博 士 論 文 (要約)

Plasmid-host functional interaction network: global proteome dynamics and molecular analysis of H-NS family proteins

プラスミド・宿主間相互作用 - プロテオーム動態および H-NS ファミリータンパク質の分子解析

ヴァシレヴァ　デリアナ　ペテヴァ

Table of contents

Abbreviations

A	adenine, Ampere
bp	base pair
BSA	bovine serum albumin
°C	degree Celsius
C-	carboxy-
Cm	chloramphenicol
Da	Dalton
(d)dH_2O	(double) distilled water
DMS	dimethyl suberimidate dihydrochloride
DNA	deoxyribonucleic acid
DNase	deoxyribonuclease
dNTP	2′-deoxynucleoside 5′-triphosphate
DTT	dithiothreitol
EDTA	ethylene diamine tetraacetate
et al.	and others
Fig.	Figure
F	Forward
g	gram
G	guanine
h	hour
IPTG	isopropyl-ß-D-thiogalactoside
k	kilo
KAT	lysine acetyltransferase
kb	kilobase
KDAC	lysine deacetylase
L	liter
LB	Luria-Bertani medium
µ	micro (10^{-6})
m	meter, milli (10^{-3})
M	molar
min	minute
mod.	modified
MS	mass spectrometry
n	nano (10^{-9})
N-	amino-
OD	optical density
ORF	Open Reading Frame
PAGE	Polyacrilamide Gel Electrophoresis
PCR	Polymerase Chain Reaction

pH	negative logarithm of the hydrogen ion concentration
PEG	polyethylene glycol
PTM	post-translational modification
R	reverse
RNase	ribonuclease
rpm	rounds per minute
RT	room temperature
s	second
SDS	sodium dodecyl sulfate
SOE	'Splicing by overlap extension'
T	thiamine
TFA	trifluoroacetic acid
T_m	melting temperature
Tris	Tris-aminomethane
U	Unit
UV	ultraviolet
WT	wild-type
w/v	weight per volume
V	volt
Vol.	volume
vs.	*versus*
v/v	volume per volume

論 文 の 内 容 の 要 旨

応用生命工学専攻
平成 27 年度博士課程入学
氏　　名　ヴァシレヴァ
　　デリアナ　ペテヴァ
指導教員名　野尻　秀昭

論文題目

Plasmid-host functional interaction network: global proteome dynamics and molecular analysis of H-NS family proteins
(プラスミド・宿主間相互作用 - プロテオーム動態および
H-NS ファミリータンパク質の分子解析)

Plasmids, one of the mobile genetic elements (MGEs), play an important role in adaptation and evolution. They can confer various novel traits to their host cells, such as resistance to antibiotics and heavy metal as well as the ability to degrade xenobiotic compounds. Novel trends in plasmid research aim at understanding the molecular mechanisms underlying the functional interaction between plasmids and host cells in order to predict the behaviour of plasmid-harbouring strains in the natural environments. Using the carbazole-degradative plasmid pCAR1 as a model, our laboratory has initiated comprehensive research, which evaluates the interplay between a catabolic plasmid and several different strains from the genus *Pseudomonas*. Previous results showed that carriage of pCAR1 differentially reshaped the chromosomal gene expression and physiology of *P. putida* KT2440, *P. aeruginosa* PAO1 and *P. fluorescens* Pf0-1. However, these and other studies have characterized the plasmid-host systems mainly at transcriptional level and only few reports addressed the effect of MGEs on the protein pools of the host cells. Furthermore, the role of post-translational modification (PTM) in plasmid-host cross-talk has not been previously explored. Therefore, the first objective of this study was to evaluate the impact of pCAR1 on the proteome of the host cells using *P. putida* KT2440 as a model. In addition, two acyl lysine modifications (acetylation and succinylation) that respond to the metabolic status of the cell and regulate diverse protein properties were investigated.

Nucleoid-associated proteins (NAPs) in bacteria are global regulators of gene expression. H-NS family proteins are one of the most abundant NAPs. They share common structural organization including a C-terminal DNA-binding domain and an N-terminal dimerization/oligomerization domain, connected by a flexible linker. Previous comprehensive transcriptome and phenotypic analyses revealed that H-NS functional homologs encoded on the pCAR1 plasmid (Pmr) and the chromosome of *P. putida* KT2440 (TurA and TurB) play a pivotal role in the plasmid-host interactions. Results suggested that the three proteins cooperatively and independently regulate the expression of both chromosomal and plasmid genes. Dimerization and subsequent oligomerization are important features of the function of these proteins. Therefore, biochemical analyses and structures of plasmid- and chromosome-born H-NS homologs would provide deeper understanding of the mechanisms of plasmid effects on host-cell physiology. The structure of an oligomerization-deficient TurB truncated variant (TurB_nt$_{61}$-R8A), which lacks the flexible linker and the DNA-binding domain, was recently resolved (Fig.1) [1]: a central dimerization site was identified and a terminal dimerization site was predicted. The second objective of this study was characterization of the N-terminal dimerization site of TurB.

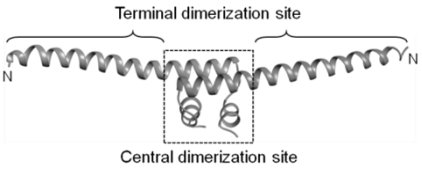

Fig. 1 Structure of TurB_nt$_{61}$-R8A [1].

Proteome and acylome analyses of the modification landscape created by the functional interaction between pCAR1 and host *Pseudomonas putida* KT2440

In order to explore the impact of pCAR1 carriage on the protein biosynthesis of the host as well as to characterize the protein lysine acetylation and succinylation profiles of the pCAR1-free and -harbouring strains, a quantitative mass spectrometry (MS) approach based on SILAC (stable isotope labeling by amino acids in cell culture) was applied. To this end, *P. putida* KT2440 and KT2440(pCAR1) lysine auxotrophic strains (KT2440L and KT2440L(pCAR1)) were constructed and employed. To evaluate the effect of pCAR1 carriage based on the physiological state of the host, the comparative proteome profiling was performed using actively growing exponential and stationary phase cells. KT2440L and KT2440L(pCAR1) were labeled in minimal succinate medium supplemented with 'light' and 'heavy' lysine, respectively. For the total proteome analysis, equal amounts of cell-free protein extracts from both strains were mixed, digested with trypsin and subjected to MS analysis. Global acylome profiling was conducted by enrichment of acetylated and succinylated peptides from the total tryptic peptide pools using anti-acetyllysine and anti-succinyllysine antibodies.

In total, 1,592 distinct proteins were detected in the pCAR1-free and -harbouring strains: 20 proteins were encoded on the pCAR1 plasmid and 1,572 proteins were encoded on the chromosome. Carriage of pCAR1 affected 10% of the detected host proteome: 7 proteins were found to be significantly induced (more than twofold) and 151 proteins were downregulated. Notably, pCAR1 reduced the abundance of key proteins involved in central metabolism (TCA cycle and glycolysis), signal transduction and motility. The overall modest correlation between the protein abundance data and the previous transcriptomic analyses

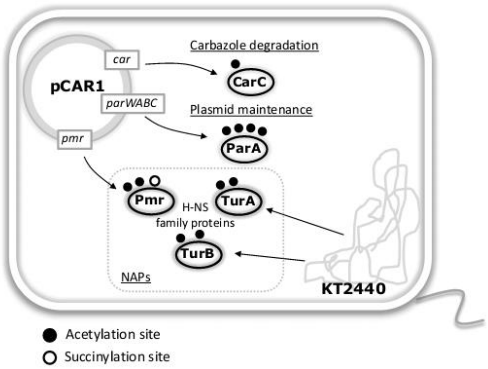

Fig. 2 Acetylation and succinylation identified on pCAR1-encoded proteins involved in carbazole degradation and plasmid maintenance and on H-NS homologs, key players in the plasmid-host cross-talk.

indicated the relevance of an integrated approach in order to better understand the effect of plasmid carriage on the host cells.

In total, 937 acetylation sites on 383 proteins and 331 succinylation sites on 150 proteins were reproducibly detected in two biologically-independent experiments in the pCAR1-free and -harbouring strains. Acetylation and succinylation mainly targeted proteins involved in translation, carbohydrate and amino acid metabolism. pCAR1 carriage resulted in changes in the acylation status of host proteins involved in the ribosome, carbohydrate and nucleotide metabolism. Furthermore, the host system invoked acetylation of important pCAR1-encoded proteins involved in carbazole degradation and plasmid maintenance (Fig. 2). Acetylation and succinylation were also detected on the pCAR1-and chromosome-encoded H-NS family proteins TurA, TurB and Pmr. Collectively, these results featured the potential of physiological cues from the host to affect plasmid-determined functions and to impact the transcriptional networks in the plasmid-harbouring systems.

Investigation of the factors affecting the acylation status in the pCAR1-free and -harbouring strains

The global proteome analyses of the pCAR1-free and -harbouring strains revealed that lysine acetylation and succinylation are abundant PTM in *P. putida* KT2440. However, the factors that affect the acylation status are still unclear. Two mechanisms for Nε-lysine acetylation have been reported in bacteria. The first relies on acetyltransferases (KATs) with acetyl-CoA as a donor of acetyl groups and the second mechanism is non-enzymatic with acetyl-phosphate (acetyl-P) serving as the acetyl group donor. Both enzymatic and non-enzymatic acetylation could be reversed by deacetylases (KDACs). Functional KATs and KDACs in *P. putida* KT2440 have not been identified yet. Bioinformatic analysis revealed more than 30 putative KATs encoded on the chromosome and one on the pCAR1 plasmid. Furthermore, *P. putida* KT2440 possesses three KDAC homologs (PP_4764, PP_5340 and PP_5402). In order to evaluate the role of the three putative KDACs, triple deletion mutants were generated (KT2440D and KT2440D(pCAR1)). To characterize also the effect of acetyl-P levels on the global acetylation status, a putative phosphotransacetylase (Pta), which catalyzes the conversion of acetyl-CoA to acetyl-P, was inactivated giving KT2440P and KT2440P(pCAR1) strains. Acetylation in the pCAR1-free and harbouring strains mainly targeted proteins involved in carbohydrate metabolism (glycolysis/gluconeogenesis, TCA cycle, pentose phosphate pathway, pyruvate metabolism), energy metabolism (oxidative phosphorylation, nitrogen, sulfur metabolism) and amino acid metabolism. Therefore, in a first set of experiments the metabolic capabilities of KT2440D and KT2440D(pCAR1) were estimated by Phenotype MicroArrays (Biolog) using 190 carbon sources, 95 nitrogen sources and 94 sulfur and phosphorous sources. KT2440D

showed no pronounced difference in comparison to the control strain under all conditions tested, whereas KT2440D(pCAR1) exhibited reduction in metabolic capabilities under most conditions. The delayed growth of KT2440D(pCAR1) in comparison to KT2440(pCAR1) was further confirmed in minimal succinate medium. Deletion of the putative KDACs genes and *pta* had no dramatic effect on the global acetylation levels of the pCAR1-free and harbouring strains, as judged by anti-acetyllysine immunoblot analyses peformed with whole-cell protein extracts from cultures grown in media supplemented with various carbon sources.

Characterization of the N-terminal dimerization site of TurB- biochemical studies and crystallization

In order to study the properties of the N-terminal dimerization site of TurB, variants truncated at the central dimerization site were constructed: TurB_ nt_{37}, TurB_nt_{40}, TurB_nt_{42} and TurB_nt_{50}. Cross-linking experiments demonstrated that all four variants formed dimers but no oligomers (results for TurB_nt_{42} and TurB_nt_{50} were published in [1]) suggesting that TurB uses both, the central and the terminal dimerization site for oligomerization. To determine the structural basis for dimerization at the N-terminal site, crystallization screening was performed with the truncated variants: TurB_ nt_{37} and TurB_nt_{40} produced no crystals, and TurB_nt_{42} produced crystals with poor diffraction. Initially, TurB_nt_{50} could not be subjected to crystallization due to formation of aggregates. Through an extensive screening 0.4 M NDSB-256 was found to prevent formation of aggregates. TurB_nt_{50} was crystallized by the hanging-drop vapour-diffusion method using a precipitant solution composed of 20% PEG3350, 0.1 M HEPES (pH 6.8), 0.1 M ammonium acetate. X-ray diffraction data were collected from TurB_nt_{50} crystals with a maximum resolution of 2.8 Å. These data are currently being analyzed.

Summary and future prospects

Through comparative proteome analyses of plasmid-free and -harbouring cells, this work determined how the catabolic plasmid pCAR1 alters the protein pools in host *P. putida* KT2440 and revealed a previously unexplored potential of metabolism-related post-translational modifications (lysine acetylation and succinylation) in the plasmid-host interactions. To examine the generality of these patterns, a broader set of host systems needs to be examined. Further studies will also be required to characterize the modulation in the pools of metabolites, whose pathways are influenced by carriage of pCAR1 in order to obtain deeper understanding of the metabolic networks in the plasmid-harbouring strains. Detailed biochemical studies are being performed to determine how acetylation and succinylation precisely affect the properties of plasmid- and chromosome-encoded NAPs. These analyses will shed light on the factors that impact the transcriptional networks in the plasmid-host systems.

In the second part of this work, the N-terminal dimerization site of the H-NS homolog TurB was characterized and crystals were obtained. Structural studies are necessary to provide more detail about the dimerization/oligomerization mechanisms of TurA and Pmr. Such information would also serve as a context for analysis of the effect of PTM on the properties of H-NS family proteins.

Reference:

[1] Suzuki-Minakuchi C, Kawazuma K, Matsuzawa J, Vasileva D, Fujimoto Z, Terada T, Okada K and Nojiri H (2016) Structural similarities and differences in H-NS family proteins revealed by the N-terminal structure of TurB in *Pseudomonas putida* KT2440. *FEBS Lett* **590**, 3583-3594.

Chapter 1

Introduction

Plasmids represent an important resource for genetic evolution and adaptation to the changing environment (Smets and Barkay, 2005). They can confer novel traits to their host cells, such as resistance to antibiotics, and heavy metals, as well as the ability to degrade xenobiotic compounds (Nojiri *et al*., 2004; Frost *et al*., 2005). Understanding the interplay between a plasmid and its host system is important in order to predict the behaviour of plasmid-harbouring strains in the natural environments.

1.1 pCAR1-a model for studies of the plasmid-host systems

Pseudomonas resinovorans CA10 was isolated from activated sludge of municipal waste water facility in 1993 (Ouchiyama *et al*., 1993). pCAR1 (Fig. 1-1), originally isolated from this strain, is a 200 kb plasmid that carries a gene cluster (*car*) involved in degradation of carbazole, a toxic and mutagenic compound (Nojiri *et al*., 2001; Nojiri, 2012). The complete nucleotide sequence of pCAR1 has been determined (Maeda *et al*., 2003; Takahashi *et al*., 2009b). pCAR1 belongs to incompatibility (Inc) group P-7 and its ability for conjugative transfer within the genus of *Pseudomonas* was demonstrated (Shintani *et al*., 2006). Using pCAR1 as a model, our lab has initiated a comprehensive research investigating the functional interactions in the plasmid-host systems. RNA mapping of pCAR1 was peformed in six different hosts and genes involved in important plasmid functions, including partitioning and carbazole degradation, were found to be differentially transcribed (Shintani *et al*., 2011). Carriage of pCAR1 also affected differentially the chromosomal gene transcription in three distinct *Pseudomonas* strains: *P. putida* KT2440, *P. aeruginosa* PAO1 and *P. fluorescens* Pf0-1 (Shintani *et al*., 2010; Takahashi *et al*., 2015). The most prominent example was the *mexEF-oprN* operon encoding an RND-efflux pump, specifically induced by pCAR1 only in host *P. putida* KT2440. Detailed analyses of the impact of pCAR1 on the physiology of the three hosts have been performed. Plasmid carriage resulted in reduced host fitness, swimming motility, resistance to osmotic and pH stresses (Takahashi *et al*., 2015) and affected biofilm formation (Lee *et al*., 2016). Comparative analyses of the metabolic capabilities have been performed between the corresponding pCAR1-free and -harbouring *Pseudomonas* strains using Biolog Phenotype MicroArrays (PM) (Takahashi *et al*., 2015). In total, cellular respiration was evaluated using different compounds as carbon (190), nitrogen (95), phosphorus (59) and sulfur (35) sources. Among all compounds tested, availabilities of 66 (KT2440), 39 (PAO1) and 31 (Pf0-1) were affected by pCAR1, suggesting modifications in the metabolic background of the host cells. For instance, carriage of pCAR1 has led to reduced cell respiration, when intermediate compounds of the TCA and those several steps away from the TCA cycle (acetic acid, L-lactic acid and propionic acid) were used as sole carbon sources (Fig. 1-2).

Collectively, the above studies indicated that novel host phenotypes arise as a result of the action of both plasmid and chromosome determined factors.

1.1.2 Role of pCAR1- and chromosome-borne nucleoid-associated proteins in the plasmid-host interactions

Nucleoid-associated proteins (NAPs) mediate compaction of chromosomal DNA and can act as global regulators of gene expression (Dorman, 2004). H-NS family proteins are one of the most abundant NAPs in Gram-negative bacteria. They share common structural organization including a C-terminal DNA-binding domain and an N-terminal dimerization/oligomerization domain, connected by a flexible linker (Rimsky, 2004). H-NS proteins can repress genes acquired through horizontal gene transfer by recognizing sequences with low GC content (Takeda *et al.*, 2011). Dimers or oligomers bind to high-affinity DNA sequences through their C-teminal domains, followed by formation of nucleoprotein complexes via protein-protein interactions. Plasmid-encoded H-NS play an important role in the regulation of the networks between plasmid and the host chromosome (Nojiri, 2013). For instance, Sfh, an H-NS protein encoded on the conjugative plasmid pSfR27 can function as a stealth protein without imposing significant fitness cost on the host (Doyle *et al.*, 2007).

MvaT-like proteins in *Pseudomonas* share low sequence homology with H-NS, but can complement *hns* deficient phenotype in *E. coli* (Tendeng *et al.*, 2003). Therefore, they belong to H-NS family proteins. Plasmid pCAR1 carries a gene encoding a MvaT-like protein Pmr. Using *P. putida* KT2440 as a host ChAP-chip analyses showed that Pmr binds numerous sites not only on pCAR1, but also on the chromosome and disruption of *pmr* resulted in significant reshaping of the transcriptome of the host (Yun *et al.*, 2010), suggesting that its function is similar to Sfh. *P. putida* KT2440 possesses five genes encoding MvaT-like proteins, *turA-E*, among which *turA* and *turB* were shown to be majorly transcribed (Yun *et al.*, 2010). ChAP-chip analyses showed that TurA, TurB and Pmr bind almost identical sites suggesting that the three proteins act cooperatively to regulate the transcriptional networks in the plasmid-host systems (Yun *et al.*, 2010). Interestingly also, transcriptome analyses of deletion mutants demonstrated that although the three proteins share high degree of amino acid homology (Fig. 1-3), their regulons did not overlap completely (Fig. 1-4) indicating that their functions are not identical. Dimerization and subsequent oligomerization are important features of the function of H-NS family proteins. Therefore, to obtain deeper undestanding of the molecular mechanism of these proteins, comparative analyses of the protein-protein interactions have been initiated (1.1.2.1).

In addtition to Pmr, pCAR1 encodes two more NAPs: Pnd (NdpA-like protein) and Phu (HU-like protein). Comprehensive phenotypic and transcriptomic analyses of single and double deletion mutants of *pmr*, *pnd* and *phu* showed that the three proteins have important roles in control of the transcriptional networks in the plasmid-harbouring strains (Suzuki-Minakuchi *et al.*, 2015).

Collectively, the results from the above studies indicated that NAPs encoded on the pCAR1 plasmid and the chromosome are key players in the plasmid-host cross-talk.

1.1.2.1 Biochemical and structural studies of the N-terminal dimerization/oligomerization domain of pCAR1- and chromosome-borne MvaT homologs

Using chemical cross-linking experiments with truncated variants of Pmr, the first 61 residues were found to constitute the dimerization/oligomerization domain and 7 residues (E6, R8, K15, Q18, R20, N27 and K49) important for oligomerization were identified (Suzuki *et al*., 2014) (Fig. 1-3). Furthemore, the crystal stucture of an oligomerization deficient variant TurB_nt$_{61}$-R8A (Fig. 1-5), which lacks the flexible linker and the DNA-binding domain was recently solved (Suzuki-Minakuchi *et al*., 2016) (Fig. 1-6 A). One protomer contained two helices: a longer N-terminal α1 helix and a shorter C- terminal α2 helix. The structure revealed a 'central dimerization site' (residues 32-58), stabilized by a hydrophobic core (Fig. 1-6 B). Furthemore, an 'terminal dimerization site' was predicted. While the central dimerization site was similar to H-NS, the terminal dimerization site predicted to form coiled-coil motif was different (Fig. 1-7) suggesting that MvaT and H-NS might have distinct oligomerization mechanisms.

1.2 Acyl lysine modifications in bacteria

1.2.1 Nε-lysine acetylation - an ubiquitous PTM in eukaryotes and bacteria

Nε-lysine acetylation was first reported as a post-translational modification (PTM) of histones in 1960s (Allfrey *et al*., 1964). The later discovery that acetylation occurs on α-tubulin and p53 (Piperno *et al*., 1987; Gu and Roeder, 1997) suggested that this PTM extends beyond histone proteins and encouraged the development of mass spectrometry (MS)-based methods for proteome-wide identification of acetylation events. These analyses include protein extraction, followed by digestion with proteases and immunoprecipitation using anti-acetyllysine antibodies. Finally, the enriched peptides are subjected to MS analysis in order to identify the acetylated sites. Early acetyl-proteomic studies provided evidence that acetylation is a common PTM in eukaryotes occuring on proteins with various functions and cellular locations (Kim *et al*., 2006; Choudhary *et al*., 2009).

Initially, lysine acetylation was considered to be rare or absent in bacteria. Until recently only two bacterial proteins were known to be acetylated: the chemotaxis protein CheY from *Escherichia coli* (Barak *et at*., 1992) and acetyl-CoA synthetase (Acs) from *Salmonella enterica* (Starai *et al*., 2002). These findings and the discovery that the mitochondrial proteome is highly acetylated (Smith and Workman, 2009) inspired global proteomic studies in prokaryotes. The first acetylome analysis in bacteria has been performed in *E. coli* (Yu *et al*., 2008). Since then, advances in MS-based proteomics and availability of anti-acetyllysine antibodies allowed the identification of hundreds of acetylated proteins involved in diverse and often essential cellular processes in various bacterial species (Table 1-1).

1.2.2 Mechanism of Nε-lysine acetylation

1.2.2.1 Enzymatic and non-enzymatic acetylation

Lysine acetyltransferases (KATs) catalyze the transfer of an acetyl group from a donor molecule such as acetyl-CoA to the target lysine residue. Five KAT protein families have been identified across all domains of life (Marmostein and Roth, 2001). The only known acetyltransferases in bacteria belong to Gcn5-related N-acetyltransferase (GNAT) superfamily. The reaction mechanism of GNAT involves a glutamate residue that deprotonates the substrate lysine, facillitating a direct nucleophile attack on the carbonyl group of

acetyl-CoA (Vetting *et al*., 2005) (Fig. 1-8). Only few acetyltransferases have been characterized so far in bacteria. Acs from *S. enterica* was the first enzyme found to be regulated by KAT (Pat) (Starai and Escalante-Semerena, 2004). Pat acetylates a conserved lysine residue in the active site of Acs and thereby inhibits its activity (Starai *et al*., 2005). This mechanism has been found to be conserved in other bacterial species (Gardner *et al*., 2006; Gardner and Escalante-Semerena, 2008; Tucker and Escalante-Semerena, 2013). Inactivation of KATs in *Bacillus subtilis* (AcuA) (Kosono *et al*., 2015; Carabetta *et al*., 2016) and *E. coli* (PatZ) (Kuhn *et al*., 2014; Castano-Cerezo *et al*. 2014; Weinert *et al*., 2013a) showed a rather minor effect on the global acetylation levels, suggesting that other mechnisms for acetylation and/or uncharacterized acetyltransferases exist in bacteria. This seems plausible, given the high number of uncharacterized GNAT-domain-containing proteins in the genomes of many bacteria.

Recent studies have proposed a second non-enzymatic mechanism for acetylation with acetyl-phosphate, the intermediate of the phosphotransacetylase (Pta)-acetate kinase (AckA) pathway (Wolfe, 2005), serving as an acetyl donor in bacteria (Weinert *et al*. 2013a; Kuhn *et al*., 2014) and acetyl-CoA as an acetyl donor in mitochondria (Wagner and Payne, 2013; Weinert *et al*., 2014) (Fig. 1-8). The results from these studies demonstrated that non-enzymatic acetylation is predominant and less specific than enzymatic acetylation.

1.2.2.2 Reversal of acetylation by deacetylases

Lysine acetylation could be reversed by deacetylases (KDACs) (Fig. 1-8). Two KDAC families are known: NAD^+-dependent sirtuins (Blander and Guarente, 2004) and metal-dependent KDACs (Yang and Seto, 2008). Zn^{2+}-dependent deacetylases are hydrolases that release acetate, whereas sirtuins use NAD^+ as a cofactor and produce nicotinamide and 2'-O-acetyl-ADP-ribose as reaction products. Bacterial homologs of each KDAC family have been identified (Hildman *et al*., 2007). Quantitative proteomic analyses provided evidence that CobB (sirtuin) in *E. coli* can deacetylate both enzymatic and non-enzymatic lysine acetylation substrates (AbouElfetouh *et al*., 2015). However, not all acetylation could be reversed by CobB suggesting that some acetylation at some sites is irreversible and/or there exist yet uncharacterized KDACs. A more recent study identified a novel deacetylase in *E. coli* (YcgC) (Tu *et al*., 2015) (Fig. 1-8). YcgC does not require Zn^{2+} or NAD^+ and uses serine residue as a catalyst for removal of acetyl groups from lysines.

1.2.3 Other acyl modification in bacteria

In addition to lysine acetylation, various novel acyl modifications including succinylation (Colak *et al*., 2013; Weinert *et al*., 2013b; Pan *et al*., 2015; Kosono *et al*., 2015; Yang *et al*. 2015; Mizuno *et al*., 2016; Okanishi *et al*., 2017a), propionylation (Okanishi *et al*., 2014; 2017b; Sun *et al*. 2016), malonylation (Qian *et al*., 2016) and glutarylation (Xie *et al*., 2016) have been reported in bacteria. Like acetylation, these modifications occur on hundreds of proteins involved in a wide variety of biological processes and the corresponding acyl-CoA molecules are considered as acyl donors. Protein lysine acetylation and succinylation have been demonstrated to occur frequently (Weinert *et al*., 2013b; Kosono *et al*., 2015). A comparative proteomic study in *E. coli* showed that CobB acts not only as a deacetylase, but also as a desuccinylase (Colak *et al*., 2013). However, enzymes catalyzing succinylation have not been identified so far.

1.2.4 Impact of lysine acylation on protein function

Acetylation results in neutralization of the positive charge of lysine. A number of studies in eukaryotes have shown that when it occurs at critical residues, acetylation could influence protein localization, stability, enzyme activity, protein-protein, and protein-DNA interactions (Gu *et al*., 1997; Glozak *et al*., 2005; Zhang *et al*., 2012; Li *et al*., 2012). The functional significance of the vast majority of the identified acetylation sites in bacteria is still unclear. However, emerging evidence from global proteomic and *in vitro* studies suggested a role in regulation of diverse cellular functions in prokaryotes including metabolic processes (Wang *et al*., 2010; Guan and Xiong, 2011; Hirschey and Zhao, 2015) motility (Ramakrishnan *et al*., 1998) and transcription (Thao *et al*., 2010; Hu *et al*., 2013). The physiological significance of many of these acylation events remains to be characterized. However, collectively, these studies suggested that acyl modifications might represent a mechanism for control of various cellular processes in response to the metabolic state of the cell.

1.3 Objectives of this study

1) The cost associated with protein biosynthesis represents an important facet of the metabolic burden imposed on the host by plasmid carriage and a fundamental aspect of evolutionary selection (Dekel and Alon, 2005; Baltrus, 2013). Multiple reports have demonstrated a weak correlation between transcriptome and proteome expression data due to factors that affect translation efficiencies, including discrepancies between mRNA and protein stabilities, amino acid availabilities and ribosome densities (Haider and Pal, 2013). However, only few studies have examined the effect of mobile genetic elements on the protein pools of the host. Furthermore, a potential role of post-translational modifications (PTM) in plasmid-host interactions has not been investigated. The first objective of this study was a comprehensive proteome analysis using the pCAR1-free and pCAR1-harboring strains to better understand the integral response of the host to pCAR1 carriage. In addition, to explore the potential role of acylation events in the previously observed phenotypic changes of the host due to pCAR1 carriage as well as in regulation of plasmid-encoded proteins in response to physiological cues of the host, comparative acetylome and succinylome analyses were performed.

2) The second part of this work aimed at clarifying the mechanism for dimerization of MvaT homologs encoded on the chromosome and the pCAR1-plasmid at the 'terminal dimerization site'.

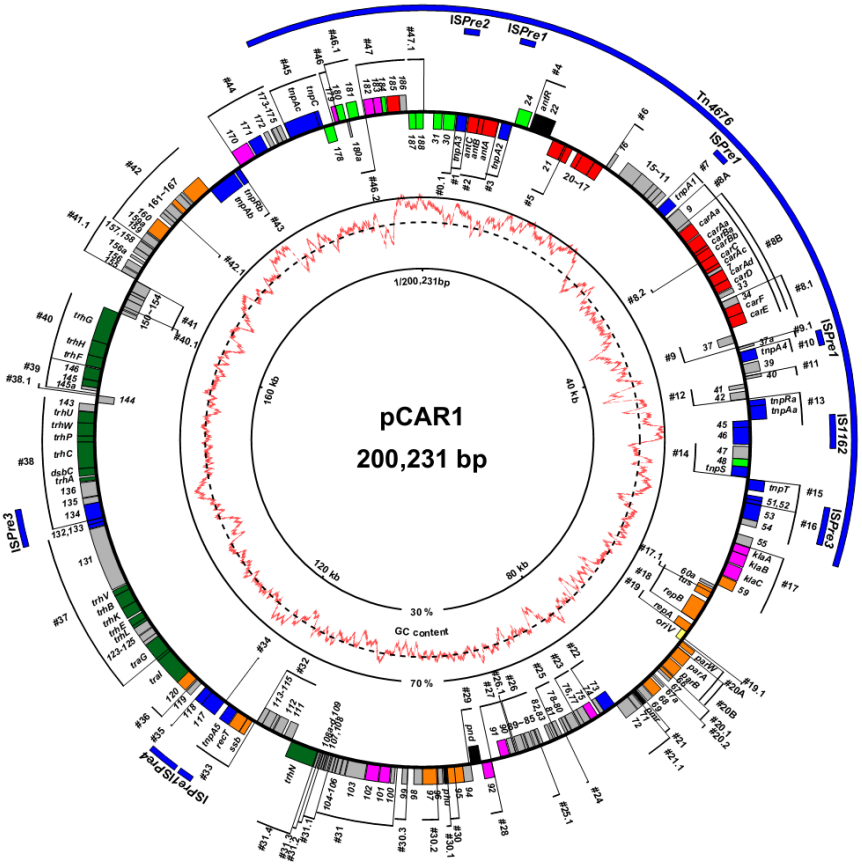

Fig. 1-1 **Circular map of pCAR1**. Genes or ORFs outside the circle are coded clockwise, those inside are coded counter-clockwise. The (putative) functions of genes or ORFs are shown by color as follows: orange, maintenance or DNA processing; dark green, conjugative transfer; blue, transposition or integration; red, degradation; light green, transport; black, regulation; magenta, other known function; gray, unknown function (homologous to hypothetical protein); and yellow, unknown function (no homology). Bars inside the circular gene map indicate the GþC contents of ORFs shown in the same color. The broken circle indicates average GC content of entire pCAR1 (56%) (Maeda *et al*., 2003; Takahashi *et al*., 2009b).

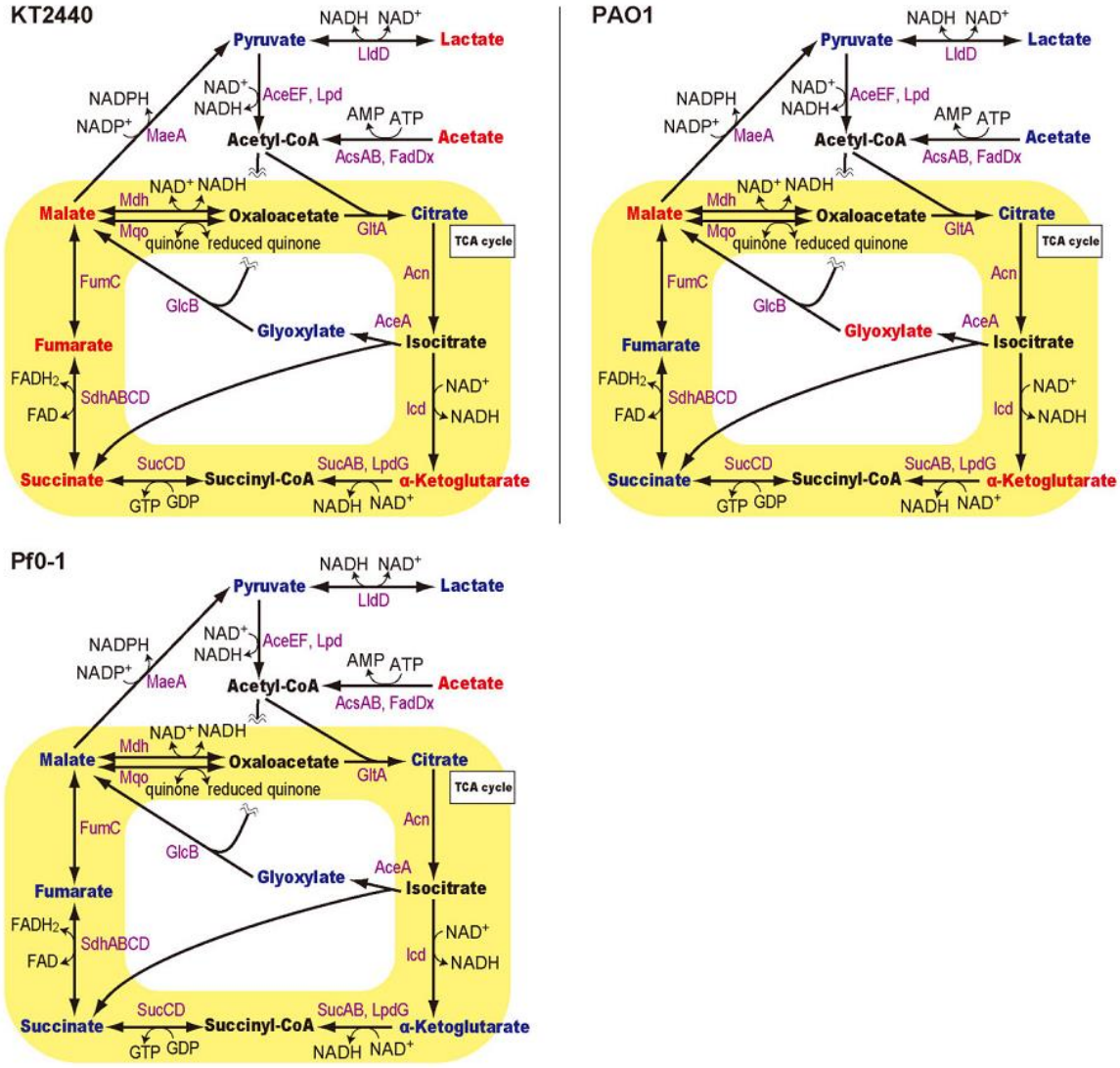

Fig. 1-2 Carriage of pCAR1 reduced the respiration activities for several compounds in the TCA cycle and its branching pathways. The TCA cycle (shown in yellow) and several steps away from the TCA cycle are presented for each host strain. Each compound shown in red or blue was supplied as a carbon source in PM. Compounds for which the host respiration activities were reduced by pCAR1 carriage are shown in red, and compounds for which the host activities did not change are shown in blue. Compounds shown in black were not contained in the PM (Takahashi *et al*., 2015; Fig. 3).

Fig. 1-3 Alignments of amino acid sequences of Pmr, TurA, TurB, and MvaT of *P. aeruginosa* PAO1. Alignments were performed using the CLUSTAL W software, version 2.1. The amino acid residues identical in two to four members are shown in red. Dimerization/oligomerization and DNA-binding domains of Pmr and the corresponding regions in the other three proteins are indicated in the panel. The seven residues important for homo-oligomerization of Pmr, and the corresponding residues in the other three proteins, are highlighted in light blue (Suzuki *et al*., 2014; Fig. 1).

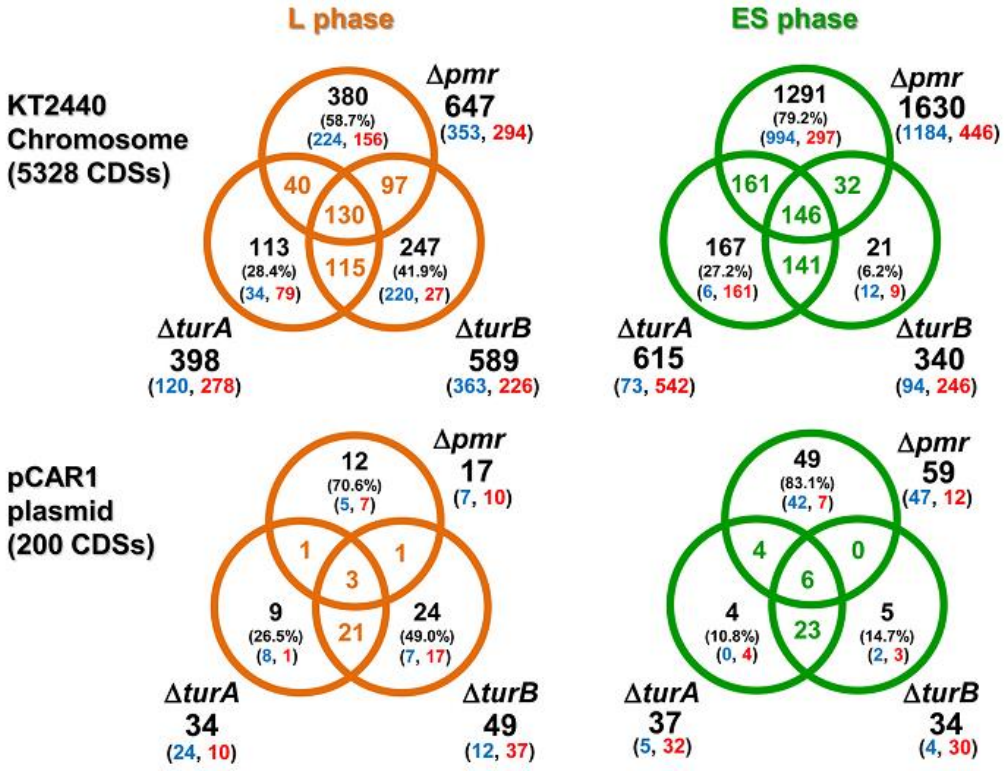

Fig. 1-4 Venn diagram of differentially transcribed CDSs in the KT2440 chromosome and the pCAR1 plasmid during the L and ES growth phases due to markerless deletion of *pmr*, *turA*, or *turB*. Blue and red numbers indicate upregulated and downregulated CDSs, respectively (Yun *et al*., 2016; Fig. 5).

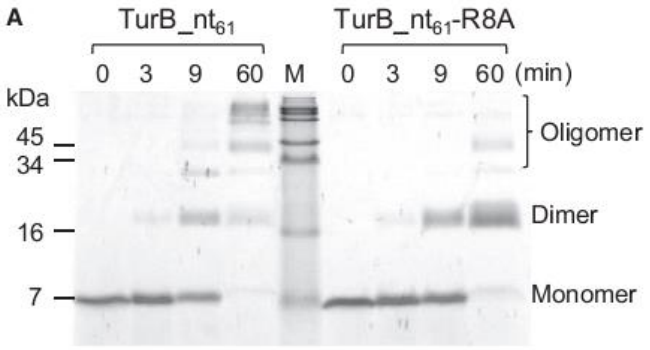

Fig. 1-5 TurB_nt$_{61}$-R8A- an oligomerization deficient derivative containing the N-terminal dimerization/ oligomerization domain. Tricine-SDS/PAGE profiles of TurB_nt61 and TurB_nt61-R8A after chemical cross-linking. Numbers indicate durations (min) of incubation with DMS. 'M' indicates the protein markers. The bands corresponding to oligomers, dimers and monomers are indicated. (Suzuki-Minakuchi *et al*., 2016; Fig. 2A).

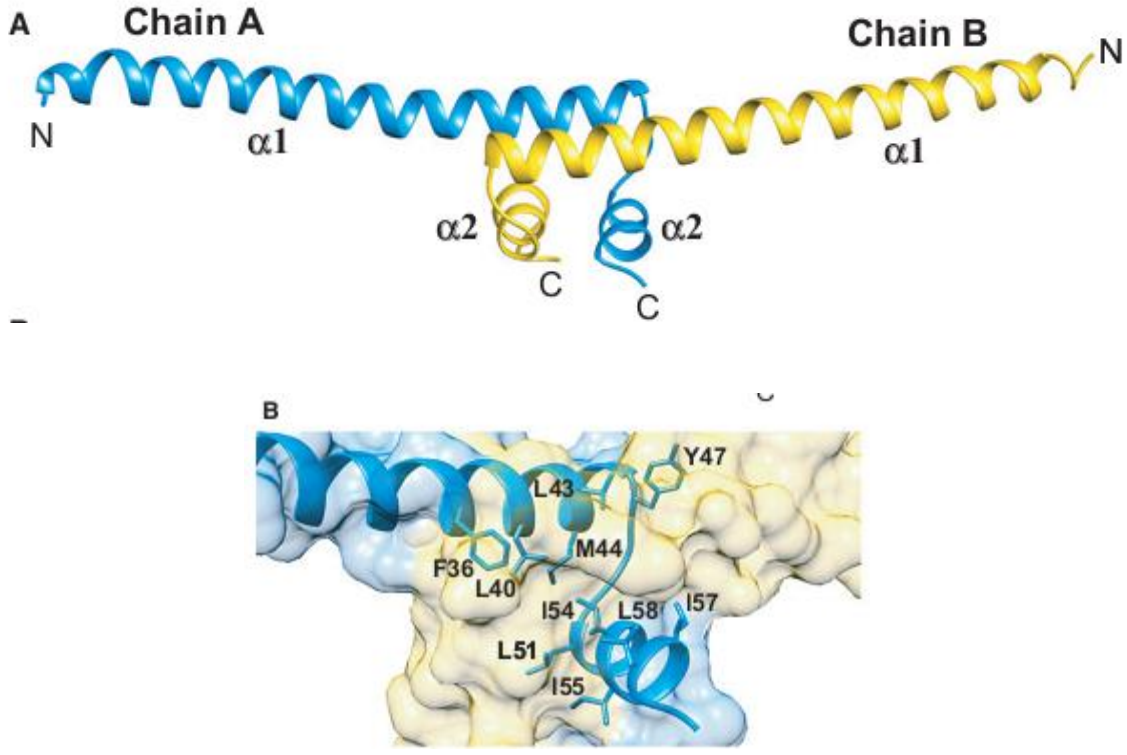

Fig. 1-6 Crystal structure of TurB_nt$_{61}$-R8A dimer. (A) Ribbon representation of the overall structure. Chain A and Chain B are shown in blue and yellow respectively. 'a1' and 'a2' are the names of helices from the N-terminus of a protomer. The N- and C-termini of the two protomers are shown as 'N' and 'C' respectively. (B) Hydrophobic core. Ribbon model and transparent surface of Chains A and B are shown. Only the surface of Chain B is shown in the left panel, whereas both the surface and the ribbon model of Chain B are shown in the right panel. Side chains of the residues included in the hydrophobic core are shown in the panels (Suzuki-Minakuchi *et al*., 2016; Fig. 3A and B).

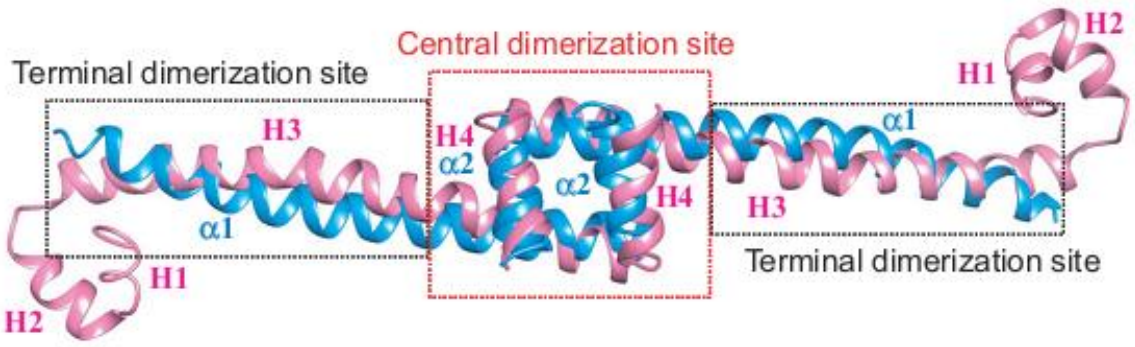

Fig. 1-7 Superimposed structure of H-NS$_{1–83}$ and TurB_nt$_{61}$-R8A. The crystal structures of H-NS$_{1–83}$ (Arold *et al*., 2010) and TurB_nt$_{61}$-R8A are shown in pink and blue respectively. Note that the H-NS$_{1–83}$ dimer in this panel is the same one shown in pink in panel A. 'a1' and 'a2' are the names of the helices in TurB_nt61-R8A. The terminal dimerization sites and the central dimerization site of TurB_nt$_{61}$-R8A are indicated in the panel (Suzuki-Minakuchi *et al*., 2016; Fig. 4B)

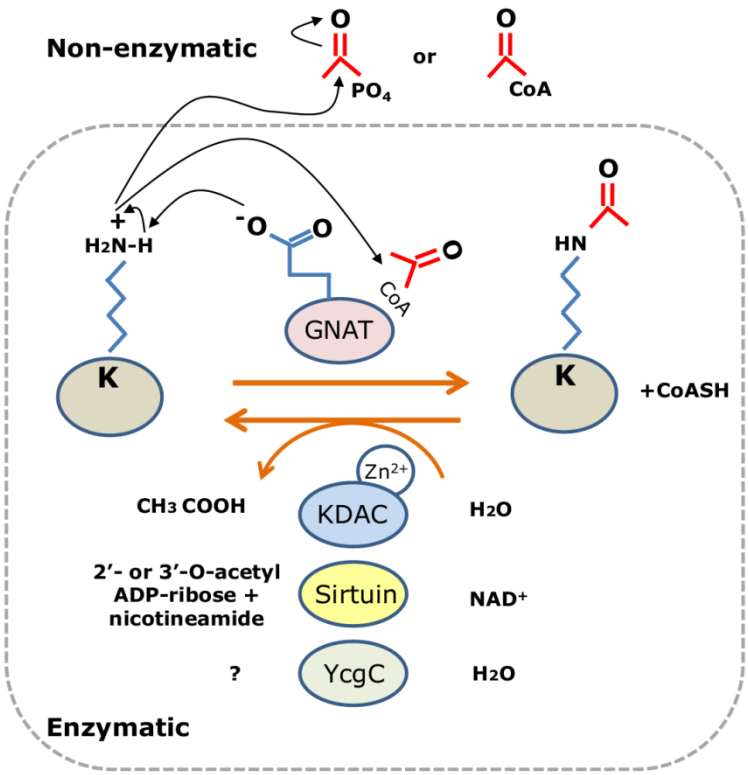

Fig. 1-8 **Mechanism of acetylation**. Acetyl groups are transferred to lysine residues from a donor molecule (acetyl-CoA) by acetyltransferases (GNAT), the only known KATs in bacteria. These enzymes deprotonate the target lysine residue through the action of a conserved glutamate residue. Non-enzymatic lysine acetylation occurs with acetyl-phosphate (bacteria) or acetyl-CoA (mitochondria) serving as the donor of acetyl groups. For both enzymatically and non-enzymatically acetylated proteins, acetyl groups are removed by KDACs: (i) metal-dependent hydrolases release acetate as a reaction product; (ii) sirtuins use NAD^+ as a cofactor and release nicotinamide and 2'-O-acetyl-ADP-ribose as products; (iii) YcgC uses a serine residue as a nucleophilic catalyst to remove acetyl groups (Carabetta and Cristea, 2017 mod.).

Table 1-1 Acetylomes in bacteria.

Species	Total number of proteins	Number of acetylated proteins	Source
Escherichia coli	4146	91	Yu *et al*., 2008*
		349	Zhang *et al*., 2013
		806	Kuhn *et al*., 2014
Bacillus subtilis	4176	185	Kim *et al*., 2013
		629	Kosono *et al*., 2015
		841	Carabetta *et al*., 2016
Mycobacterium tuberculosis	4034	137	Liu *et al*., 2014
		658	Xie *et al*., 2015
Mycobacterium abscessus	4920	289	Guo *et al*., 2016
Vibrio parahemolyticus	3079	656	Pan *et al*., 2015
Streptomyces roseosporus	6315	667	Liao *et al*., 2014
Thermus thermophilus	2238	128	Okanishi *et al*., 2013
Pseudomonas aeruginosa PA14	5878	320	Ouidir *et al*., 2015
Salmonella enterica	4525	191	Zhao *et al*., 2010
Geobacillus kaustophilus	3653	114	Lee *et al*., 2013
Bacillus amyloliquefaciens	3811	1254	Liu *et al*., 2016
Corynebacterium glutamicum	2959	604	Mizuno *et al*., 2016
Haloferax mediterranei	2923	643	Liu *et al*., 2017

* The first characterized acetylome in bacteria.

Chapter 2

Proteome and acylome analyses of the modification landscape created by the functional interaction between pCAR1 and host *P. putida* KT2440

2.1 Introduction

For accurate evaluation of the impact of pCAR1 on the global protein biosynthesis in host cells, as well as to characterize the protein acylation (acetylation and succinylation) profiles of the pCAR1-free and -harbouring strains, a quantitative proteomic MS approach based on SILAC (Stable Isotope Labeling by Amino acids in Cell culture) method was applied (Ong *et al*., 2002). Among the three hosts previously investigated, *P. putida* KT2440 was considered as a suitable model because harbouring of pCAR1 resulted in the most marked effect on the physiology of this host (Takahashi *et al*., 2015). *P. putida* KT2440 is also the best studied soil bacterium featured by its versatile metabolism, robustness towards stress and biosafety, which highlight its value for application in bioremediation (Nikel *et al*., 2014). Furthermore, global analysis of protein lysine acylation in this strain has not been reported yet.

2.2 Materials and Methods

2.2.1 Bacterial strains and plasmids

The bacterial strains, vectors and recombinant plasmids employed in this chapter are listed in Table 2-1.

Table 2-1 Bacterial strains and plasmids.

Bacterial strain or plasmid	Relevant characteristic(s)	Source or reference(s)
Bacterial strains		
Escherichia coli		
DH5α	F$^-$, ϕ80d*lacZ*ΔM15, Δ(*lacZYA-argF*)U169, *endA1*, *recA1*, *hsdR17*($r_K^- m_K^+$), *deoR*, *thi-1*, *supE44*, *gyrA96*, *relA1*, λ^-, *phoA*	Toyobo
S17-1λ*pir*	*recA*, *thi*, *pro*, *hsdR*; RP4-2 integrated into the chromosome (*kan*::Tn*7* *ter*::Mu) λ*pir*	de Lorenzo and Timmis, 1994
Pseudomonas putida		
KT2440	Naturally Cm^r	Bagdasarian *et al*., 1981
KT2440(pCAR1)	KT2440 harbouring pCAR1	Miyakoshi *et al*., 2007
KT2440L	KT2440 double-deletion mutant lacking *lysA1* and *lysA2* genes	This study
KT2440L(pCAR1)	KT2440(pCAR1) double-deletion mutant lacking *lysA1* and *lysA2* genes	This study
Plasmids		
pZErO-2	Km^r, T7 promoter, ColE1 and f1 origin, *ccdB* lethal gene, M13 priming sites	Invitrogen
pPS856	Ap^r, Km^r, FRT sites	Hoang *et al*., 1998
pK19mobsacB	Km^r, *oriT* (RP4), *sacB* , *lacZ*α, pMB1 replicon	Schäfer *et al*., 1994
pK19mobsacBΔlysA1	pK19mobsacB containing 5′- and 3′-flanking regions of *lysA1* and Gm^r cassette, which is flanked by FRT sites	This study
pK19mobsacBΔlysA2	pK19mobsacB containing 5′- and 3′-flanking regions of *lysA2* and Gm^r cassette, which is flanked by FRT sites	This study
pFLP2Km	pFLP2, Km^r gene cassette inserted into its ScaI site	Yun *et al*., 2010

2.2.2 Media and growth conditions

All media and thermostable supplements were autoclaved for 20 min at 121°C. Thermolabile additives were sterilized by filtration (0.22 μm pore size, Millex®GP, Merck Millipore Ltd.). Cells of *E. coli* strains were routinely grown at 37°C in lysogeny broth (LB) (Sambrook and Russell, 2001), whereas *Pseudomonas* strains were grown at 30°C in LB or carbon-free nitrogen plus mineral medium 4 (NMM-4) (Shintani *et al*., 2005) containing succinate or carbazole at the indicated concentrations as the sole carbon and energy sources. Solid media were prepared by addition of 1.6% [w/v] agar powder (Nacalai Tesque,

Kyoto, Japan). For the purpose of selection and screening, media contained antibiotics or additives listed in Table 2-2. Stock solutions were prepared according to Sambrook and Russell (2001) and stored at -20°C.

LB medium

Trypton	10	g
Yeast extract	5	g
NaCl	10	g
dH_2O	up to 1000	ml

NMM-4 medium

Na_2HPO_4	2.2	g
KH_2PO_4	0.8	g
NH_4NO_3	3	g
$FeCl_3 \cdot 6H_2O$*	0.01	g
$MgSO_4 \cdot 7H_2O$*	0.2	g
$CaCl_2 \cdot 6H_2O$*	0.01	g
MilliQ water	up to 1000	ml

* These components were added from sterile stock solutions to the medium after autoclavation.

Table 2-2 Antibiotics and additives.

Antibiotics or additives	Stock solution/Solvent	Final concentration	
		E. coli	***P. putida***
Chloramphenicol (Cm)	34 mg/ml/ 96% ethanol [v/v]	-	34 µg/ml
Kanamycin (Km)	50 mg/ml/ MilliQ water	50 µg/ml	50 µg/ml
Gentamicin (Gm)	120 mg/ml/ 96% ethanol [v/v]	30 µg/ml	120 µg/ml
Sucrose	20% [w/v]/ MilliQ water	-	10% [w/v]
L-lysine ($^{12}C_6$ or $^{13}C_6$)	50 mg/ml/ MilliQ water	-	50 µg/ml

2.2.3 Extraction of nucleic acids

2.2.3.1 Isolation of plasmid DNA from *E. coli*

Analytical and preparative plasmid isolation from cells of *E. coli* was performed using the alkaline lysis method. Cells grown overnight in 5 ml LB medium supplemented with the appropriate antibiotics for selection were pelleted by centrifugation (5,000 rpm; 10 min; 4°C) and handled according to the following protocol:

1) Resuspend the cell pellets in 300 µl Buffer 1.
2) Add 300 µl Buffer 2 and incubate for 3 min at RT.
3) Add 300 µl Buffer 3 and incubate for 3 min at RT.
4) Centrifugation (13,000 rpm; 15 min; 4°C). Transfer the samples into new 2-ml tubes.
5) Add 1 Vol. of Phenol:Chloroform:IAA (25:24:1) (Nacalai Tesque, Kyoto, Japan) and mix by vortexing.
6) Centrifugation (13,000 rpm; 15 min; 4°C). Transfer the upper aqueous phase into new 1.5-ml tubes.
7) Add 640 µl isopropanol and invert.

8) Centrifugation (13,000 rpm; 15 min; 4°C).
9) Discard the supernatants and wash the pellets with 500 µl 70% ethanol.
10) Dry the pellets.
11) Resuspended the pellets in 50 µl MilliQ water and incubate with RNase A (Nippon Gene) for 30 min at 37°C.
12) Store the samples at -20°C.

Buffer 1

Tris-HCl, pH 8.0	25	mM
EDTA	10	mM
Glucose	50	mM

* The buffer was sterile filtered and stored at 4°C.

Buffer 2

NaOH	0.2	N
SDS	1	mM

* The buffer was prepared freshly prior to use.

Buffer 3 (pH 6.0)

Potassium acetate	3	M

* The pH value was adjusted with glacial acetic acid and the buffer was strored at RT.

2.2.3.2 Isolation of chromosomal DNA from *P. putida*

For isolation of chromosomal DNA from *P. putida*, 5-ml LB cultures were grown at 30°C overnight. Cells were then harvested by centrifugation (6,000 rpm; 5 min; 4°C) and stored at -20°C until further use. Extraction of chromosomal DNA was conducted according to Ausubel *et al.* (1990).

1) Resuspend the pellets in 567 µl TE buffer.
2) Add 30 µl 10% SDS and 3 µl Proteinase K solution (20 mg/ml) to each sample. Rotation mixing for 15 min at RT (Rotator RT-50, TAITEC).
3) Incubate the samples for 1 h at 37°C.
4) Add 100 µl 5M NaCl to each sample. Rotation mixing for 5 min at RT.
6) Add 80 µl pre-incubated at 65°C CTAB/NaCl solution to each sample. Rotation mixing for 7 min at RT.
7) Incubate for 10 min at 65°C.
8) Add 800 µl chloroform to each sample. Rotation mixing for 10 min at RT.
9) Centifugation (15,000 rpm; 15 min; RT). Transfer the upper aqueous phase into new 2-ml tubes.
10) Add 1 Vol. of Phenol:Chloroform:IAA (25:24:1) to each sample. Rotation mixing for 10 min at RT.
11) Centrifugation (15,000 rpm; 15 min; RT). Transfer the upper aqueous phase was transferred into new 1.5-ml tubes.
12) Add isopropanol to each sample. Rotation mixing for 30 min at RT.
13) Centrifugation (15,000 rpm; 15 min; RT). The supernatants were discarded.
14) Wash the pellets with 500 µl 70% ethanol.
15) Dry the pellets.

16) Resuspend the pellets in 50 µl MilliQ water. Incubate with RNase A (Nippon Gene) for 4 h at 37°C and store at -20°C until further use.
17) The quality of the isolated DNA was monitored on a 1% agarose gel (2.2.4.2).

TE buffer

Tris-HCl, pH 8.0	10	mM
EDTA	1	mM

* The buffer was autoclaved and stored at RT.

CTAB/NaCl solution

Hexadecyltrimethyl ammonium bromide	10	%[w/v]
NaCl	0.7	M

* The buffer was prepared freshly and pre-incubated at 65°C prior to use.

2.2.4 Standard molecular biology techniques

2.2.4.1 Extraction of DNA from agarose gels

Wizard® SV Gel and PCR Clean-Up System (Promega Corporation) was routinely used for isolation of electrophoretically separated DNA fragments in the course of this work. After sufficient separation on an agarose gel and staining with ethidium bromide (2.2.4.2), the fragments of interest were cut with a sterile scalpel under UV light and placed in clean tubes. The DNA fragments were afterwards subjected to purification as recommended by the manufacturer.

2.2.4.2 Agarose gel electrophoresis

Analytical and preparative agarose gel elecrophoresis of DNA fragments was carried out in horizontal electrophoresis tanks (Mupid-α, Advance) using Agarose ME (Nacalai Tesque, Kyoto, Japan) and 1x TAE electrophoresis buffer. Samples were mixed with 10x Loading Dye (Takara Bio) and loaded in the wells of the gel. Electrophoresis was performed at 100V for 30-40 min. The gels were then stained with ethidium bromide (Nippon Gene) for 15 min, destained in dH_2O for 15 min, and visualized using FAS (Toyobo). One STEP marker 6 (Nippon Gene) DNA ladder and 100 bp maker (GeneDirex) were routinely used in the course of this study.

50x TAE buffer

Tris	242	g
EDTA (0.5M, pH 8.0)	50	ml
Glacial acetic acid	57	ml
dH_2O	up to 1000	ml

* The buffer was stored at RT and diluted to 1x before use.

2.2.5 Manipulation of nucleic acids

2.2.5.1 Primers

Primer design for PCR assays (2.2.5.4) was performed using the Primer3Plus online-based platform (http://www.bioinformatics.nl/cgi-bin/primer3plus/primer3plus.cgi/) and T_m values were calculated employing the OligoCalc software (http://biotools.nubic.northwestern.edu/OligoCalc.html). All oligonucleotides (Life Technologies, Japan) used in Chapter 2 are listed in Table 2-3.

Table 2-3 Oligonucleotide primers.

Primer	Sequence (5' → 3')*	Reference
Construction of lysine auxotrophic strains		
lysA1_del_up_F	GGATCCCTGGGCAAAGCGATCGATC	This study
lysA1_del_up_R	TCAGAGCGCTTTTGAAGCTAATTCGGGTCATGGTGGCGTTACTC	This study
lysA1_del_down_F	AGGAACTTCAAGATCCCCAATTCGTTTCTAAAGATCGCCCCTGG	This study
lysA1_del_down_R	AAGCTTACGAGTCCATGTATAGCTCCA	This study
Gm_lysA1_F	GAGTAACGCCACCATGACCCGAATTAGCTTCAAAAGCGCTCTGA	This study
Gm_lysA1_R	CCAGGGGCGATCTTTAGAAACGAATTGGGGATCTTGAAGTTCCT	This study
lysA1_verif_F	CGCGGTATCTGTTCGACTTC	This study
lysA1_verif_R	GCACAGTTCGAGGGTTTCTT	This study
lysA2_del_up_F	GGATCCCTGCGCAGAGGCTAAGCA	This study
lysA2_del_up_R	TCAGAGCGCTTTTGAAGCTAATTCGAAAGCGTTCATCTGGTTTCC	This study
lysA2_del_down_F	AGGAACTTCAAGATCCCCAATTCGCGAACTGTATGCTGGCGAAA	This study
lysA2_del_down_R	AAGCTTATGATGCCGCTCTTGGTTTC	This study
Gm_lysA2_F	GGAAACCAGATGAACGCTTTCGAATTAGCTTCAAAAGCGCTCTGA	This study
Gm_lysA2_F	TTTCGCCAGCATACAGTTCGCGAATTGGGGATCTTGAAGTTCCT	This study
lysA2_verif_F	CCTCGAAATTGGCTGCGTTA	This study
lysA2_verif_R	GGATTTCGGCAGGGATGAAG	This study
Confirmation of pCAR1 carriage		
carF_F	CGAAAGTAGCAATTATCGGGTCG	Takahashi *et al*., 2009a
carF_R	CGCCTTTCCTTTCGATGCTCCGCC	Takahashi *et al*., 2009a

* *Hin*dIII and *Bam*HI restriction sites are underlined. Overlapping sequences in primers used for construction of *lysA1* and *lysA2* deletion cassettes are highlighted in the same color (see Fig. 2-1).

2.2.5.2 Digestion with restriction endonucleases

All restriction endonucleases used in this chapter are listed in Table 2-4.

Table 2-4 Restriction endonucleases.

Restriction endonuclease	Target sequence	Buffer system (Takara Bio)
*Bam*HI	5′-G^G A T C C-3′ 3′-C C T A G^G-5′	1x Buffer K
*Hin*dIII	5′-A^A G C C T-3′ 3′-T T C G G^A-5′	1x Buffer K
*Eco*RV	5′-G A T^A T C-3′ 3′-C T A^T A G-5′	1x Buffer H

^ Indicates restriction sites.

2.2.5.3 Ligation

Ligation was performed using Ligation high Ver.2 (Toyobo) as recommended by the manufacturer.

2.2.5.4 PCR methods

Ex Taq DNA polymerase (Takara Bio) was routinely used for analytical PCR assays in the course of this study. PCR reactions contained the following components:

Template DNA	50-100	ng
Primer F (20 µM)	1	µl (0.4 µM final conc.)
Primer R (20 µM)	1	µl (0.4 µM final conc.)
dNTP mix (2.5 mM each)	4	µl
Ex Taq-Polymerase (5 U/µl)	0.25	µl
10x *Ex Taq* buffer	5	µl
MilliQ water	up to 50	µl

Amplification was performed using PCR Thermal Cycler Dice (Takara Bio) according to the following program:

Pre-denaturation	94°C	3	min	
Denaturation	98°C	10	s	30 cycles
Annealing	T_m (Primer) - 3°C	30	s	
Extension	72°C	1	min/kb	
Storage	4°C	∞		

Preparative PCR ampification was performed using KOD-Plus-Neo polymerase (Toyobo). PCR reactions contained the following components:

Template DNA	50-200	ng
Primer F (20 µM)	1	µl (0.4 µM final conc.)
Primer R (20 µM)	1	µl(0.4 µM final conc.)
dNTPs (2 mM)	5	µl
KOD-Plus-Neo (1 U/µl)	1	µl
10x Buffer for KOD-Plus-Neo	5	µl
$MgSO_4$ (25 mM)	3	µl
MilliQ water	up to 50	µl

Amplification was performed according to the following PCR program:

Pre-denaturation	94°C	2	min	
Denaturation	98°C	10	s	30 cycles
Annealing	T_m (Primer) - 3°C	30	s	
Extension	68°C	30	s/kb	
Storage	4°C	∞		

2.2.6 Construction of recombinant strains

2.2.6.1 Preparation of *E. coli* competent cells by $CaCl_2$ treatment

For transformation of *E. coli* DH5α and S17-1λ*pir*, cells were made competent according to Hanahan (1983, mod.).

1) Inoculate a single colony into 5 ml LB medium and grow the culture overnight at 37 °C.

2) Inoculate 100 ml fresh LB medium with 1 ml preculture and propagate the cells at 37 °C until an OD_{600} of 0.4-0.6.
3) Chill the culture on ice and pellet by centrifugation (5,000 rpm; 5 min; 4°C).
4) Rinse the tubes and the pellets with TFB I to remove traces of medium.
5) Resuspend the cell pellets gently in 40 ml ice-cold TFB I. Incubate for 5 min on ice.
6) Centrifugation (5,000 rpm; 5 min; 4°C). Discard the supernatants.
7) Resuspend the cell pellets in 4 ml ice-cold TFB II. Incubation for 60 min on ice.
8) Aliquot the cell suspension into sterile 1.5-ml tubes (100 µl) and flash-freeze in liquid N_2.
9) Store at -80°C.

TFB I (pH 5.8)

RbCl	100	mM
$MnCl_2$	50	mM
Potassium acetate	30	mM
$CaCl_2.H_2O$	10	mM
Glycerol	15	%[v/v]

* The pH value was adjusted with 0.2M acetic acid. The buffer was sterile filtered and stored at 4°C.

TFB II (pH 6.5)

MOPS	10	mM
RbCl	10	mM
$CaCl_2.H_2O$	10	mM
Glycerol	15	%[v/v]

* The pH value was adjusted with 1N NaCl. The buffer was sterile filtered and stored at 4°C.

2.2.6.2 Transformation into $CaCl_2$-competent *E. coli* cells

Transformation of $CaCl_2$-competent cells of *E. coli* was performed according to the following protocol.

1) Add plasmid DNA or ligation assay to 100 µl competent cells and incubate for 30 min on ice.
2) Perform heat shock at 42°C for 1 min.
3) Incubate for 3 min on ice.
4) Add 500 µl LB and incubate the cells for 1 h at 37°C with shaking (300 rpm).
5) Plate 100-200 µl of the cell suspension on LB agar plates supplemented with the appropriate antibiotics for selection and incubate overnight at 37°C.

2.2.6.3 Transformation of *P. putida* via conjugation (filter mating)

Transformation of *P. putida* cells was performed via conjugative transfer using *E. coli* S17-1 λ*pir* as a donor.

1) Grow cell of the donor and recipient overnight in 5 ml LB medium supplemented with the appropriate antibiotics for selection.
2) Pellet 1 ml culture of each strain by centrifugation (3,000 rpm; 5 min; RT).
3) Discard the supernatants and resuspend both pellets in 500 µl CF buffer.
4) Dispense the mixed culture onto a cellulose membrane filter (0.45 µm, Millipore) that had been placed on a LB agar plate.
5) After allowing the culture to dry into the filter, incubate the plate at 30°C for 16 h.

6) Transfer the filter into a 50-ml tube and suspend the culture with 500 µl CF buffer.
7) Prepare serial dilutions in CF buffer and plate 100 µl of each dilution on LB agar plates suppemented with the appropriate antibiotics for selection.

CF buffer

Na_2HPO_4	2.2	g
KH_2PO_4	0.8	g
NH_4NO_3	3	g
MilliQ water	up to 1000	ml

* The buffer was autoclaved and stored at RT.

2.2.7 Protein techniques

2.2.7.1 Determination of protein concentration

Protein concentrations in whole-cell (2.2.7.2) and cell-free protein extracts (2.2.8.3) were quantified by the method of Bradford (Bradford, 1976) using Protein Assay Dye Reagent Concentrate (Bio-Rad Laboratories, Hercules, CA). Appropriate dilutions (1:2 to 1:50) were prepared with MilliQ water and 20 µl from each dilution were mixed with 1 ml of 1:5 diluted Protein Assay Dye Reagent Concentrate in a 1-ml plastic single-use cuvette. After 5 min of incubation at RT, the absorbance at 595 nm wavelength was measured (Beckman Coulter DU800) against a blank made up of 20 µl MilliQ water and 1 ml reagent solution. The protein concentrations were estimated using a standard curve prepared with BSA (Bovine serum albumin, Bio-Rad) in the 0 mg/ml to 0.5 mg/ml range.

2.2.7.2 Preparation of whole-cell protein

Whole-cell protein was prepared as previously described (Sun *et al.*, 2017) with modifications. Cells of *P. putida* strains were collected by centrifugation (6,000 rpm; 5 min; 4°C) at the indicated time points and washed with ice-cold PBS buffer supplemented with 20 mM nicotinamide (Sigma Aldrich, class III or sirtuin KDAC inhibitor) and 10 mM sodium butyrate (Sigma Aldrich, class I, II KDAC inhibitor). The pellets were then flash frozen in liquid N_2 and stored at -80°C until further use.

1) Resuspend the pellets in 250 µl Buffer A. Incubation for 10 min on ice.
2) Add 50 µl Buffer B. Incubation for 20 min on ice.
3) Lysis: incubate the samples with 0.6% Nonidet-40 (Nacalai Tesque, Kyoto, Japan) and 100 µl Buffer C for 20 min on ice.
4) Supplement the lysates with 0.2M KCl, 0.01M $MgCl_2$, 10 µg RNase A, and 12.5 µg DNaseI (Sigma Aldrich). Incubation for 10 min at 37°C.
5) Sonication for 10 min (10 sec ON/30 sec OFF) using Bioruptor II, Cosmo Bio.
6) Protein concentration was determined using Protein Assay Dye Reagent Concentrate (Bio-Rad Laboratories, Hercules, CA) (2.2.7.1).

PBS buffer (pH 7.4)

NaCl	137	mM
KCl	2.7	mM
Na_2HPO_4	10	mM

KH_2PO_4	1.8	mM
Sodium butyrate	1	mM

* The buffer was autoclaved and stored at 4°C.

Buffer A

Tris-HCl (pH 8.1)	40	mM
Sucrose	25	%[w/v]
PMSF	1	mM
Nicotinamide (Sigma Aldrich)	2	mM
Sodium butyrate (Sigma Aldrich)	1	mM

* The buffer was sterile filtered and stored at 4°C.

Buffer B

Tris-HCl (pH 8.2)	40	mM
EDTA	10	mM
Lysozyme	1	mM

* The buffer was freshly prepared prior to use.

Buffer C

Tris-HCl (pH 8.2)	40	mM
EDTA	10	mM
Brij®58 (Sigma Aldrich)	1	%[w/v]
Sodium deoxycholate (Sigma Aldrich)	0.4	%[w/v]

* The buffer was stored at 4°C.

2.2.7.3 SDS-PAGE

Electrophoretic separation of proteins was performed on 13% polyacrylamide gels using Mini-PROTEAN® 3 Cell (Bio-Rad) according to the procedure of Laemmli (1970). The following solutions were used for preparation and running of the polyacrylamide gels:

4x Resolving gel buffer

Tris-HCl (pH 8.8)	1.5	M
SDS	0.4	%[w/v]

* The pH value was adjusted with 1N HCl and SDS was added after autoclavation.

4x Stacking gel buffer

Tris-HCl (pH 6.8)	0.5	M
SDS	0.4	%[w/v]

* The pH value was adjusted with 1N HCl and SDS was added after autoclavation.

2x SDS sample buffer

Tris-HCl (pH 6.8)	100	mM
Glycerol	20	%[v/v]
SDS	4	%[w/v]
DTT	200	mM

Bromophenol blue	0.2	%[w/v]

* Aliquots were stored at -20°C.

10x SDS Running buffer

Tris	0.25	M
Glycine	1.92	M
SDS	1	%[w/v]

* The buffer was stored at RT and diluted to 1x before use.

Resolving and stacking gels were prepared as indicated in Table 2-5. Protein samples were mixed with 2x Sample buffer, followed by denaturation for 5 min at 100°C. Running conditions were set at 10 mA/gel until the samples have entered the resolving gel and at 20 mA/gel for the rest of the run. The gels were afterwards rinsed twice with MilliQ water and proteins were visualized by staining with ready-to-use SimplyBlue™ SafeStain (Thermo Fisher Scientific) for 1h at RT. The gels were finally destained with MilliQ water for 2-3 hours at RT.

Table 2-5 Composition of SDS-PAGE gels used in this study.

Solution	13% Resolving gel*	4% Stacking gel*
40% Acryamide/Bis (37.1:1) (Bio-Rad)	3.25 ml	562 µl
4x Resolving gel buffer	2.5 ml	-
4x Stacking gel buffer	-	1.25 ml
10% [w/v] APS solution	100 µl	50 µl
TEMED	5 µl	5 µl
MilliQ water	4.2 ml	3.2 ml

* The indicated volumes were used for preparation of 2 gels.

2.2.7.4 Western blotting for detection of protein lysine acetylation and succinylation

Aliquots containing 70 µg of whole-cell protein (2.2.7.2) were loaded on a 13% glycine-SDS-PAGE gel (2.2.7.3) and transferred to a Sequi-Blot polyvinylidene difluoride (PVDF) membrane (Bio-Rad, Foster city, CA) at 4ºC for 12 h using a tank blotting system (Mini Trans-Blot® electrophoretic transfer cell, Bio-Rad). To set up the western blot, six pieces of Whatman filter paper (GE Healthcare) and a PVDF membrane were cut to the dimensions of the gel, followed by activation of the membrane for 1 min in methanol. The SDS-PAGE gels and the membrane were equillibrated for 15 min in Transfer buffer. Fiber pads and filter papers were soaked in Transfer buffer. The blotting sandwich was built up in the following order: a fiber pad, two Whatman filter papers, the PVDF membrane, the SDS-PAGE gel, two Whatman filter papers, and a fiber pad on top. Air bubbles captured between layers were removed by careful rolling with a clean reaction tube over the top of the membrane. The blotting tank was filled with Transfer buffer and a constant voltage of 30V was applied. Successful transfer of proteins onto the PVDF membrane was confirmed by staining of the gels with SimplyBlue™ SafeStain (Thermo Fisher Scientific) (2.2.7.3).

Transfer buffer

Glycine	192	mM
Tris	25	mM

* The buffer was sterile filtered and stored at 4°C.

The blot was blocked with 3% [w/v] skimmed milk (Nacalai Tesque, Kyoto, Japan) in TBST buffer, washed three times (5 min each) with TBST and incubated overnight at 4ºC with a combination of two commercial anti-acetyllysine antibodies (Cell Signaling Technology, #9441 and Rockland Immunochemicals Inc., #606-401-939) or anti-succinyllysine antibody (Kosono *et al*., 2015) at a 1:1000 dilution in TBST with 5% [w/v] bovine serum albumin (BSA). After three washing steps with TBST buffer, the blot was incubated with a goat horseradish peroxidase-conjugated anti-rabbit secondary antibody (Sigma Aldrich #A0545) at a 1:5000 dilution in TBST with 3% [w/v] skimmed milk for 1 h at room temperature. Finally, the blot was washed three times with TBST buffer, probed for 5 min with Immobilon Western Chemiluminescent HRP Substrate (Millipore, Billerica, MA) and then detected using an ImageQuant LAS 500 image analyzer (GE Healthcare).

TBST buffer

Tris	50	mM
NaCl	138	mM
Tween-20	0.05	%[v/v]

* The buffer was sterile filtered and stored at 4°C.

2.2.8 Quantitative proteome and acylome analyses

2.2.8.1 Preparation of lysine auxotrophic strains

For quantitative proteomic analyses of the pCAR1-free and -harbouring *P. putida* KT2440, lysine auxotrophic strains were constructed by a gene replacement system based on homologous recombination that incorporate suicide vectors, antibiotics resistance selection and sucrose counterselection (Choi and Schweizer, 2005). The basic strategy for generation of the mutant strains is illustrated on Fig. 2-1. The upstream and downstream regions of *lysA1* and *lysA2* genes were amplified using the primer pairs: lysA1_del_up_F/lysA1_del_up_R, lysA1_del_down_F/ lysA1_del_down_R, lysA2_del_up_F/ lysA2_del_up_R, and lysA2_del_ down_F/ lysA2_del_down_R, respectively, and KT2440 genomic DNA as template. Gm_lysA1_F/Gm_lysA1_R and Gm_lysA2_F/Gm_lysA2_R primers were used for amplification of the Gm^r cassette flanked by flippase recognition sites (FRT) from pPS856 (Hoang *et al*., 1998). 'A splicing by overlap extension' (SOE) PCR was then performed using the three partially overlapping fragments amplified in the first PCR round as templates. The resultant deletion cassettes were cloned into the *Eco*RV site of the pZErO-2^{TM} vector. The recombinant plasmid was introduced into *E. coli* DH5α for *in vivo* amplification. Transformants were plated on LB agar medium supplemented with Km and Gm and positive clones were identified by purified plasmid test digestion. After verification of their sequence, the fragments were excised using *Hin*dIII and *Bam*HI and subsequently cloned into the suicide vector pK19mobsacB (Schäfer *et al*., 1994) to yield pK19mobsacBΔlysA1 and pK19mobsacBΔlysA2,

respectively. Using *E. coli* S17-1 λ*pir* as a donor, pK19mobsacBΔlysA1 was introduced into KT2440 and KT2440(pCAR1) strains by conjugal transfer. The transconjugants resulting from a single-crossover event were selected on LB agar plates supplemented with Cm, Km and Gm. Double-crossover recombinants were obtained by *sacB*-mediated sucrose counterselection on LB agar plates supplemented with 10% sucrose in the presence of Gm. The Gm cassette was finally removed by Flp recombinase-catalyzed excision using the Flp-expressing pFLP2Km (Yun *et al*., 2010). pFLP2Km was introduced into the double-crossover recombinants by conjugal transfer using *E. coli* S17-1 λ*pir* as a donor. The transconjugants were selected on LB agar plates supplemented with Cm and Km and single colonies were screened for Gm sensitivity. Plasmid pFLP2Km was cured by growing Gm sensitive clones on LB agar plates supplemented with 10% sucrose and Cm. Loss of pFLP2Km was tested by screening of sucrose resistant colonies for Km sensitivity. KT2440L and KT2440L(pCAR1) double mutant strains were obtained in a second event of gene replacement by introduction of pK19mobsacBΔlysA2, followed by excision of the Gm cassette as described above. PCR analyses using genomic DNA were performed to verify the construction of the mutant strains.

2.2.8.2 Metabolic labeling and sampling

SILAC is a metabolic labeling strategy for quantitative proteomics, which relies on protein synthesis to incorporate stable isotope-containing amino acids such as lysine containing $^{13}C_6$ atoms (heavy isotope) into the proteome. Cells grown under different conditions or different strains to be compared are supplied with the natural light isotope of the amino acid and the heavy SILAC isotope, respectively. Thereby, this method creates two versions of each peptide, and the ratio of the areas of the MS peaks associated with those peptides is proportional to the difference in their abundance between both states that are to be compared (Fig. 2-2). Metabolic labeling of *P. putida* KT2440L and *P. putida* KT2440L(pCAR1) lysine auxotrophic strains was carried out according to the scheme illustrated in Fig. 2-3. Cells of both strains were grown for 3 days at 30°C on NMM-4 plates supplemented with 0.1% [w/v] glucose as the sole carbon source and 50 µg/ml $^{12}C_6$-lysine ('light' lysine) or $^{13}C_6$-lysine ('heavy' lysine; Cambridge Isotope Laboratories, Inc.). Single colonies were then inoculated into fresh NMM-4 medium containing 0.4% [w/v] glucose and 'light' lysine or 'heavy' lysine for pre-cultivation. The main cultures were grown in 400 ml NMM-4 medium supplemented with 0.2% [w/v] succinate and the pCAR1-free and pCAR1-harbouring strains were labeled with 'light' and 'heavy' lysine, respectively. At the indicated time points in the log and stationary phases 250 ml and 150 ml cells, respectively, were harvested by centrifugation (6,000 rpm; 5 min; 4°C), washed with 5 ml PBS buffer supplemented with 20 mM nicotinamide (Sigma Aldrich, class III or sirtuin KDAC inhibitor) and 10 mM sodium butyrate (Sigma Aldrich, class I, II KDAC inhibitor), flash frozen in liquid N_2 and stored at -80°C until further processing.

2.2.8.3 Preparation of cell-free protein extracts

Cells were resuspended in NET buffer supplemented with 1 mM PMSF, 1 mM DTT, 2 mM nicotinamide, 1 mM sodium butyrate, 10 µg/ml DNaseI (Sigma Aldrich), and 10 µg/ml RNase A (Nippon Gene), disrupted by sonication for 10 min (10 sec ON/30 sec OFF) (Bioruptor II, Cosmo Bio) and clarified by

centrifugation (15,000 rpm; 15 min; 4°C). After filtration of the samples through a 0.45-µm filter (Nanosep® MF GHP, Pall Life Sciences), protein concentration was measured by Protein Assay Dye Reagent (Bio-Rad Laboratories, Hercules, CA) (2.2.7.1).

NET buffer

Tris-HCl (pH 7.6)	50	mM
NaCl	150	mM
EDTA	1	mM

* The buffer was sterile filtered and stored at RT.

2.2.8.4 Preparation of samples for HPLC-MS/MS analysis. Tryptic digestion and enrichment of acetylated and succinylated peptides

Total proteome

To estimate modifications in the total proteome associated with pCAR1 carriage, aliquots containing 25 µg of cell-free protein extract from *P. putida* KT2440L and KT2440L(pCAR1) strains grown to the log and stationary phases, respectively, were mixed and treated according to the following protocol:

1) Add 10 µl LC/MS grade acetonitrile (Fisher Scientific) to each sample.
2) Add 2 µl 1M DTT (Nacalai Tesque, Kyoto, Japan) and incubate at 56°C in a water bath for 30 min.
3) Add 10 µl 333 mM iodoacetamide (Nacalai Tesque, Kyoto, Japan) and incubate for 60 min at 37°C in the dark.
4) Incubate the samples with 0.3 µl (300 ng) mass spectrometry grade Trypsin Gold (Promega, Fitchburg, WI, USA) at a 1:100 enzyme:substrate ratio [w/v] overnight at 37°C in the dark.
5) Add 1 µl TFA (trifluoroacetic acid) to each sample.
6) Concentrate the samples to about 10 µl using centrifugal concentrator (TOMY, CC-105) (Heat Low; air ON).
7) Store at -20°C and subject to nano HPLC-MS/MS analysis.

Acetylome and succinylome

For characterization and quantification of the acetylome and succinylome of the pCAR1-free and pCAR1-harbouring strains, equal amounts of protein (5-7 mg) from both strains were mixed and handled according to the following protocol:

I. Acetone precipitation and tryptic digestion

1) Precipitate the protein samples with 4 Vol. of ice-cold acetone at -20°C for at least 2h.
2) Centrifugation in high speed Falcon tubes (10,000 rpm; 10 min; 4°C). Discard the supernatants carefully.
3) Add 20 ml 70% ice-cold acetone.
4) Centrifugation in high speed Falcon tubes (10,000 rpm; 10 min; 4°C). Discard the supernatants carefully.
5) Add 20 ml 100% ice-cold acetone.
6) Centrifugation in high speed Falcon tubes (9,500 rpm; 10 min; 4°C). Discard the supernatants carefully.
7) Repeat steps 5) and 6).

8) Dry the pellets on air (care should be taken not to let the pellets dry completely as it will decrease their solubility).
9) Add 0.9 ml 0.1M NH_4HCO_3 (Sigma Aldrich, ≥99%) and dissolve the pellets carefully with a homogenization stick.
10) Add 0.1 ml LC/MS grade acetonitrile (Fisher Scientific).
11) Add 20 µl 1M DTT (20 mM final conc.) and incubate the samples at 56°C in a water bath for 30 min.
12) Add 100 µl 333 mM iodoacetamide (30 mM final conc.), cover the tubes with aluminium foil and incubate for 30 min at 37°C in the dark.
13) Incubate the samples with mass spectrometry grade Trypsin Gold (Promega, Fitchburg, WI, USA) at a 1:100 enzyme:substrate ratio [w/w] for 16h at 37°C in the dark.
14) Incubate the samples with Trypsin Gold at a 1:200 enzyme:substrate ratio [w/w] for 4h at 37°C in the dark.

II. Incubation with anti-acetyllysine and anti-succinyllysine antibodies

1) Centrifugation (10,000 rpm; 2 min; 4°C) to remove the insoluble precipitates.
2) Transfer the soluble phase into 1.5-ml low-protein-binding tubes (APRO cat# PT 2001).
3) Centrifugation (10,000 rpm; 2 min; 4°C). Transfer the samples into 1.5-ml low-protein-binding tubes.
4) Concentrate the samples to about 50 µl using centrifugal concentrator (TOMY, CC-105) (Heat Low; air ON).
5) Add 500 µl NETN buffer and mix thorougly.
6) Enrichment of acetylated and succinylated peptides by incubation with a combination of two commercial anti-acetyllysine antibodies (Cell Signaling Technology, #9441 and Rockland Immunochemicals Inc., #606-401-939) and pan-anti-succinyllysine antibody (Kosono *et al*., 2015), respectively, at a 1:100 antibody:substrate ratio overnight at 4°C.

III. Immunoprecipitation using Protein G magnetic beads (Thermo Fisher Scientific)

1) Pipet 250 µl magnetic beads per 50 µg antibody into 1.5-ml low-protein-binding tubes.
2) Equillibrate the beads with 500 µl NETN buffer (500 rpm flash→magnet).
3) Repeat step 2).
4) Add the peptide samples and incubate at 4°C under constant rotation for at least 2h.
5) Wash the beads 3 times with 500 µl NETN buffer (500 rpm flash→magnet).
6) Wash the beads 3 times with 500 µl NET buffer (500 rpm flash→magnet).
7) Wash the beads once with 500 µl MilliQ water (500 rpm flash→magnet).
8) Elution: add 50 µl 0.1% TFA and incubate for 5 min at RT (500 rpm flash→magnet). Place the 50 µl sample into a new 1.5-ml low-protein-binding tube.
9) Repeat step 8) for a total of 150 µl.
10) Add 20 µl MS grade acetonitrile and pipet thoroughly.
11) Concentrate the samples to about 20 µl using centrifugal concentrator (TOMY, CC-105) (Heat Low; air ON).

IV. Purification and concentration of the samples using ZipTip-scx microtips (Millipore)

1) Attach a ZipTip to a 20 µl pipette and adjust the volume to 20 µl.
2) Equillibration: withdraw Wash buffer slowly through the ZipTip and pipet out carefully (repeat at least 3 times).
3) Binding: withdraw the peptide samples slowly and pipet out carefully (repeat at least 10 times).

4) Washing: withdraw Wash buffer slowly and pipet out in a separate tube (repeat at least 10 times).
5) Elution: pipet 5 µl Elution buffer into a new 1.5-ml low-protein-binding tube. Slowly withdraw and pipet out (repeat at least 10 times).
6) Repeat steps 1) to 5) twice more for a total volume of 15 µl.
7) Store at -20°C and subject to nano HPLC-MS/MS analysis.

NETN buffer

Tris-HCl (pH 7.6)	50	mM
NaCl	150	mM
EDTA	1	mM
Nonidet P-40	0.1	% [v/v]

* The buffer was sterile filtered and stored at RT.

Wash buffer (12 ml)

TFA	12	µl
Methanol	3.6	ml
MilliQ water	8.4	ml

* The buffer was dispensed into 1.5-ml tubes. For each washing step a new tube was used (3 tubes per sample).

Elution buffer (1 ml)

NH_4OH	170	µl
Methanol	300	µl
MilliQ water	530	µl

Two independent biological experiments (ex1 and ex2) were performed with log and stationary phase cells for the proteome, acetylome and succinylome analyses: a single replicate for ex1 (ex1-log and ex1-stat) and analytical duplicates for ex2 (ex2-log-n1, ex2-log-n2, ex2-stat-n1 and ex2-stat-n2).

2.2.8.5 Mass spectrometry analysis and peptide identification

Total proteome, acetyllysine and succinyllysine enriched peptide samples were analysed by reverse-phase nano HPLC-MS/MS using an EASY-nLC 1000 HPLC system connected to a Q Exactive mass spectrometer (Thermo Fisher Scientific, Waltham, MA, USA) as previously described (Kosono *et al*., 2015). The acquired MS raw data were processed using Proteome Discoverer (Ver.1.4; Thermo Fisher Scientific). For identification, data were searched against *P. putida* KT2440 and pCAR1 protein sequence databases (NC_002947 and NC_011838) using the MASCOT search engine (Ver. 2.5.1). The search parameters were set to allow for up to two missed cleavages. Carbamidomethylation on cysteine was specified as a fixed modification and variable modifications included $^{13}C_6$-labeled lysine, methionine oxidation, acetylation (lysine and protein N-terminus) for the acetylome and succinylation (lysine and N-terminus) for the succinylome. Precursor ion and fragment mass tolerance were set to 6 ppm and 20 mmu, respectively. To ensure high stringency of the MS data, false discovery rate (FDR) threshold for peptide identification was set at less than 1% and validated by the Percolator algorithm. For protein identification, only proteins with Mascot ion score greater than 60 and coverage (percentage of the protein sequence

covered by the identified peptides) greater than 10% were regarded as confident identifications and subjected to further analysis.

2.2.8.6 SILAC quantification

Quantification was performed based on SILAC heavy/light ratio of the peak area for each peptide in the pCAR1-free and pCAR1-harbouring strain. Peptide ratios were calculated using the same number of isotopes (two or more). Protein ratios were calculated based on previously reported algorithm (Silva *et al*., 2006). Quantitative evaluation of acyl modifications was performed based on the R-value, which was calculated from the SILAC heavy/light ratio of the peptide peak area, normalized to the ratio of the protein area. In case multiple peptides with identical lysine modification were detected, the peptide with the highest Mascot ion score was chosen. The mass spectrometry data have been deposited to the ProteomeXchange Consortium (http://proteomecentral. proteomexchange.org) via the PRIDE partner repository (Vizcaino *et al*., 2016) with the dataset identifier PXD007089 and PXD007133 for ex1, and PXD007722 and PXD007090 for ex2.

2.2.9 Bioinformatic analyses

For protein functional annotation Kyoto Encyclopedia of Genes and Genome (KEGG) pathway database was employed. Functional enrichment analyses were performed using the Database for Annotation, Visualization, and Integrated Discovery (DAVID) (Huang *et al*., 2009). Motif analysis of the lysine acetylation and succinylation amino acid sequence context was conducted using the obtained MS data. Sequences encompassing 21 amino acids, which represent 10 amino acids on either side of each modification site were analyzed and a consensus logo was generated using the motif-X webserver (Schwartz and Gygi, 2005).

2.3 Results and Discussion

2.3.1 Generation and phenotypic verification of *P. putida* KT2440 and KT2440(pCAR1) lysine auxotrophic strains

To facilitate SILAC labeling for the quantitative proteomic analysis, lysine auxotrophic strains were generated by deletion of *lysA* encoding diaminopimelate decarboxylase, which catalyzes the final step in the biosynthesis of lysine. The genome of *P. putida* KT2440 revealed two *lysA* genes, *lysA1* (PP_2077) and *lysA2* (PP_5227) (Fig. 2-4) (Nelson *et al*., 2002). PP_2077 and PP_5227 showed 60% and 33% amino acid identity to the diaminopimeate decarboxylase from *E. coli*, respectively, and 32% amino acid identity between each other. KT2440L and KT2440L(pCAR1) double deletion mutants were obtained by two consecutive events of gene replacement (2.2.8.1). In order to avoid polar effects on downstream genes, the deletion of *lysA2* left the first 3 and the last 12 codons. Confirmation of gene deletion was carried out by PCR using the primer pairs: lysA1_verif_F/ lysA1_verif_R and lysA2_verif_F/lysA2_verif_R, respectively, and genomic DNA extracted from four representative mutant clones and the corresponding parental strains (Fig. 2-5 A and B). The *car* operon in pCAR1 is flanked by the insertion sequences ISPre1 and ISPre2 (Nojiri, 2001). Previous reports demonstrated that a population deficient for the *car* operon could arise as a result of homologous recombination between the two ISs (Takahashi *et al*., 2009a). Therefore, carriage of pCAR1 plasmid in the KT2440L(pCAR1) strain was verified by PCR amplification of the CarF (acetadehyde dehydrogenase) encoding gene employing the primer pair carF_F/carF_R (Fig. 2-5 C). Furthermore, the presence of an intact *car* gene cluster was demonstrated by formation of clear zones on NMM-4 agar plates supplemented with 0.1% carbazole as the sole carbon source (Fig. 2-5 C).

To confirm their phenotype, KT2440L and KT2440L(pCAR1) were grown on NMM-4 succinate agar plates with and without L-lysine supplementation. In contrast to the Δ*lysA1* and Δ*lysA2* single-deletion mutants, KT2440L and KT2440L(pCAR1) were not able to grow in the absence of L-Lysine (Fig. 2-6). Addition of 50 µg/ml L-lysine to liquid NMM-4 succinate medium was determined to be sufficient to restore the growth rate of the mutants to that of their parental strains (Fig. 2-7). Therefore, this concentration was employed for further experiments.

2.3.2 Experimental workflow

Comparative analysis at various time points of the growth demonstrated that the transcriptional alterations in *P. putida* KT2440 invoked by pCAR1 are most pronounced in the transition and early stationary phases (Takahashi *et al*., 2015). These results suggested that the effect of pCAR1 is related to the physiological status of the host cell. Therefore, in this study proteome profiles of the pCAR1-free and pCAR1-harbouring strains were compared using actively growing, exponential phase cells and early stationary phase cells. In order to ensure maximum incorporation of isotopic lysine into the proteome, the lysine auxotrophic strains were adapted on medium supplemented with 'light' and 'heavy' lysine, respectively (2.2.8.2 and Fig. 2-3). The experimental workflow and sampling points are illustrated on Fig.

2-8. For total proteome profiling, equal amounts of cell-free protein extract from both strains were mixed, digested with trypsin and subjected to MS analysis (2.2.8.4). Global acylome analysis was performed by affinity enrichment of acetylated and succinylated peptides from the total tryptic peptide pool using anti-acetyllysine and anti-succinyllysine antibodies, respectively (2.2.8.4). The incorporation level of 'heavy' lysine was monitored by examining the percentage of lysine labeled peptides versus all possible labeling targets using total trypsinized peptides from log and stationary phase cells of KT2440L(pCAR1) (Table 2-6). The corresponding SILAC labeling efficiencies were estimated to be above 99%. The proteomic data in this study were acquired from two independent biological experiments (ex1 and ex2) and samples were analysed in a single replicate for ex1 and analytical replicates for ex2 (ex2-n1 and ex2-n2) yielding a total of 6 datasets: 3 datasets from the log (ex1-log, ex2-log-n1 and ex2-log-n2) and 3 datasets from the stationary phase (ex1-stat, ex2-stat-n1 and ex2-stat-n2).

2.3.3 Proteome profiling of the pCAR1-free and -harbouring strains

In total, 1,592 distinct proteins were identified in the pCAR1-free and -harbouring strains. Among them, 835 and 1,259 proteins were reproducibly detected in at least two of the three datasets in the log and stationary phases, respectively (Fig. 2-9 A). Those were defined as the proteome in each growth state (Fig. 2-9 B). Among them, 40 proteins were unique to the log phase; 464 proteins were unique to the stationary phase and 795 proteins were detected in both growth phases. Highly produced pCAR1-encoded proteins and the dynamic reshaping of the host proteome by pCAR1 carriage were determined.

2.3.3.1 Identification of pCAR1-encoded proteins

It has been suggested that the expression level of plasmid-encoded proteins represents one of the major factors for loss of host fitness. Seventy-four transcriptional units encompassing 201 putative open reading frames (ORFs) have been previously identified on the pCAR1 plasmid (Miyakoshi *et al*., 2009; Shintani *et al*., 2011; Takahashi *et al*., 2015). Similarly to the effects of plasmid carriage on the transcriptional network of the host, expression of genes on the pCAR1 plasmid is differentially affected by different host backgrounds and 86% of the ORFs were shown to be actively transcribed in *P. putida* KT2440 grown in minimal succinate medium (Shintani *et al*., 2011). Under the culture conditions used in the present study, 20 distinct pCAR1-encoded proteins were identified (Table 2-7), corresponding to 10% of the number of predicted ORFs. Among them, 8 proteins were reproducible. Due to the bias of MS analysis to detect abundant proteins more often than low-abundance proteins, the most highly abundant soluble pCAR1-encoded proteins were expected to be sampled. The function of numerous genes carried on plasmids has not been elucidated. A large portion of the ORFs on pCAR1 (91/201, 45%) code for hypothetical proteins. Therefore, global approaches coupled with functional characterization are necessary in order to capture plasmid-encoded proteins with novel functionality. Notably, along with proteins involved in core and accessory functions, including partitioning (ParA, ParB and ParC), and carbazole degradation (CarAc, CarBb, CarC and CarF), 8 pCAR1-encoded proteins were detected, which could be classified now as uncharacterized and might play an important role in the functional interaction with the host. Among them, 5 proteins (ORF67, ORF76, ORF77, ORF111, ORF159a) were conserved in at least one of the other

sequenced IncP-7 plasmids, including the naphthalene-catabolic plasmid pND6-1 (Li *et al*., 2012), and the TOL plasmids pWW53 and pDK1 (Yano *et al*., 2007; 2010).

2.3.3.2 Remodeling of the proteome of the host by pCAR1 carriage

Among all identified proteins in this study, 1,572 were encoded on the chromosome, which reflects 29% of the 5,507 predicted ORFs from the genome sequence of *P. putida* KT2440 after removal of pseudogenes and non-coding RNAs. Among the reproducibly detected proteins (Fig. 2-9), those that exhibited a fold change in abundance of at least two (≥ 2 or ≤ 0.5) in all three datasets obtained from either growth state were defined as differentially regulated by carriage of pCAR1. A total of 7 proteins (1 in the log phase and 7 in the stationary phase) were found to be significantly induced and a total of 151 proteins (51 in the log phase and 119 in the stationary phase) were significantly downregulated (Table 2-8).

2.3.3.3 Proteins with increased abundance by pCAR1 carriage

Most notably induced in the presence of pCAR1 was the multidrug RND transporter MexF (PP_3426) (above 70-fold increase in abundance in the stationary phase). These results are in line with the transcriptomic profiling analyses, which showed a strong induction of the *mexEF-oprN* operon, encoding an efflux system, in *P. putida* KT2440 upon carriage of pCAR1 (Shintani *et al*., 2010; Takahashi *et al*., 2015). MexT, a LysR-type transcriptional regulator, has been demonstrated to positively regulate the expression of the *mexEF-oprN* operon (Tian *et al*., 2009). However, the transcriptional level of *mexT* (PP_2826) in *P. putida* KT2440 did not change due to carriage of pCAR1 (Shintani *et al*., 2010; Takahashi *et al*., 2015). The MexT protein could not be detected and quantified in this study, probably due to its low intracellular level. Thus, the mechanism of MexT activation by pCAR1 harbouring remains unclear. Significantly upregulated in the log phase was PP_3099, a homologue of TssC1 protein, which is involved in type VI secretion system (T6SS), demonstrated to be functional in *P. putida* KT2440 in a recent study (Bernal *et al*., 2017). Furthermore, glycine dehydrogenase (PP_0988), heme oxygenase (PP_1005), a putative ABC transporter ATP-binding protein (PP_1895), a homologue of ClpV ATPase (PP_3095) involved in T6SS and a putative large subunit of acetolactate synthase (PP_3365) displayed increased abundance in the stationary phase. Given that a homologue of PP_1895 in *P. aeruginosa* PAO1 (PA2812) was previously reported as a direct target of MexT activation (Tian *et al*., 2009), a similar pattern of regulation might be expected in *P. putida* KT2440. Comparison with the previous transcriptome data (Shintani *et al*., 2010; Takahashi *et al*., 2015) showed that the transcript level of all upregulated proteins except for PP_3095 was significantly elevated in the pCAR1-containing strain. Thus, the increased abundance of this protein could be attributed to post-translational regulation or protein stabilities that exceed mRNA stabilities.

Taken together, these results suggested that elevated production of components of the MexT regulon, T6SS and the iron deprivation response set might have contributed substantially to the increased translational and energy demand associated with pCAR1 carriage in *P. putida* KT2440.

2.3.3.4 Proteins with reduced abundance by pCAR1 carriage

In order to gain further insight into the cellular processes affected at proteome level by carriage of pCAR1 in the host, functional classification analysis of the proteins with decreased abundance was conducted using the Kyoto Encycopedia of Genes and Genomes (KEGG) pathway database (Fig. 2-10). Among the proteins that could be assigned to at least one functional category, the largest groups were represented by amino acid metabolism (15 proteins, 9.9% of the number of downegulated proteins), followed by signal transduction and motility (14 proteins, 9.3%), carbohydrate metabolism (10 proteins, 6.6%) and nucleotide metabolism (8 proteins, 5.3%). These results suggested that the adaptive reshaping of the proteome of the host associated with pCAR1 carriage was reflected by differential regulation of proteins for cell energy management. Notably, only in a few cases, a direct correlation between the proteome and the previous transcriptome profiling data (Shintani *et al*., 2010; Takahashi *et al*., 2015) was observed. Out of 151 proteins with decreased abundance in both growth phases, 10 were found also to be significantly downregulated (more than twofold) at transcriptional level (see Table 2-8).

2.3.3.5 Modifications in metabolism

Carriage of pCAR1 reduced the abundance of various proteins involved in metabolic processes (Table 2-8). Carriage of pCAR1 reduced the respiration activities for intermediate metabolites of the tricarboxylic acid (TCA) cycle and those several steps away from the TCA cycle (acetic acid and L-lactic acid), as well as utilization of a number of amino acids in the host cells (Takahashi *et al*., 2015). In this study, proteins related to the TCA cycle (aconitase, PP_2112 and isocitrate dehydrogenase, PP_4011), glycolysis/gluconeogenesis (glyceradehyde-3-phosphate dehydrogenase, PP_3443), acetate metabolism (acetyl-CoA synthetase, PP_4487) and amino acid metabolism (Table 2-8) were reduced in abundance by pCAR1 carriage. Furthermore, the β and ε subunits of the ATP synthase (PP_5412 and PP_5414) were significantly downregulated.

2.3.3.6 Alterations in the motility apparatus

The quantitative proteomic analysis in this study revealed reduced accumulation of flagellum components including flagellin encoded by *fliC* (PP_4378), flagellar cap encoded by *fliD* (PP_4376), and the flagellar motor complex protein MotB (PP_4904) in the pCAR1-containing strain. Furthermore, the amounts of several proteins involved in chemotaxis were decreased (Table 2-8). Assembly and rotation of the flagella are energy-demanding processes. In *E. coli*, the biosynthesis of the flagellum consumes about 2% of the cellular metabolic resources (Macnab, 1996). Therefore, repression of the motility apparatus might provide a means to ameliorate the metabolic burden associated with pCAR1 carriage by redirecting energy and reducing power and thus improving survival under stress.

2.3.3.7 Oxidative stress response and iron metabolism

In addition to proteins related to metabolism and motility, proteins involved in oxidative stress response were present at lower levels in the pCAR1-containing strain, including superoxide dismutase (SodB, PP_0915), catalase/peroxidase (KatB, PP_3668) and alkyl hydroxyperoxidase (AhpC, PP_2439).

Expression of KatB and AhpC in *P. putida* KT2440 is controlled by OxyR, which senses intracellular oxidative species (Hishinuma *et al*., 2006) and regulation of superoxide dismutase in *P. aeruginosa* is mediated by the ferric uptake regulator (Fur) (Vasil, 2007). Futhermore, bacterioferritin encoded by *bfr*α (PP_0482) and *bfr*β (PP_1082) were downregulated. Carriage of pCAR1 resulted in iron deficiency in the host, in part due to constitutive expression of iron-containing carbazole-degrading enzymes (Shintani *et al*., 2010). Therefore, decreased abundance of the proteins involved in oxidative stress defence and iron storage could be explained by the iron shortage, as well as the reduced metabolism in the host cell as a consequence of pCAR1 carriage.

2.3.3.8 Differential expression of NAPs

As described in the introduction part, comprehensive transcriptome and phenotypic analyses of single gene mutants and double gene mutants of the three pCAR1-encoded NAPs (Pmr, Phu and Pnd) demonstrated that these proteins are key determinants of the transcriptional networks in pCAR1-harbouring host cells (Suzuki-Minakuchi *et al*., 2015). The proteome data in this study showed that several NAPs encoded on the chromosome, including the HU proteins HupA (PP_5313) and HupN (PP_0975), and NdpA (PP_0973), were downregulated in the pCAR1-harbouring strain, suggesting that carriage of pCAR1 might result in additional modifications in the composition of the nucleoid in the host.

2.3.4 Detection of lysine acyl-modifications in the pCAR1-free and -harbouring strains

To evaluate the relative abundance of protein lysine acetylation and succinylation in the proteome of the pCAR1-free and -harbouring strains, whole-cell protein from KT2440 and KT2440(pCAR1) cells grown to the log and early stationary phases, respectively, was subjected to western blot analysis using anti-acetyllysine and anti-succinyllysine antibodies (Fig. 2-11). These results provided evidence that protein lysine acetylation and succinylation commonly occur in *P. putida* KT2440 and KT2440(pCAR1) under the culture conditions employed in this study.

To gain a detailed view of the potential role of acetylation and succinylation events in *P. putida* KT2440 and in the plasmid-host functional interaction, acylated proteins and the specific modification sites were determined in the pCAR1-free and pCAR1-containing lysine auxotroph strains by selective enrichment of acetylated and succinylated peptides followed by MS analysis. In order to ensure that the observed differences occur irrespective of changes in protein abundance, the differences in acyl modifications at the individual sites between both strains were assessed by estimating the R-value, which was calculated from the ratio of peptide peak areas (SILAC ratios) normalized to the ratio of protein abundance (2.2.8.6).

2.3.5 Acetylome and succinylome of the pCAR1-free and -harbouring strains

2.3.5.1 Overview

In total, 1,359 unique acetyl lysine sites occurring on 637 proteins were detected in both strains investigated. Among them, 1,344 sites were identified on 627 proteins encoded on the chromosome of the host and 15 sites were detected on 10 proteins encoded on the pCAR1 plasmid (50% of the detected total

pCAR1 proteome). To examine the cellular functions that can be potentially affected by lysine acetylation, all identified acetylated proteins were classified based on the KEGG pathway database (Fig. 2-12 A). Most abundant groups were represented by proteins involved in translation (69 proteins, 10.8% of the total), amino acid metabolism (68 proteins, 10.7%), and carbohyrate metabolism (59 proteins, 9.3%). Although a direct comparison cannot be made due to different genetic background and growth conditions, a report from *P. aeruginosa* PA14 identified 320 acetylated proteins predominantly involved in energy metabolism and amino acid metabolism (Ouidir *et al*., 2015). Previous studies demonstrated that lysine acetylation frequently targets proteins involved in central metabolic processes in bacteria (Wang *et al*., 2010; Guan and Xiong, 2011; Hirschey and Zhao, 2015; Kosono *et al*., 2015; Mizuno *et al*., 2016). Similarly, many enzymes involved in glycolysis, gluconeogenesis and the TCA cycle were found to be acetylated in this study. Assessment of the distribution of acetylation sites per proteins showed that 46% of the acetylated proteins were modified at two or more sites and several proteins were found to be heavily acetylated, including heat-shock protein 90 (PP_4179, 21 sites), molecular chaperone DnaK (PP_4727, 18 sites), DNA-directed RNA polymerase β' (PP_0448, 18 sites), and elongation factor G (PP_0451, 14 sites).

The succinylome analysis of the pCAR1-free and pCAR1-harbouring strains revealed 567 unique succinylation sites occurring on 259 proteins: 565 sites on 257 proteins encoded on the chromosome of the host and 2 sites on 2 pCAR1-encoded proteins. Functional classification of the succinylated proteins demonstrated that the cellular processes predominantly targeted by lysine succinylation are translation (51 proteins, 19.7% of the total), carbohydrate metabolism (31 proteins, 12.0%) and amino acid metabolism (29 proteins, 21.6%) (Fig. 2-12 A). Analysis of the distribution of the succinylation sites per protein showed that 44.7% of the succinylated proteins were modified at more than one site. The most heavily succinylated proteins were chaperone DnaK (PP_4727, 16 sites), chaperone GroEL (PP_1361, 14 sites), elongation factor G (PP_0451, 13 sites), and 30S ribosomal protein S1 (PP_1772, 12 sites).

2.3.5.2 Overlap between acetylome and succinylome

Lysine residues in bacteria are a subject of wide range of acyl modifications. Previous global proteomic studies raised the possibility of cross-talk between acetylation and succinylation in bacteria (Colak *et al*., 2013; Pan *et al*., 2014; Kosono *et al*., 2015; Pan *et al*., 2015; Mizuno *et al*., 2016). Therefore, the acetylome and succinylome data obtained in this study was compared. Although both modifications targeted similar functional categories (Fig. 2-12 A), the extent of overlap was limited (Fig. 2-12 B). Only 244 sites (43% of the detected succinylome) were shared between the acetylome and succinylome. The degree of overlap between both acyl modifications was lower than that reported for *E. coli* (66% of the detected succinylome overlapped with the acetylome) (Weinert *et al*., 2013b), and comparable with reports from *Bacillus subtilis* (35%) (Kosono *et al*., 2015) and *Corynebacterium glutamicum* (37%) (Mizuno *et al*., 2016). Overlapping sites were mainly detected in proteins associated with the ribosome (51 sites on 31 proteins), carbohydrate metabolism (23 sites on 15 proteins), and amino acid metabolism (24 sites on 14 proteins).

2.3.5.3 Amino acid context of lysine acetylation and succinylation

To examine the possibility for a specific acetylation and succinylation pattern, the amino acid sequences surrounding the modified lysines from position -10 to position +10 were analyzed by using the motif-X program (2.2.9). Survey of the flanking regions of the identified acetylation sites revealed overrepresentation of aspartate (D), leucine (L), and phenylalanine residues (F) (Fig. 2-13 A). The high prevalence for acidic and aromatic residues in the proximity of acetyl lysine sites was consistent with previously reported global acetylome analyses in diverse bacteria (Kuhn *et al*., 2014; AbouElfetouh *et al*., 2015; Kosono *et al*., 2015) as well as in mitochondria (Lundby *et al*., 2012). It has been suggested that these motifs might serve as a recognition signature for acetyltransferases and deacetylases, or might facilitate non-enzymatic acetylation events. However, the existence of specific determinants for protein acetylation has not been rigorously explored.

Analysis of the amino acid sequences surrounding the identified succinyllysine sites revealed only a weak preference for alanine (A), in contrast to the pattern derived from the local sequence context of lysine acetylation (Fig. 2-13 B). These results were different from the succinylomes of *E. coli* (Colak *et al*., 2013), *B. subtilis* (Kosono *et al*., 2015) and *Mycobacterium tuberculosis* (Yang *et al*., 2015; Xie *et al*., 2016), which showed a strong bias for charged amino acids in the vicinity of the succinylated lysines.

Only the partial overlap between the acetylome and succinylome detected in this study and the differences in amino acid sequence context in the proximity of the acetylation and succinylation sites suggested that these two acyl modifications occur by distinct mechanisms in *P. putida* KT2440.

2.3.5.4 Acetylome and succinylome in the log and stationary phases

Of 1,359 acetylation sites, 415 and 522 sites were reproducibly identified in at least two of the three datasets from the log and stationary phases, respectively. Those were defined as the acetylome in each growth state (Fig. 2-14 A). Although no dramatic change in the overall acetylation level was observed, as demonstrated also by the western blot analysis (Fig. 2-11), the extent of overlap between acetylated sites in both growth phases was limited (Fig. 2-14 B). These differences in the protein acetylation pattern suggested the potential for dynamic regulation. In order to identify the pathways that might be influenced by acetylation, enrichment analysis of the acetylated proteins from the log and stationary phases was carried out using DAVID (Huang *et al*., 2009) and the KEGG database (Table 2-9). Proteins involved in the ribosome were enriched in the acetylome from both growth states, whereas categories related to different metabolic pathways were specifically targeted in the stationary phase.

Of 567 unique succinylation sites, 224 and 107 sites reproducibly detected in the log and stationary phases, respectively, were defined as the succinylome in each growth state (Fig. 2-15 A). Although the extent of protein succinylation was similar, the succinylation pattern differed (Fig. 2-15 B), suggesting temporal regulation. To reveal the biological processes that could be potentially affected in a growth-stage-dependent manner, enrichment analysis of the two succinylome datasets against the detected proteomes in the log and stationary phases was performed (Table 2-10). In both growth states, succinylated proteins were significantly enriched in the category ribosome, whereas succinylation in the log phase also preferentially targeted proteins associated with the TCA cycle.

2.3.6 Potential role of protein lysine acetylation and succinylation in the plasmid-host cross-talk

Among the reproducible acetylation sites, those that exhibited greater than twofold change in all three datasets were defined as differentially regulated by pCAR1 carriage (Table 2-11). Six sites in the log phase and 7 sites in the stationary phase were upregulated (R > 2) or unique to the pCAR1-containing strain. Those were found on proteins involved in the ribosome, carbohydrate metabolism and nucleotide metabolism. On the other hand, acetylation at 1 site in the log phase and 2 sites in the stationary phase on elongation factor EF-Tu (PP_0440) and a putative diguanylate cyclase (PP_1144) were found to be unique to the pCAR1-free strain. The remaining sites exhibited a fold change of less than two, indicating that the change in acetylation level was proportional to the change in protein abundance. These results suggested that carriage of pCAR1 resulted in changes in the status of acyl modifications in the host. Furthermore, the host system invoked acetylation of pCAR1-encoded protein, including the *meta*-cleavage compound hydrolase CarC, the partitioning protein ParA, the three NAPs proteins Phu, Pnd and Pmr, as well as two uncharacterized proteins encoded by ORF111 and ORF165, respectively (Fig. 2-16). Pmr is composed of a C-terminal DNA binding domain (residues 74-119) and an N-terminal oligomerization domain (residues 1-61), connected by a flexible linker (residues 62-73) (Suzuki *et al*., 2014). Acetylation was identified at position K49, which is located in the N-terminal oligomerization domain and at position K72, which is located in the flexible linker. The solved structure of the N-terminal dimerization/oligomerization domain of TurB showed that K49 forms a salt bridge (Suzuki-Minakuchi *et al*., 2016). Furthermore, cross-linking experiments demonstrated that substitution of K49 with alanine reduces the oligomerization ability of Pmr (Suzuki *et al*., 2014). In addition, acetylation was identified also on the chromosome-encoded MvaT homologues TurA (K39 and K49) and TurB (K39 and K61).

Functional KATs and KDACs in *P. putida* KT2440 have not been identified yet. In prokaryotes all characterized KATs so far possess Gcn5-related acetyltranserase (GNAT) motifs. The genome of *P. putida* KT2440 revealed more than 30 proteins with GNAT motifs (Nelson *et al*., 2002), some of which might functions as KATs. Furthermore, *P. putida* KT2440 possesses three KDAC homologues (PP_4764, PP_5340 and PP_5402). PP_5402 showed 40% amino acid identity to the sirtuin deacetylase CobB from *E. coli*, whereas PP_4764 and PP5340 showed 28% amino acid identity to the metal-dependent deacetylase AcuC from *B. subtilis*. Carriage of the pCAR1 plasmid induced the transcription of two of the putative acetyltranserases (PP_2957 and PP_3243) and the transcription of one putative deacetylase (PP_5340) (Takahashi *et al*., 2015). Furthermore, in the proteomic data a protein encoded on the pCAR1 plasmid that contains a GNAT motif (ORF76) was identified. Therefore, the possibility that some of these factors might have contributed to the observed changes in protein acetylation in the pCAR1-containing strain cannot be ruled out.

Among the reproducible succinylation sites, only one (K317) on elongation factor EF-Tu (PP_0440) was upregulated in the pCAR1-free strain (Table 2-11), suggesting that carriage of pCAR1 did not cause significant change in the intracellular pools of succinyl-CoA under the growth conditions used in this study. However, succinylation was detected on the pCAR1-encoded H-NS family protein Pmr (K64) only in the

stationary phase, suggesting that the acylation status of this protein might be linked to the metabolic state of the cell.

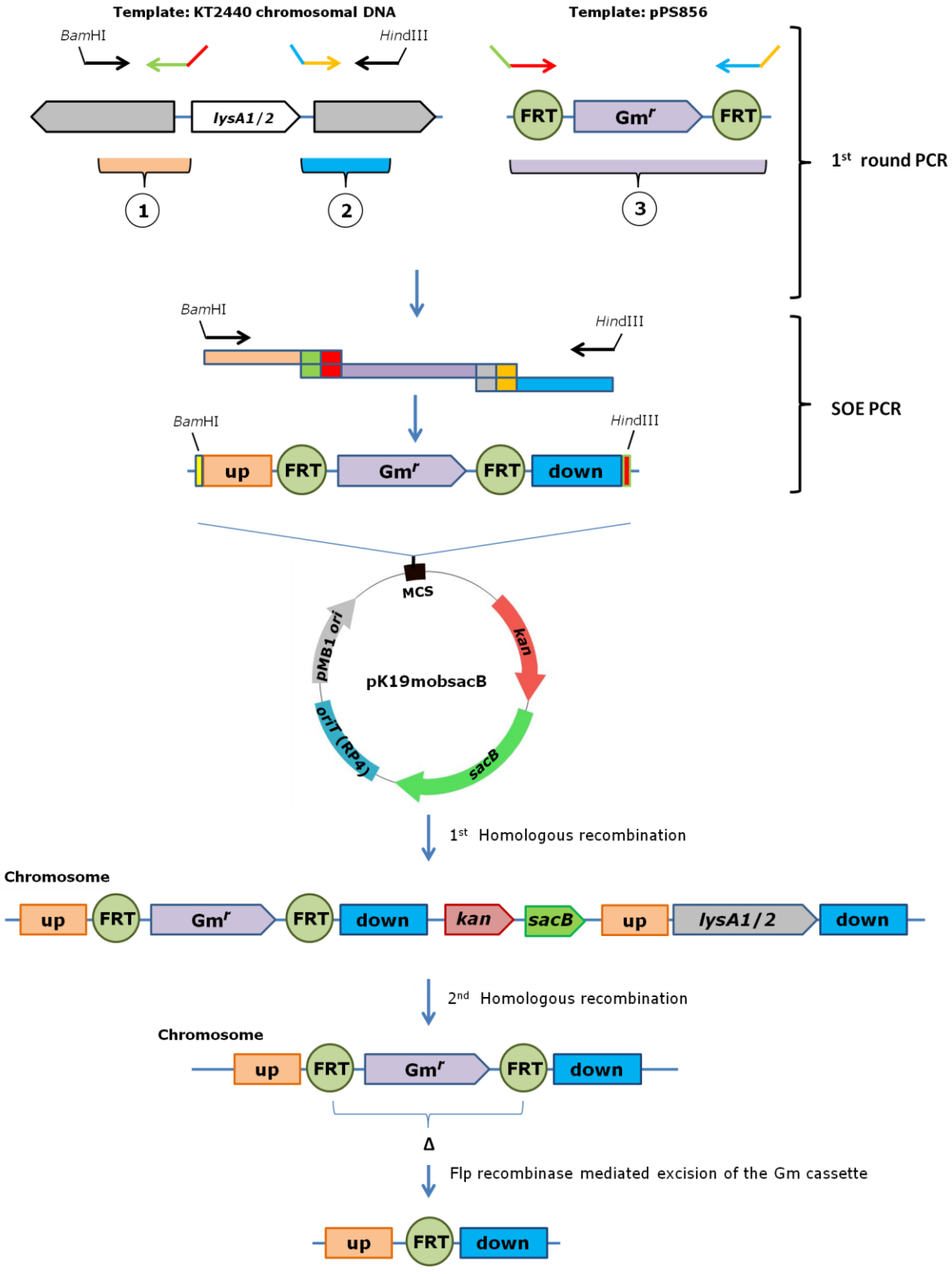

Fig. 2-1 Strategy for generation of *P. putida* KT2440 and KT2440(pCAR1) lysine auxotrophic strains. The deletion cassettes for inactivation of *lysA1* and *lysA2* genes were assembled by SOE PCR using the 5'- and 3'- flanking regions and Gm^r cassette, and subsequently cloned into the suicide vector pK19mobsacB. Double cross-over recombinants were generated by two consecutive homologous recombination events. Markerless mutant strains were obtained by Flp-recombinase mediated excision of the Gm^r cassette.

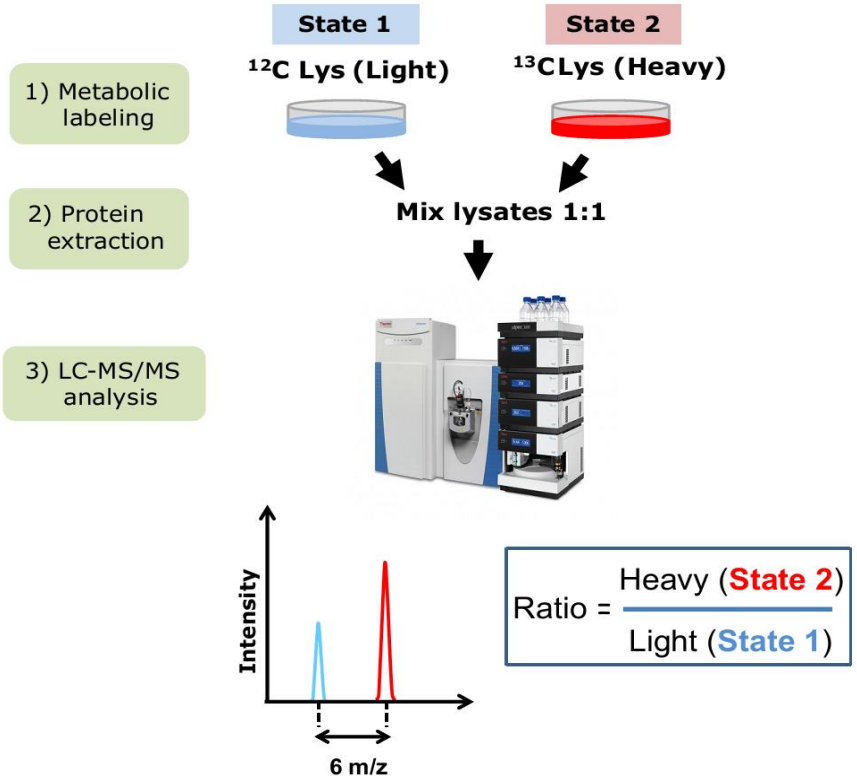

Fig. 2-2 Overview of the SILAC strategy for quantitative proteomics.

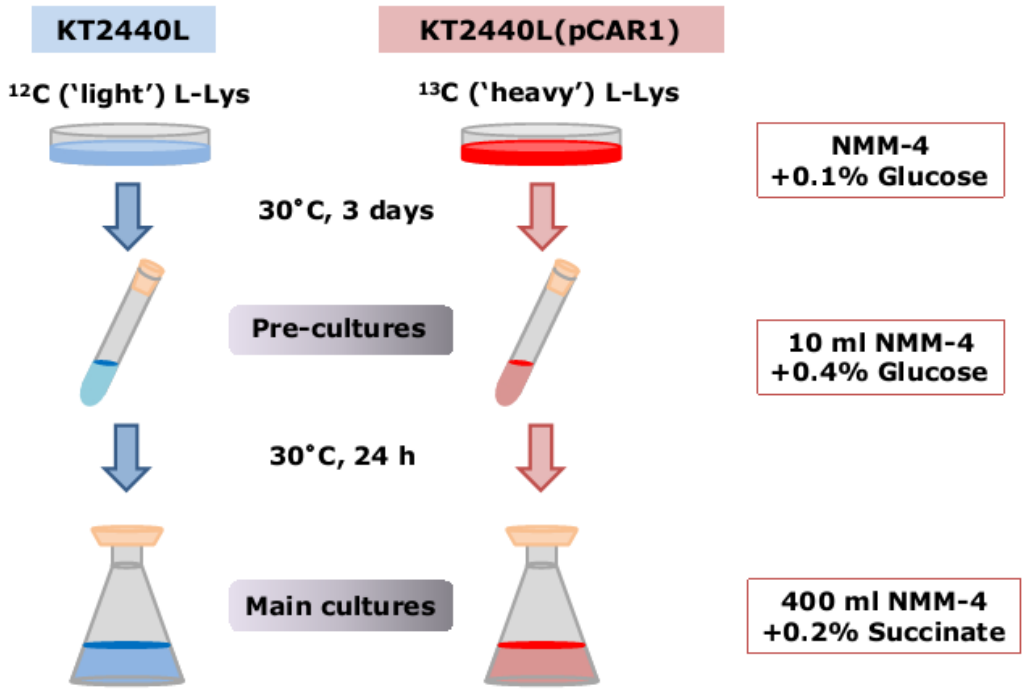

Fig. 2-3 Metabolic labeling of *P. putida* KT2440L and KT2440L(pCAR1) lysine auxotrophic strains for quantitative proteomics. The lysine auxotrophic strains were adapted in minimal medium suppemented with 'light' or 'heavy' L-lysine: KT2440L and KT2440L(pCAR1) were grown on NMM-4 agar plates with 0.1% [w/v] glucose for 3 days at 30°C, single colonies were inoculated in 10 ml NMM-4 medium supplemented with 0.4% [w/v] glucose and propagated for 24 h at 30°C, precultures were transferred to fresh NMM-4 medium with 0.2% [w/v] succinate. All media contained 50 µg/ml 'light' or 'heavy' L-lysine.

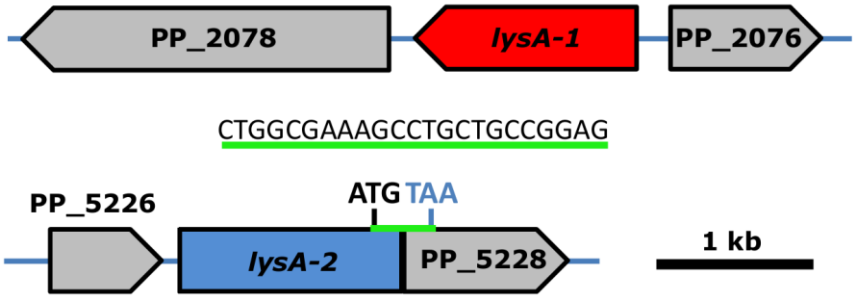

Fig. 2-4 Genetic organization of the *lysA1* and *lysA2* locuses in *P. putida* KT2440. The *lysA1* gene is flanked upstream by PP_2076, which encodes an uncharacterized hypothetical protein, and downstream by PP_2078, which encodes a LysR family transcriptional regulator. The *lysA2* gene is flanked upstream by PP_5226, which encodes an LppI family protein, and downstream by PP_5228, which encodes a diaminopimelate epimerase. ATG, start codon of PP_5228; TAA, stop codon of *lysA2*. The nucleotide sequence between the start codon of PP_5228 and the stop codon of *lysA2* is highlighted in green.

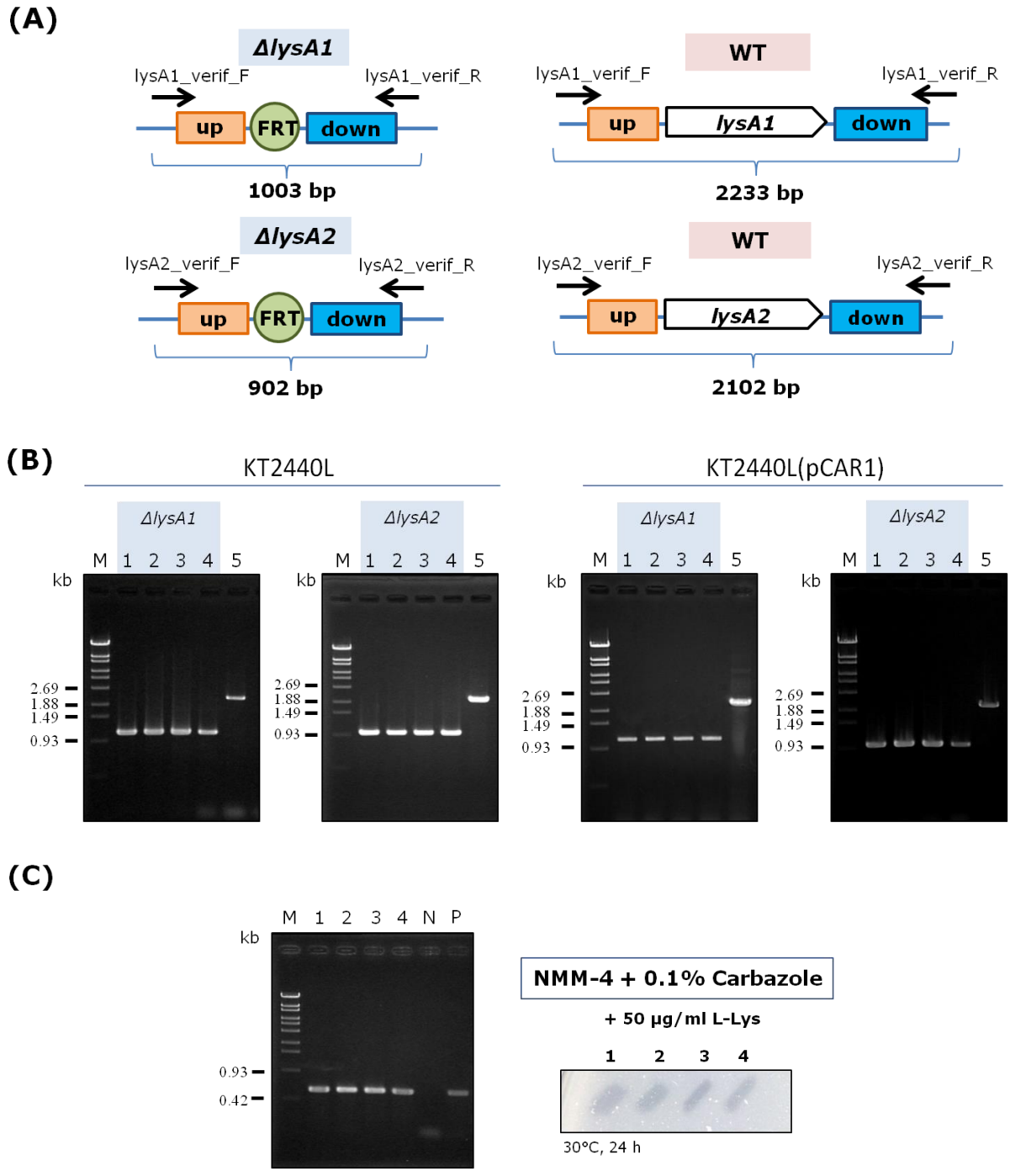

Fig. 2-5 Verification of *P. putida* KT2440 and KT2440(pCAR1) lysine auxotrophic strains. A) Schematic representation of the PCR strategy employed for confirmation of *lysA1* and *lysA2* genes deletion; B) Amplification was performed using genomic DNA extracted from four representative mutant strains (lanes 1-4) and the corresponding parental strains (lane 5); M, OneSTEP Marker 6 (Nippon, Japan) DNA ladder; C) Amplification of the *carF* gene region and formation of clear zones on NMM-4 agar plates supplemented with 0.1% carbazole confirmed that the KT2440L(pCAR1) contains pCAR1 and the presence of an intact *car* gene cluster. Agarose gel: lanes 1-4, genomic DNA from four representative KT2440L(pCAR1) clones; N, genomic DNA from KT2440; P, genomic DNA from KT2440(pCAR1).

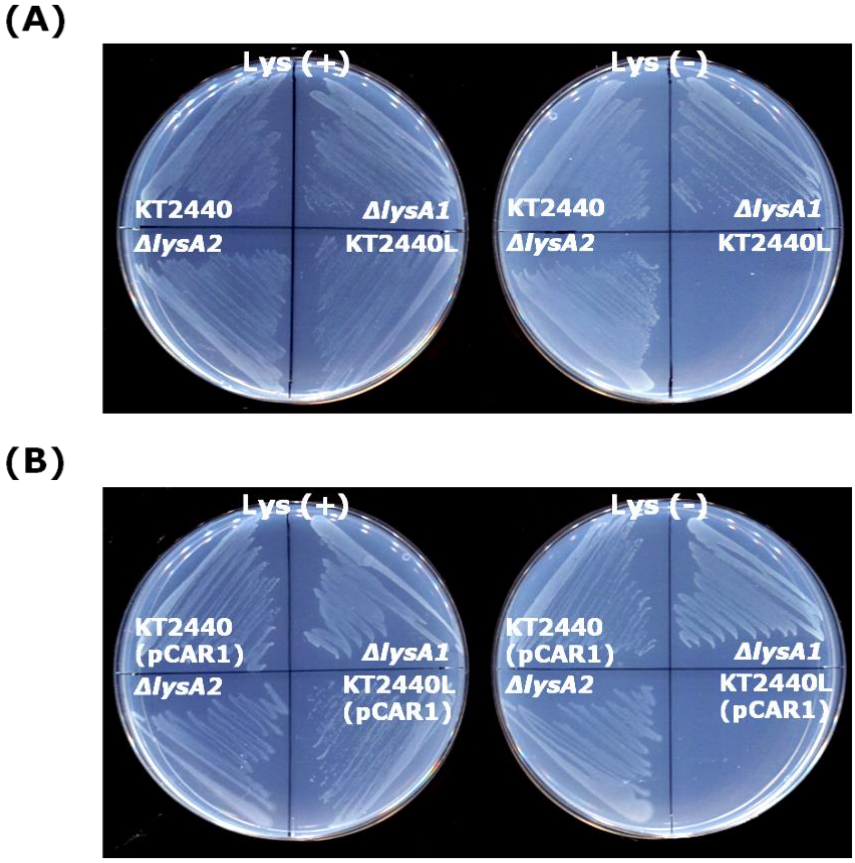

Fig. 2-6 Phenotypic confirmation of *P. putida* KT2440L and KT2440L(pCAR1) lysine auxotrophic strains. Growth of (A) KT2440 and (B) KT2440(pCAR1) wild-type, Δ*lysA1* and Δ*lysA2* single and double mutant strains on NMM-4 agar plates with and without suppementation of L-lysine.

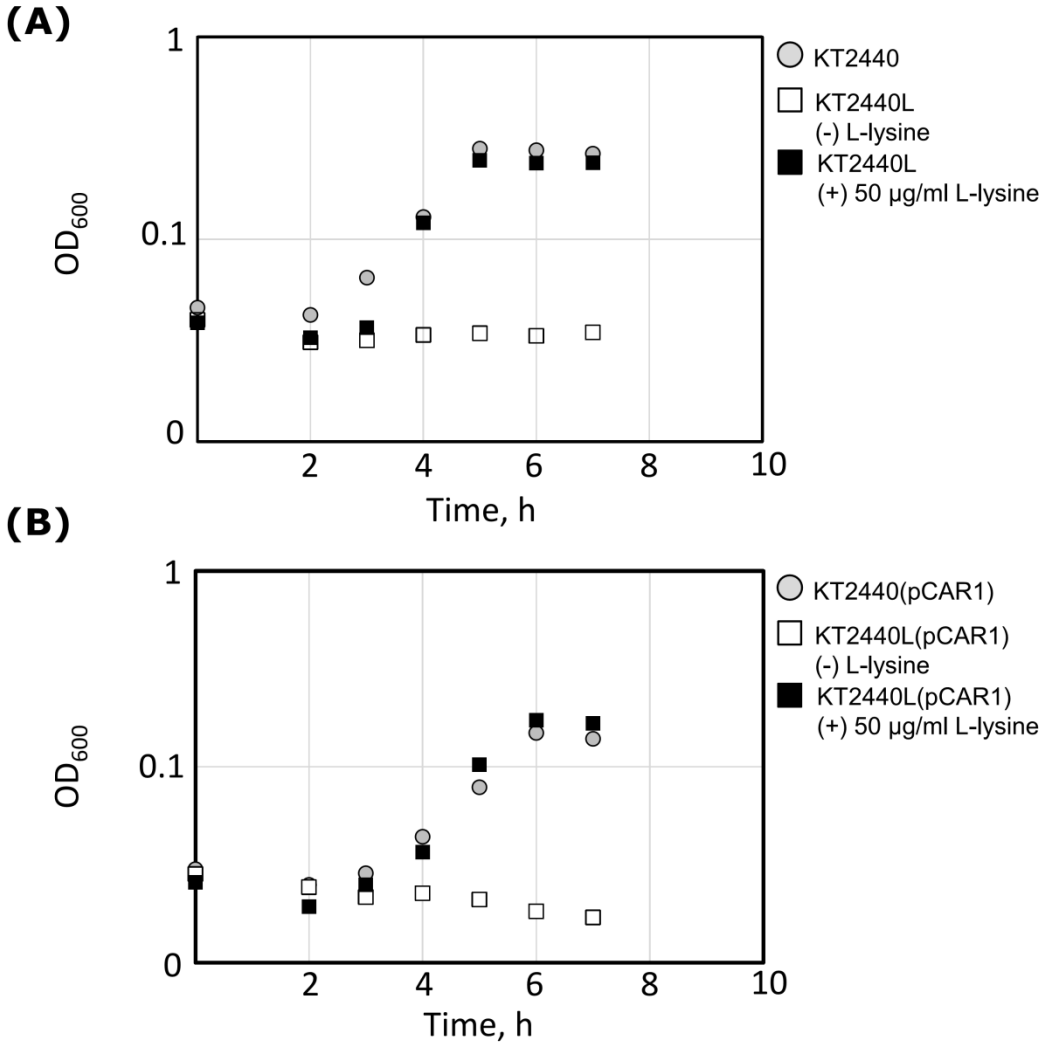

Fig. 2-7 Growth of *P. putida* KT2440L (A) and KT2440L(pCAR1) (B) lysine auxotrophic strains in comparison to their parental strains. Growth curves of KT2440 and KT2440(pCAR1) in NMM-4 minimal medium with 0.1% succinate as the sole carbon source are indicated with grey circles and growth curves of KT2440L and KT2440L(pCAR1) in NMM-4 succinate medium without L-lysine and with 50 µg/ml L-Lysine are indicated with open and closed squares, respectively.

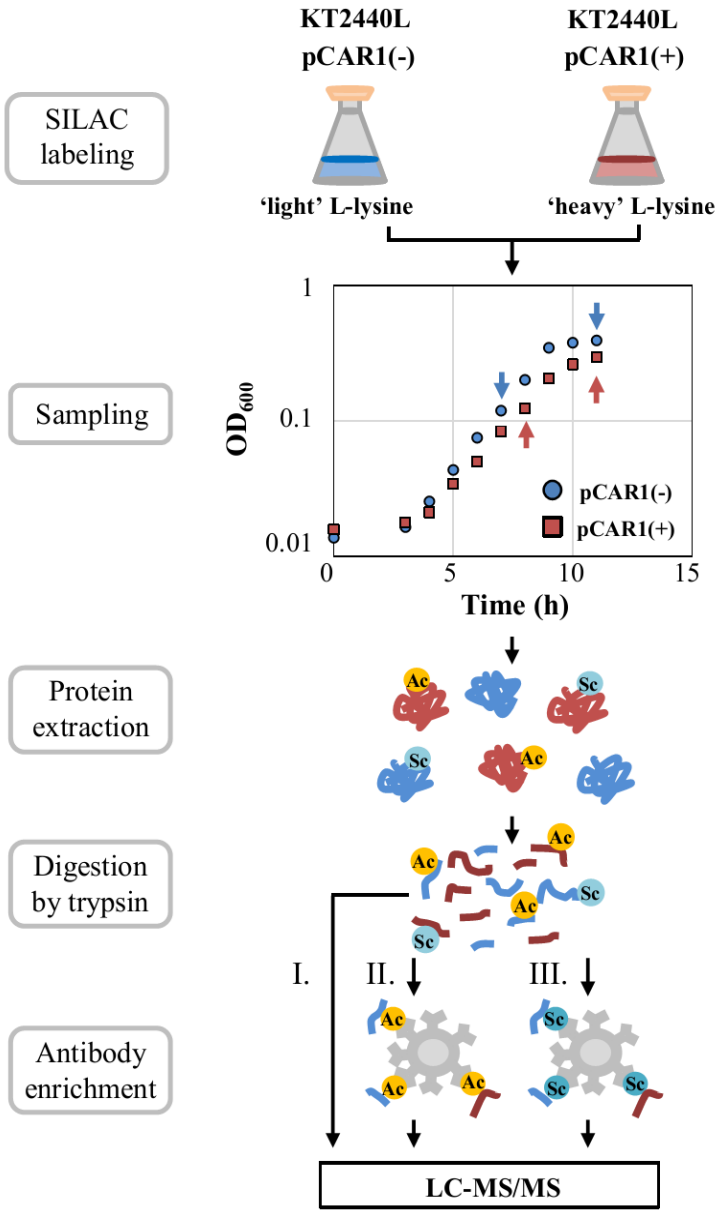

Fig. 2-8 Experimental workflow for global quantification of the total proteome and acylome (acetylome and succinylome) in *P. putida* KT2440 and KT2440(pCAR1) using lysine auxotrophic strains. SILAC method was used to quantify the changes in the total proteome and acylome invoked by pCAR1 carriage. pCAR1-free and pCAR1-harbouring lysine auxotrophic strains (KT2440L and KT2440L(pCAR1)) were grown in 0.2% succinate NMM-4 medium supplemented with 'light' lysine and 'heavy' lysine, respectively. Cells were harvested in the log and early stationary phases (indicated by arrows). Cell-free protein extracts were prepared, mixed in a 1:1 ratio, and subjected to digestion by trypsin. An aliquot from the peptide pool was used for the total proteome analysis (I). Acetyllysine (II) and succinyllysine (III) peptides were enriched by immuno-precipitation with anti-acetyllysine and anti-succinyllysine antibodies, respectively. Peptides were analysed by MS and relative abundance was determined by comparing the intensities of 'light' and 'heavy' labeled peptides.

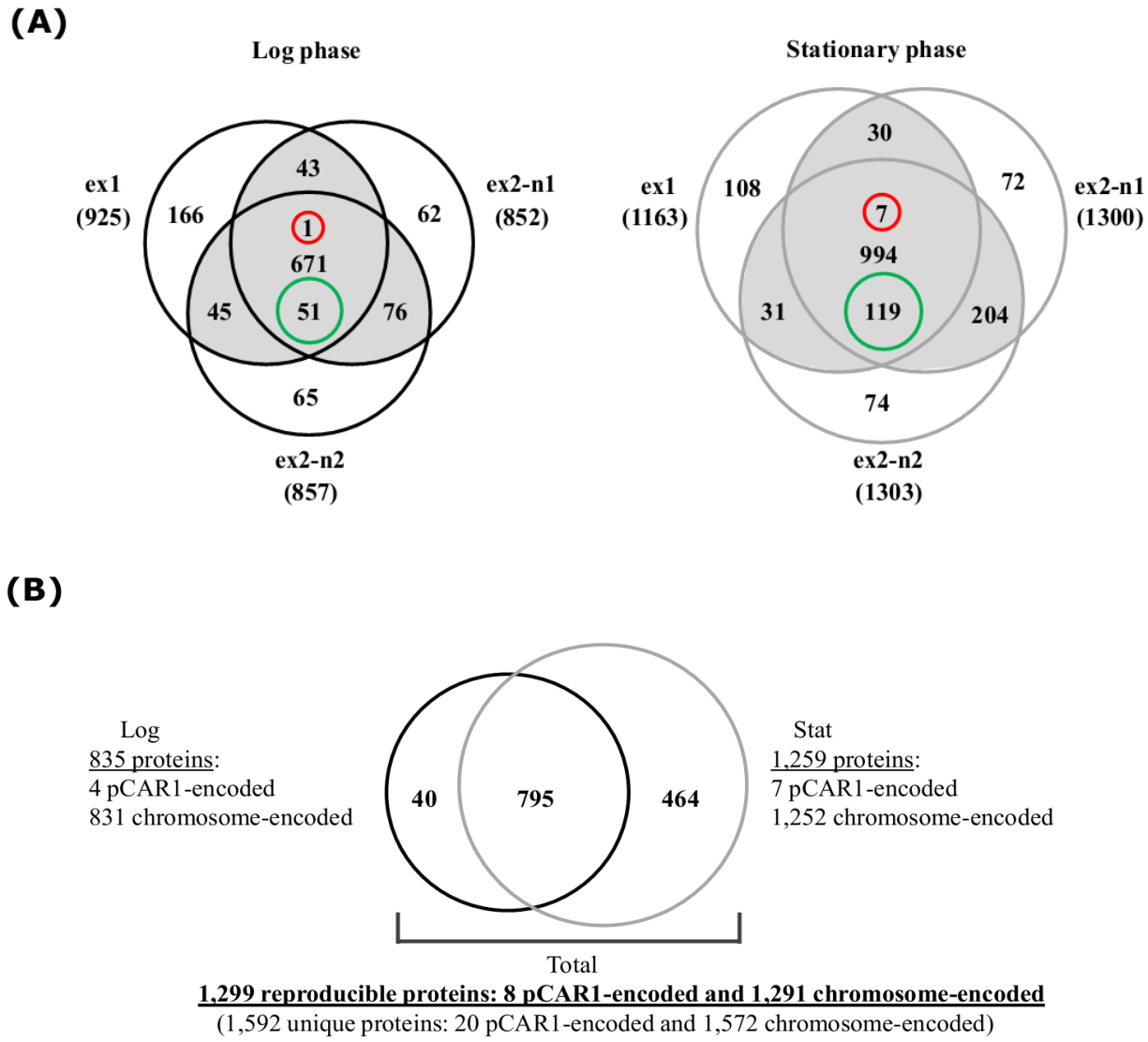

Fig. 2-9 Proteome of *P. putida* KT2440 and KT2440(pCAR1) in the log and stationary phases. (A) Total number of proteins identified in the log (black circles) and stationary (grey circles) phases. Diagrams show the overlap and total number (in parenthesis) of proteins identified in ex1, ex2-n1 and ex2-n2, respectively. Proteins detected reproducibly in at least two of the three datasets from the log (835) and stationary (1,259) phases were defined as the proteome in each growth state (highlighted in grey). Among the reproducible proteins, those that exhibited a fold change in abundance of at least two (≥ 2 or ≤ 0.5) in all three datasets obtained from either growth state were defined as differentially regulated by carriage of pCAR1. The number of upregulated proteins (1 in the log and 7 in the stationary phase) is shown in red, and the number of downregulated proteins (51 in the log and 119 in the stationary phase) is indicated in green circles. (B) Venn diagrams showing the growth-stage-dependent distribution and overlap of reproducible proteins identified in the log (853) and stationary (1,259) phases.

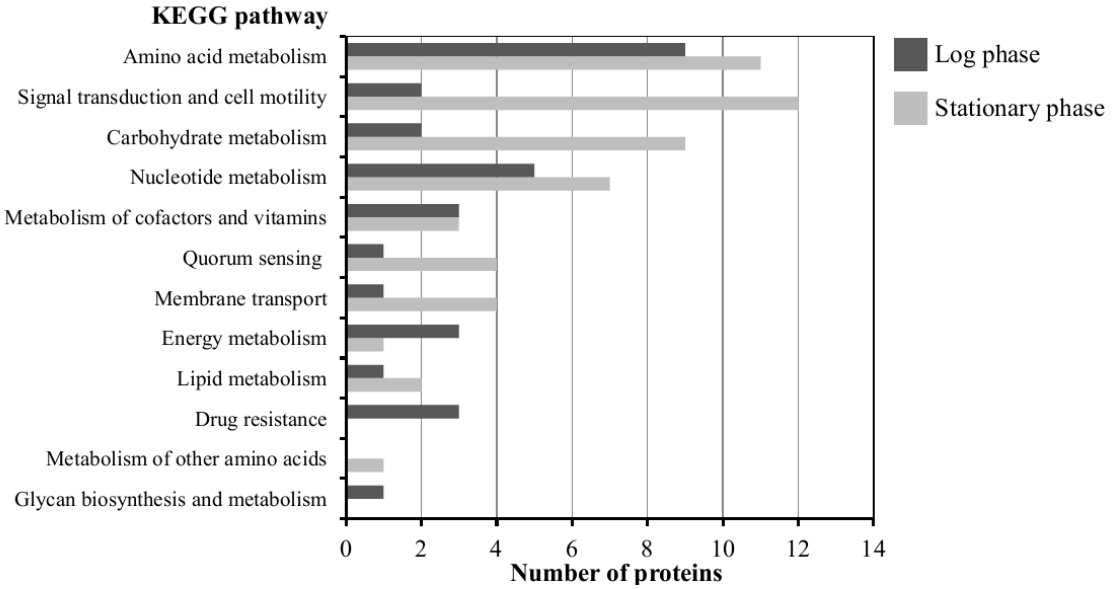

Fig. 2-10 Functional categorization of 151 proteins with reduced abundance by carriage of pCAR1 in *P. putida* KT2440 based on KEGG.

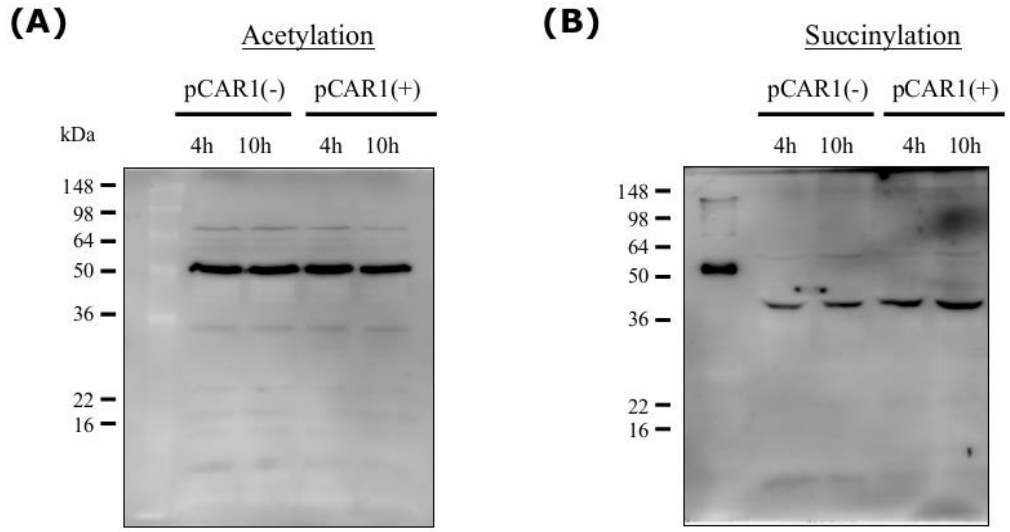

Fig. 2-11 Identification of acetylated and succinylated proteins in *P. putida* KT2440 and KT2440(pCAR1) using western blot. Cells of both strains were grown in NMM-4 succinate medium and harvested at three time points (mid-log [4 h] and early stationary phase [10 h], respectively). Aliquots containing 70 µg of whole-cell protein were loaded in each lane and subjected to anti-acetyllysine and anti-succinyllysine immunoblot analysis.

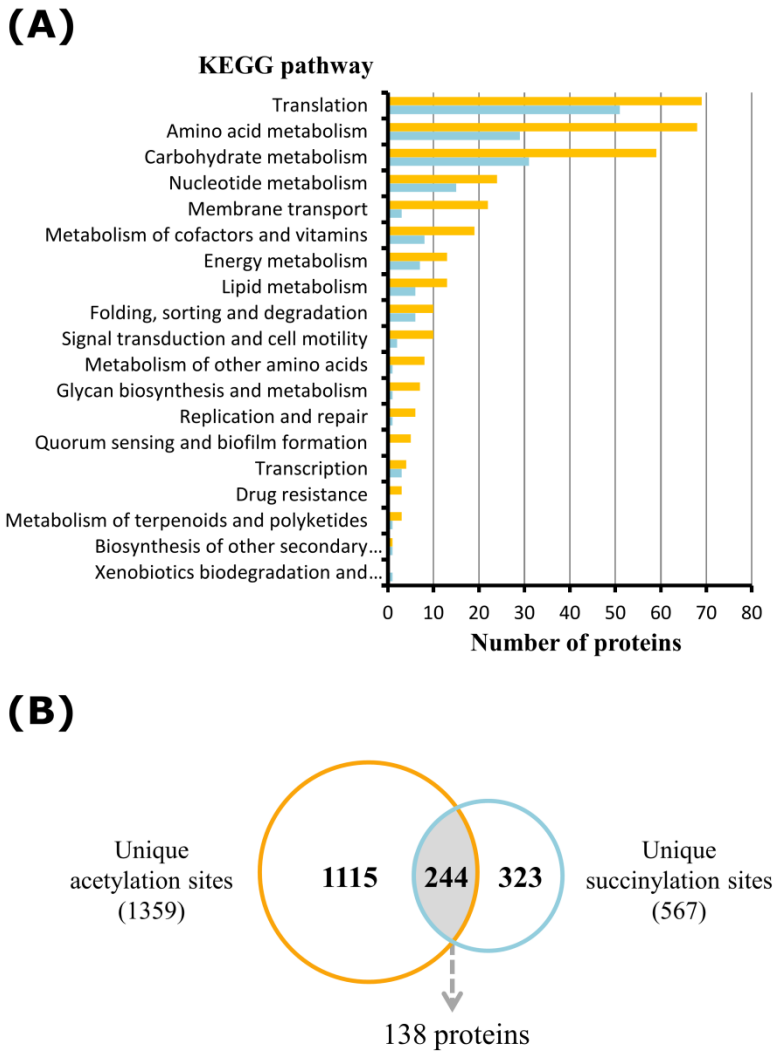

Fig. 2-12 Acetylome and succinylome of the pCAR1-free and pCAR1-harbouring strains. (A) Functional categorization of all identified acetylated (637) and succinylated (259) proteins based on KEGG pathway database. Orange and blue bars indicate the number of acetylated and succinylated proteins, respectively. (B) Venn diagram comparing the total number of unique acetylation (1,359) and succinylation (567) sites identified in this study: 244 sites on 138 proteins were found to be shared between the acetylome and succinylome. Orange and blue circles represent the number of acetylated and succinylated sites, respectively.

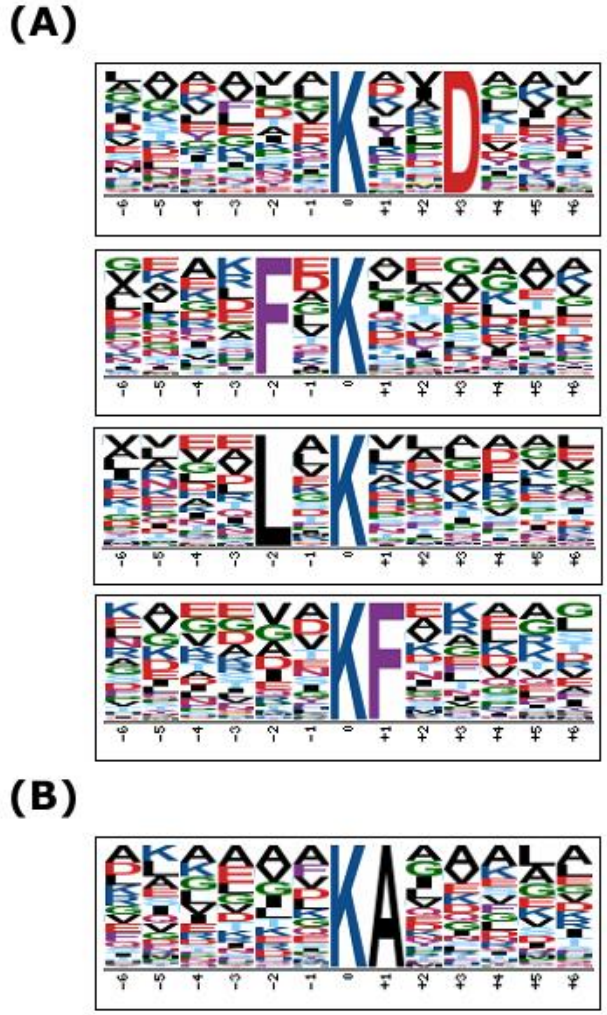

Fig. 2-13 Analysis of amino acid context of lysine acetylation and succinylation in *P. putida* KT2440. To examine the possibility for a specific acetylation and succinylation pattern, the amino acid sequences surrounding the modified lysines were analysed using the motif-X program (Schwartz and Gygi, 2005). The generated acetylation motifs (A) revealed overrepresentation of negatively charged aspartate residues at position +3, hydrophobic leucine residues at position -2 and aromatic phenylalanine residues at positions -2 and +1. In contrast, the obtained succinylation motif (B) showed only a weak preference for alanine at position +1. The parameters used were as follows: width, 21 residues (10 residues on each side of the modification site); occurrence threshold, 20; *P*-value threshold, 0.000001 for generation of the acetylation motif and 0.0001 for generation of the succinylation motif. Unaligned motif data was used as a background.

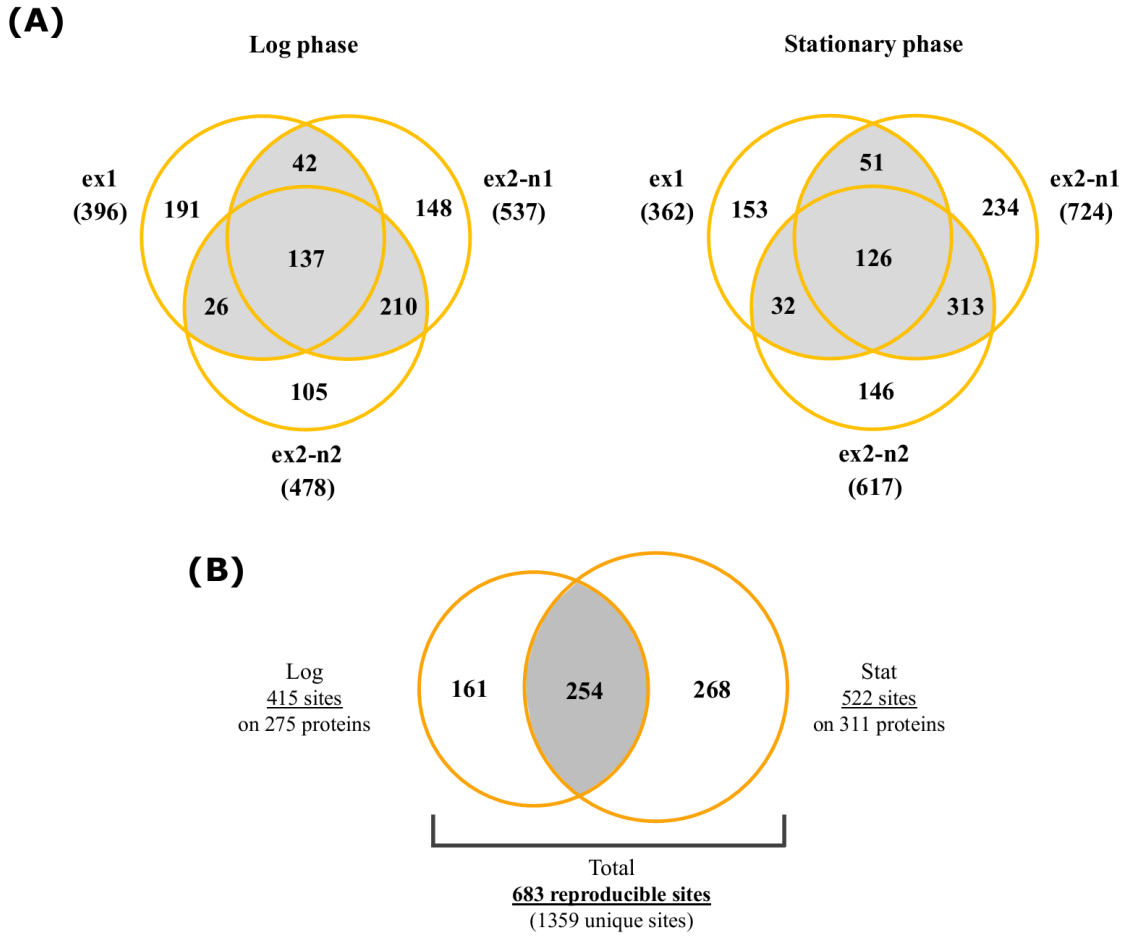

Fig. 2-14 Acetylome of the pCAR1-free and pCAR1-harbouring strains in the log and stationary phases. (A) Total number of acetylation sites identified in the log and stationary phases. Diagrams show the overlap and total number (in parenthesis) of acetylation sites identified in ex1 (396 in the log and 362 in the stationary phase), ex2-n1 (537 in the log and 724 in the stationary phase) and ex2-n2 (478 in the log and 617 in the stationary phase), respectively. Acetylation sites detected reproducibly in at least two of the three datasets from the log and stationary phases were defined as the acetyome in each growth state (highlighted in grey). (B) Venn diagrams showing the growth-stage-dependent distribution and overlap of reproducibly identified acetylation sites: 254 acetylation sites were identifed both in the log and stationary phases.

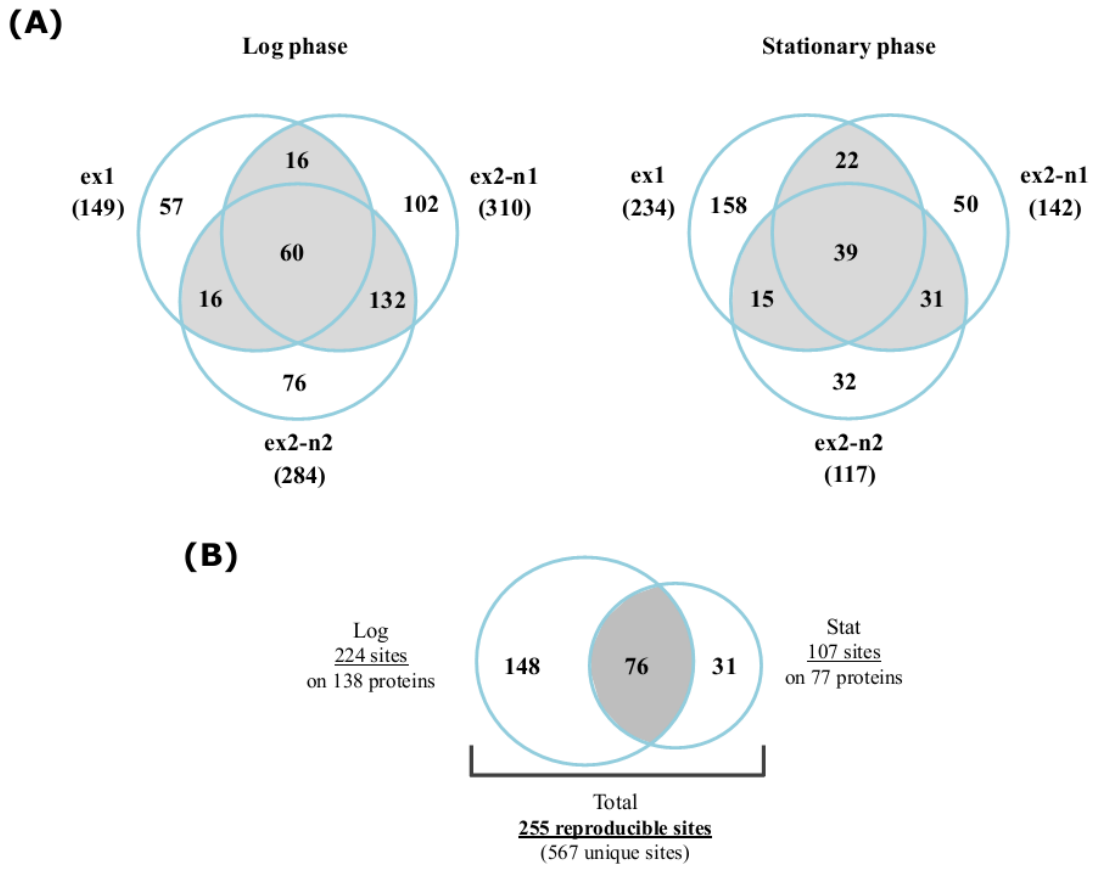

Fig. 2-15 Succinylome of the pCAR1-free and pCAR1-harbouring strains in the log and stationary phases. (A) Total number of succinylation sites identified in the log and stationary phases. Diagrams show the overlap and total number (in parenthesis) of succinyation sites identified in ex1 (149 in the log and 234 in the stationary phase), ex2-n1 (310 in the log and 124 in the stationary phase) and ex2-n2 (284 in the log and 117 in the stationary phase), respectively. Succinylation sites detected reproducibly in at least two of the three datasets from the log and stationary phases were defined as the succinylome in each growth state (highlighted in grey). (B) Venn diagrams showing the growth-stage-dependent distribution and overlap of reproducibly identified succinylation sites: 76 succinylation sites were identified in both the log and the stationary phases.

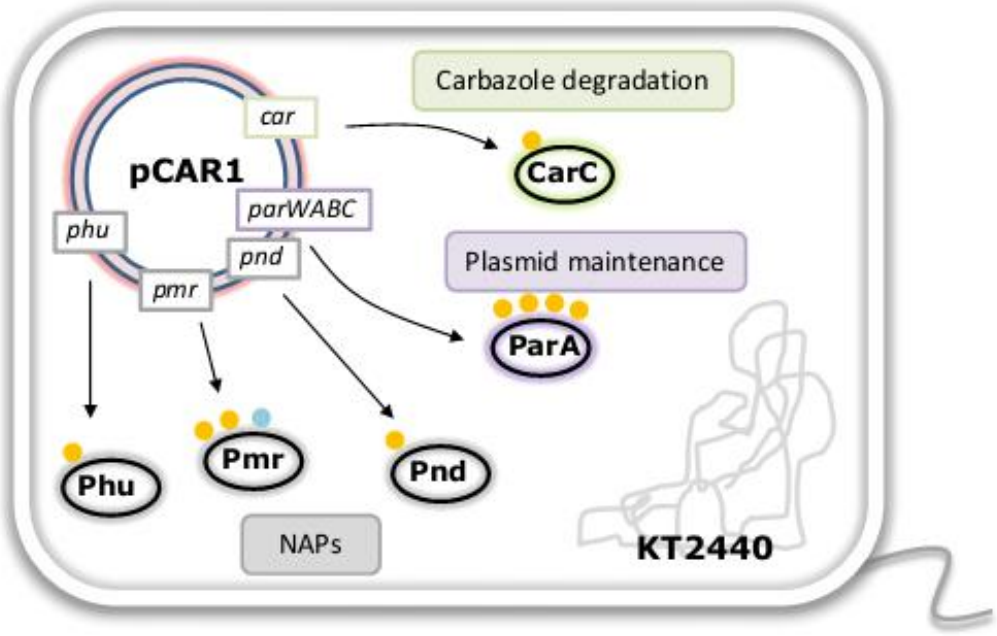

Fig. 2-16 Acyl modifications identified on key pCAR1-encoded proteins. Orange and blue circles represent acetylated and succinylated sites, respectively. The number of circles represents the number of modification sites. Green, purple and grey boxes indicate the *car* operon, involved in carbazole degradation, the *parWABC* gene region, involved in plasmid partitioning (Shintani *et al*., 2006) and the three NAPs encoding genes, respectively. CarC, *meta*-cleavage compound hydrolase.

Table 2-6 SILAC labeling efficiency.

Feature	Log phase	Stationary phase
Total number of lysines[a]	2,542	3,483
Number of ^{13}C-labeled lysines	2,526	3,458
Incorporation efficiency	99.37%	99.28%

[a] Total number of lysines in all identified proteins.

Table 2-7 pCAR1-encoded proteins identified in this study.

Protein	Description
ParA*	Partitioning protein
ParB*	Partitioning protein
ParC	Partitioning protein
CarAc	Ferredoxin component of carbazole
CarBc	Catalytic subunit of meta cleavage enzyme
CarC*	Meta cleavage compound hydrolase
CarF	Acetaldehyde dehydrogenase
Phu*	Nucleoid-associated protein (an HU homolog)
Pmr*	Nucleoid-associated protein (an H-NS homolog)
Pnd	Nucleoid-associated protein (an NdpA homolog)
KlaB*	Putative tellurite resistant protein
ORF170	Putative methyl-accepting chemotaxis protein
ORF111*	Uncharacterized protein
ORF159a	Uncharacterized protein
ORF163	Uncharacterized protein
ORF42	Uncharacterized protein
ORF67	Uncharacterized protein
ORF7	Uncharacterized protein
ORF76	Uncharacterized protein
ORF77*	Uncharacterized protein

*Reproducibly identified pCAR-encoded proteins. Green indicates proteins involved in carbazole degradation; purple, proteins involved in plasmid maintenance and grey, pCAR1-encoded NAPs.

Table 2-8 Differentially regulated proteins in *P. putida* KT2440 by pCAR1 carriage in the log and stationary phases.

Locus tag	Description	KEGG BRITE 1[a]	KEGG BRITE 2[b]	Protein ratio (fold change)					
				ex1-log	ex2-log-n1	ex2-log-n2	ex1-stat	ex2-stat-n1	ex2-stat-n2
Proteins with increased abundance by pCAR1 carriage (≥2)									
PP_0988*	Glycine dehydrogenase	Metabolism	Amino acid metabolism	0.4	0.52	0.5	**2.42**	**3.08**	**3.2**
PP_1005*	Heme oxygenase	Others	Unknown	1.4	N.D.	N.D.	**38.5**	**18.9**	**19.0**
PP_1895*	ABC transporter ATP-binding protein	Others	Unknown	N.D.	N.D.	**4.3**	**11.0**	**5.8**	**4.1**
PP_3095	T6SS related protein	Environmental information processing	Membrane transport	N.D.	**2.5**	**3.9**	**4.5**	**2.4**	**2.6**
PP_3099*	T6SS related protein	Cellular processes	Biofilm formation	**3.4**	**2.4**	**3.0**	**3.7**	**3.0**	**2.4**
PP_3365*	Acetolactate synthase	Metabolism	Carbohydrate metabolism	1.5	**2.3**	**2.7**	**2.5**	**3.3**	**2.6**
PP_3426*	Hydrophobe/amphiphile efflux-1 family transporter (MexF)	Others	Unknown	**19.9**	**12.4**	N.D.	**72.7**	**81.1**	**54.5**
Proteins with decreased abundance by pCAR1 carriage(≤0.5)									
PP_0013	DNA gyrase subunit B	Others	Unknown	**0.4**	**0.4**	**0.4**	**0.4**	**0.4**	**0.4**
PP_0100	Carbonate dehydratase	Metabolism	Energy metabolism	**0.4**	**0.4**	**0.4**	0.6	**0.4**	**0.2**
PP_0120	Zinc ABC transporter substrate-binding protein	Environmental information processing	Membrane transport	N.D.	N.D.	N.D.	**0.4**	**0.3**	**0.2**
PP_0126	Cytochrome c4	Others	Unknown	N.D.	N.D.	N.D.	**0.3**	**0.08**	**0.01**
PP_0127	DsbA family thiol:disulfide interchange protein	Human disease	Drug resistance	**0.5**	**0.5**	**0.5**	0.6	**0.3**	**0.3**
PP_0133	Alginate biosynthesis transcriptional regulatory protein AlgB	Environmental information processing	Signal transduction	N.D.	N.D.	N.D.	**0.5**	**0.2**	**0.4**
PP_0158	Acyl-CoA dehydrogenase	Metabolism	Lipid metabolism	N.D.	1.3	1.3	**0.4**	**0.2**	**0.2**
PP_0159	CAIB/BAIF family protein	Others	Unknown	N.D.	N.D.	N.D.	**0.3**	**0.1**	**0.2**
PP_0168	Surface adhesion protein	Others	Unknown	0.7	**0.5**	**0.5**	**0.5**	**0.3**	**0.3**
PP_0181	Uncharacterized protein	Others	Unknown	N.D.	N.D.	N.D.	**0.1**	**0.05**	**0.08**
PP_0182	Uncharacterized protein	Others	Unknown	N.D.	N.D.	N.D.	**0.2**	**0.3**	**0.3**
PP_0185	LytTR family two component transcriptional regulator	Environmental information processing	Signal transduction	N.D.	N.D.	N.D.	**0.1**	**0.1**	**0.2**

PP_0234*	Porin	Others	Unknown	**0.1**	**0.1**	**0.1**	**0.1**	**0.2**	**0.1**
PP_0258	LysM domain/BON superfamily protein	Others	Unknown	**0.02**	N.D.	N.D.	**0.08**	**0.2**	**0.3**
PP_0335	Glutathione S-transferase	Others	Unknown	**0.2**	**0.06**	**0.2**	**0.3**	**0.3**	**0.2**
PP_0395	SpoVR family protein	Others	Unknown	N.D.	N.D.	N.D.	**0.4**	**0.02**	**0.04**
PP_0396	UPF0229 protein	Others	Unknown	N.D.	N.D.	N.D.	**0.2**	**0.1**	**0.1**
PP_0397	Serine protein kinase PrkA	Others	Unknown	**0.2**	**0.3**	**0.2**	**0.2**	**0.07**	**0.06**
PP_0412	Polyamine ABC transporter substrate-binding protein	Cellular processes	Quorum sensing	N.D.	N.D.	N.D.	**0.4**	**0.2**	**0.1**
PP_0482	Bacterioferritin	Metabolism	Metabolism of cofactors and vitamins	**0.2**	N.D.	N.D.	**0.3**	**0.2**	**0.2**
PP_0509	Uncharacterized protein	Others	Unknown	N.D.	N.D.	N.D.	**0.4**	**0.4**	**0.3**
PP_0545	Aldehyde dehydrogenase	Metabolism	Carbohydrate metabolism	**0.4**	**0.5**	**0.5**	**0.2**	**0.2**	**0.2**
PP_0574	LuxR family transcriptional regulator	Others	Unknown	N.D.	N.D.	**0.2**	**0.07**	**0.06**	**0.07**
PP_0742	Uncharacterized protein	Others	Unknown	N.D.	0.6	**0.4**	**0.5**	**0.2**	**0.2**
PP_0753	Lipoprotein	Others	Unknown	**0.4**	**0.5**	**0.3**	**0.2**	0.8	**0.5**
PP_0766	Uncharacterized protein	Others	Unknown	**0.3**	**0.3**	**0.3**	**0.2**	**0.1**	**0.1**
PP_0768	Response regulator/hypothetical protein	Others	Unknown	**0.2**	N.D.	N.D.	**0.3**	**0.2**	**0.3**
PP_0885	Peptide ABC transporter substrate-binding protein	Cellular processes	Cell motility	N.D.	N.D.	N.D.	**0.4**	**0.5**	**0.3**
PP_0888	Fis family transcriptional regulator	Environmental information processing	Signal transduction	N.D.	**0.1**	N.D.	**0.5**	**0.4**	**0.3**
PP_0893	Pfpi family intracellular protease	Others	Unknown	N.D.	0.51	0.51	**0.2**	**0.4**	**0.4**
PP_0915	Superoxide dismutase [Fe]	Others	Unknown	**0.5**	**0.5**	0.6	**0.5**	**0.5**	**0.5**
PP_0942	PmbA protein	Others	Unknown	N.D.	N.D.	**0.4**	**0.5**	**0.3**	**0.4**
PP_0963	BolA family protein	Others	Unknown	N.D.	N.D.	**0.2**	**0.3**	**0.3**	**0.5**
PP_0973	Nucleoid-associated protein (NdpA)	Others	Unknown	**0.3**	**0.3**	N.D.	**0.4**	**0.1**	**0.5**
PP_0975	Nucleoid-associated protein (HupN)	Others	Unknown	**0.2**	**0.3**	**0.3**	**0.4**	**0.3**	**0.3**
PP_0986	Glycine cleavage system T protein	Metabolism	Amino acid metabolism	**0.4**	**0.4**	**0.4**	**0.4**	**0.3**	**0.3**

PP_0998	Uncharacterized protein	Others	Unknown	N.D.	N.D.	N.D.	**0.3**	**0.2**	**0.07**
PP_0999	Carbamate kinase	Metabolism	Energy metabolism	N.D.	N.D.	N.D.	**0.3**	**0.3**	**0.3**
PP_1000	Ornithine carbamoyltransferase	Metabolism	Amino acid metabolism	N.D.	1.0	N.D.	**0.2**	**0.2**	**0.2**
PP_1001	Arginine deiminase	Metabolism	Amino acid metabolism	0.6	**0.3**	0.6	**0.2**	**0.2**	**0.2**
PP_1071	Amino acid ABC transporter substrate-binding protein	Environmental information processing	Membrane transport	0.53	0.6	0.6	**0.5**	**0.3**	**0.3**
PP_1082	Bacterioferritin	Metabolism	Metabolism of cofactors and vitamins	**0.1**	**0.4**	N.D.	**0.3**	**0.1**	**0.1**
PP_1085	Ribonuclease T	Others	Unknown	N.D.	0.51	**0.4**	**0.5**	**0.5**	**0.3**
PP_1088	Argininosuccinate synthase	Metabolism	Amino acid metabolism	**0.4**	**0.5**	**0.5**	0.54	**0.5**	**0.5**
PP_1091	Uncharacterized protein	Others	Unknown	**0.3**	**0.4**	**0.5**	N.D.	N.D.	N.D.
PP_1121	OmpA/MotB domain-containing protein	Others	Unknown	**0.2**	N.D.	N.D.	**0.2**	**0.1**	**0.2**
PP_1141	ABC transporter substrate-binding protein	Environmental information processing	Membrane transport	**0.4**	**0.5**	**0.4**	**0.2**	**0.1**	**0.1**
PP_1169	TRAP dicarboxylate transporter subunit DctP	Others	Unknown	**0.5**	**0.4**	0.8	**0.3**	**0.1**	**0.1**
PP_1179	Ribonucleotide-diphosphate reductase subunit alpha	Metabolism	Nucleotide metabolism	**0.4**	**0.4**	**0.4**	0.6	**0.5**	0.6
PP_1184*	Dienelactone hydrolase	Others	Unknown	N.D.	0.7	N.D.	**0.3**	**0.2**	**0.2**
PP_1223	Peptidoglycan-associated lipoprotein	Others	Unknown	**0.3**	**0.5**	**0.4**	**0.4**	0.6	0.8
PP_1245	Uncharacterized protein	Others	Unknown	**0.4**	**0.4**	**0.3**	N.D.	N.D.	1.6
PP_1291	PhoH family protein	Others	Unknown	N.D.	N.D.	**0.3**	**0.4**	**0.05**	**0.08**
PP_1297	Amino acid ABC transporter substrate-binding protein	Environmental information processing	Membrane transport	N.D.	N.D.	N.D.	**0.07**	**0.07**	**0.04**
PP_1332	UDP-N-acetylmuramoyl-L-alanyl-D-glutamate-2,6-diaminopimelate ligase	Metabolism	Amino acid metabolism	**0.4**	0.6	**0.4**	**0.4**	**0.5**	**0.5**
PP_1347	Glutathione S-transferase	Metabolism	Metabolism of other amino acids	0.6	**0.5**	**0.4**	**0.3**	**0.2**	**0.4**
PP_1348	Uncharacterized protein	Others	Unknown	N.D.	**0.2**	**0.5**	**0.3**	**0.4**	**0.4**
PP_1372	Uncharacterized protein	Others	Unknown	N.D.	N.D.	N.D.	**0.5**	**0.3**	**0.3**
PP_1457	GAR transformylase 2	Metabolism	Nucleotide metabolism	**0.1**	**0.4**	**0.4**	**0.4**	**0.4**	**0.4**
PP_1478	NADH:flavin oxidoreductase	Others	Unknown	N.D.	**0.4**	**0.4**	**0.01**	**0.03**	**0.05**

PP_1481	Gamma-aminobutyraldehyde dehydrogenase	Metabolism	Amino acid metabolism	N.D.	N.D.	N.D.	**0.1**	**0.2**	**0.1**
PP_1486	Polyamine ABC transporter substrate-binding protein	Cellular processes	Quorum sensing	N.D.	N.D.	N.D.	**0.07**	**0.03**	**0.06**
PP_1488	Methyl-accepting chemotaxis sensory transducer	Environmental information processing	Signal transduction	**0.3**	N.D.	N.D.	**0.3**	**0.3**	**0.3**
PP_1603	Acyl-[acyl-carrier-protein]--UDP-N-acetylglucosamine O-acyltransferase	Metabolism	Glycan biosynthesis and metabolism	**0.3**	**0.3**	**0.3**	N.D.	N.D.	**0.2**
PP_1623	RNA polymerase sigma factor RpoS	Others	Unknown	N.D.	N.D.	N.D.	**0.5**	**0.4**	**0.06**
PP_1659*	Uncharacterized protein	Others	Unknown	N.D.	N.D.	N.D.	**0.08**	**0.08**	**0.07**
PP_1665	Phosphoribosylformylglycinamidine cyclo-ligase	Metabolism	Nucleotide metabolism	**0.3**	**0.4**	**0.4**	**0.2**	**0.4**	**0.4**
PP_1719	Carboxyl-terminal protease	Others	Unknown	0.56	0.7	0.8	**0.5**	**0.4**	**0.4**
PP_1726	ABC transporter substrate-binding protein	Cellular processes	Quorum sensing	**0.1**	**0.2**	**0.2**	**0.09**	**0.07**	**0.08**
PP_1765	Ubiquinone biosynthesis O-methyltransferase	Metabolism	Metabolism of cofactors and vitamins	N.D.	N.D.	**0.3**	**0.5**	**0.4**	**0.4**
PP_1767	DNA gyrase subunit A	Others	Unknown	**0.4**	**0.5**	**0.3**	**0.4**	**0.4**	**0.4**
PP_1771	Cytidylate kinase	Metabolism	Nucleotide metabolism	**0.1**	**0.07**	**0.1**	**0.1**	**0.3**	**0.4**
PP_1776	Mannose-6-phosphate isomerase	Metabolism	Carbohydrate metabolism	N.D.	N.D.	N.D.	**0.2**	**0.3**	**0.2**
PP_1859	OsmC family protein	Others	Unknown	**0.4**	N.D.	N.D.	**0.3**	**0.5**	**0.5**
PP_1893	Acyl-CoA dehydrogenase	Metabolism	Lipid metabolism	N.D	N.D.	N.D.	**0.2**	**0.1**	**0.1**
PP_1916	3-oxoacyl-ACP synthase	Metabolism	Lipid metabolism	**0.4**	**0.5**	**0.4**	0.54	0.7	0.6
PP_2000	Amidophosphoribosyl transferase	Metabolism	Nucleotide metabolism	**0.3**	**0.4**	**0.4**	**0.4**	**0.5**	**0.4**
PP_2112	Aconitate hydratase	Metabolism	Carbohydrate metabolism	N.D.	N.D.	N.D.	**0.2**	**0.1**	**0.07**
PP_2130	Lytic transglycosylase	Others	Unknown	N.D.	N.D.	N.D.	**0.07**	**0.2**	**0.4**
PP_2187	Universal stress protein	Others	Unknown	N.D.	N.D.	N.D.	**0.1**	**0.08**	**0.1**
PP_2320	ErfK/YbiS/YcfS/YnhG family protein	Others	Unknown	**0.2**	**0.4**	**0.4**	N.D.	**0.04**	**0.04**
PP_2338	2-methylcitrate dehydratase	Metabolism	Carbohydrate metabolism	N.D.	N.D	N.D.	**0.5**	**0.3**	**0.4**

PP_2396	Uncharacterized protein	Others	Unknown	N.D.	**0.4**	**0.3**	**0.3**	**0.1**	**0.2**
PP_2422	Alkylhydroperoxidase	Others	Unknown	N.D.	N.D	N.D.	**0.4**	**0.4**	**0.4**
PP_2439	Alkyl hydroperoxide reductase	Others	Unknown	**0.3**	**0.4**	**0.4**	0.6	**0.4**	**0.5**
PP_2453	Glutaminase-asparaginase	Metabolism	Amino acid metabolism	**0.2**	**0.3**	**0.3**	**0.3**	**0.3**	**0.3**
PP_2648	Universal stress protein	Others	Unknown	N.D.	**0.2**	**0.3**	**0.2**	**0.4**	**0.3**
PP_2876	Beta-lactamase	Human disease	Drug resistance	**0.05**	**0.3**	**0.4**	0.501	**0.3**	**0.3**
PP_3079	Peptidyl-prolyl cis-trans isomerase	Others	Unknown	**0.4**	0.6	0.6	**0.5**	**0.5**	**0.5**
PP_3128	Protein-tyrosine kinase	Others	Unknown	N.D.	N.D.	N.D.	**0.07**	**0.02**	**0.02**
PP_3431*	ThiJ/PfpI domain-containing protein	Others	Unknown	N.D.	N.D.	N.D.	**0.08**	**0.1**	**0.07**
PP_3443	Glyceraldehyde-3-phosphate dehydrogenase	Metabolism	Carbohydrate metabolism	N.D.	1.0	0.7	**0.4**	**0.5**	**0.4**
PP_3455	RND family efflux transporter MFP subunit	Human disease	Drug resistance	**0.4**	**0.4**	**0.5**	0.7	0.7	0.7
PP_3600	D-galactonate transporter	Others	Unknown	**0.3**	**0.4**	**0.3**	**0.3**	**0.5**	**0.4**
PP_3649	GntR family transcriptional regulator	Others	Unknown	**0.3**	**0.4**	**0.4**	N.D.	**0.4**	**0.4**
PP_3668	Catalase-peroxidase	Metabolism	Amino acid metabolism	**0.1**	**0.4**	**0.4**	**0.2**	**0.2**	**0.2**
PP_3765	transcriptional regulator MvaT, P16 subunit	Others	Unknown	N.D.	N.D.	N.D.	**0.1**	**0.05**	**0.04**
PP_3775*	Sarcosine oxidase	Metabolism	Amino acid metabolism	**0.4**	**0.4**	**0.4**	0.506	**0.5**	**0.5**
PP_3779	LysR family transcriptional regulator	Others	Unknown	N.D.	N.D.	N.D.	**0.2**	**0.4**	**0.4**
PP_3781*	Oxygen-independent coproporphyrinogen III oxidase	Others	Unknown	**0.3**	**0.3**	**0.3**	1.2	**0.4**	**0.4**
PP_3783*	Uncharacterized protein	Others	Unknown	**0.3**	**0.4**	**0.5**	0.8	0.7	0.7
PP_3786*	Aminotransferase	Metabolism	Amino acid metabolism	**0.2**	**0.3**	**0.4**	N.D.	N.D.	N.D.
PP_3839*	Zinc-dependent alcohol dehydrogenase	Metabolism	Carbohydrate metabolism	**0.3**	**0.3**	**0.4**	0.8	N.D.	N.D.
PP_3984	ISPpu13, transposase Orf3	Others	Unknown	N.D.	N.D.	N.D.	**0.08**	**0.1**	**0.1**
PP_4011	Isocitrate dehydrogenase	Metabolism	Carbohydrate metabolism	**0.5**	N.D.	**0.5**	**0.4**	**0.3**	**0.3**
PP_4034	Allantoate amidohydrolase	Metabolism	Nucleotide metabolism	N.D.	N.D.	N.D.	**0.05**	**0.05**	**0.1**
PP_4055	Glycogen debranching enzyme	Metabolism	Carbohydrate metabolism	N.D.	N.D.	N.D.	**0.3**	**0.2**	**0.2**

PP_4111	Elongation factor G 2	Others	Unknown	N.D.	N.D.	N.D.	**0.2**	**0.1**	**0.2**
PP_4138	Chromate reductase	Others	Unknown	N.D.	**0.3**	N.D.	**0.3**	**0.4**	**0.2**
PP_4288	Ureidoglycolate lyase	Metabolism	Nucleotide metabolism	N.D.	N.D.	N.D.	**0.4**	**0.3**	**0.3**
PP_4332	Purine-binding chemotaxis protein CheW	Environmental information processing	Signal transduction	**0.4**	**0.5**	**0.5**	0.503	**0.4**	**0.4**
PP_4337	Chemotaxis response regulator protein-glutamate methylesterase of group 1 operon	Environmental information processing	Signal transduction	**0.4**	N.D.	0.51	**0.3**	**0.3**	**0.3**
PP_4339	Protein phosphatase CheZ	Cellular processes	Cell motility	**0.4**	**0.2**	**0.2**	0.6	**0.1**	**0.2**
PP_4364	Anti-sigma-factor antagonist	Environmental information processing	Signal transduction	N.D.	N.D.	N.D.	**0.4**	**0.2**	**0.2**
PP_4373	Fis family transcriptional regulator	Environmental information processing	Signal transduction	N.D.	N.D.	N.D.	**0.4**	**0.2**	**0.4**
PP_4376	Flagellar cap protein FliD	Cellular processes	Cell motility	**0.4**	N.D.	**0.5**	**0.3**	**0.2**	**0.2**
PP_4378	Flagellin FliC	Cellular processes	Cell motility	**0.3**	0.505	0.503	**0.5**	**0.4**	**0.4**
PP_4397	Flagellar brake protein YcgR	Others	Unknown	**0.3**	0.55	**0.5**	**0.4**	**0.4**	**0.2**
PP_4448	Uncharacterized protein	Others	Unknown	N.D.	**0.4**	0.53	**0.4**	**0.3**	**0.4**
PP_4487	Acetyl-coenzyme A synthetase 1	Metabolism	Carbohydrate metabolism	N.D.	N.D.	0.6	**0.3**	**0.3**	**0.2**
PP_4519	TolC family type I secretion outer membrane protein	Others	Unknown	**0.3**	**0.5**	**0.3**	0.51	**0.5**	0.6
PP_4593	Uncharacterized protein	Others	Unknown	**0.03**	N.D.	**0.3**	**0.09**	**0.05**	**0.02**
PP_4616	Uncharacterized protein	Others	Unknown	N.D.	N.D.	**0.2**	**0.3**	**0.4**	**0.3**
PP_4666	3-hydroxyisobutyrate dehydrogenase	Metabolism	Amino acid metabolism	N.D.	N.D.	N.D.	**0.1**	**0.03**	**0.04**
PP_4760	Zinc-containing alcohol dehydrogenase	Others	Unknown	0.55	**0.1**	**0.3**	**0.4**	**0.4**	**0.4**
PP_4782	Phosphomethylpyrimidine kinase	Metabolism	Metabolism of cofactors and vitamins	**0.4**	**0.06**	**0.4**	N.D.	N.D.	**0.3**
PP_4789	Uncharacterized protein	Others	Unknown	N.D.	N.D.	N.D.	**0.5**	**0.5**	**0.5**
PP_4836	Uncharacterized protein	Others	Unknown	N.D.	**0.4**	N.D.	**0.4**	**0.2**	**0.2**
PP_4867	ABC transporter substrate-binding protein	Cellular processes	Quorum sensing	N.D.	N.D.	N.D.	**0.1**	**0.06**	**0.05**
PP_4869	NH(3)-dependent NAD(+) synthetase	Metabolism	Metabolism of cofactors and vitamins	**0.3**	**0.4**	**0.4**	0.6	**0.4**	**0.5**

PP_4870*	Azurin	Others	Unknown	N.D.	**0.3**	N.D.	**0.4**	**0.1**	**0.1**
PP_4871	Uncharacterized protein	Others	Unknown	N.D.	N.D.	N.D.	**0.2**	**0.01**	**0.4**
PP_4890	ATP phosphoribosyltransferase regulatory subunit	Metabolism	Amino acid metabolism	**0.3**	**0.4**	**0.4**	**0.2**	**0.3**	**0.4**
PP_4904	Flagellar motor protein MotB	Cellular processes	Cell motility	N.D.	N.D.	N.D.	**0.4**	**0.4**	**0.5**
PP_4967	S-adenosylmethionine synthase	Metabolism	Amino acid metabolism	**0.4**	**0.4**	**0.4**	0.53	**0.4**	**0.4**
PP_4977	5,10-methylenetetrahydrofolate reductase	Metabolism	Metabolism of cofactors and vitamins	**0.4**	**0.4**	**0.4**	0.51	**0.5**	**0.4**
PP_4983	Amine oxidase	Metabolism	Amino acid metabolism	**0.1**	**0.4**	**0.5**	**0.3**	**0.4**	**0.3**
PP_4991	Response regulator receiver protein	Environmental information processing	Signal transduction	N.D.	N.D.	N.D.	**0.5**	**0.4**	**0.3**
PP_5024	Amino acid ABC transporter substrate-binding protein	Others	Unknown	0.54	**0.4**	**0.4**	**0.4**	**0.4**	**0.4**
PP_5153	Fumarylacetoacetate (FAA) hydrolase	Others	Unknown	N.D.	**0.3**	**0.3**	**0.4**	**0.4**	**0.3**
PP_5156	Uncharacterized protein	Others	Unknown	**0.4**	**0.5**	**0.5**	0.53	**0.3**	**0.3**
PP_5192	Glycine dehydrogenase (decarboxylating) 2	Metabolism	Amino acid metabolism	N.D.	N.D.	N.D.	**0.08**	**0.06**	**0.05**
PP_5267	Cytochrome c5	Others	Unknown	N.D.	N.D.	**0.4**	**0.3**	**0.3**	**0.3**
PP_5313	Histone family protein DNA-binding protein (HupN)	Others	Unknown	N.D.	N.D.	N.D.	**0.3**	**0.3**	**0.4**
PP_5324	Response regulator receiver protein	Others	Unknown	N.D.	N.D.	**0.3**	**0.1**	**0.3**	**0.3**
PP_5335	Phosphoribosylaminoimidazole carboxylase ATPase subunit	Metabolism	Nucleotide metabolism	0.53	0.7	0.7	**0.1**	**0.4**	**0.5**
PP_5365	Cyclopropane-fatty-acyl-phospholipid synthase	Others	Unknown	N.D.	N.D.	N.D.	**0.2**	**0.08**	**0.2**
PP_5395	Uncharacterized protein	Others	Unknown	**0.1**	**0.3**	**0.3**	**0.4**	**0.3**	**0.2**
PP_5409	Glutamine--fructose-6-phosphate aminotransferase [isomerizing]	Metabolism	Carbohydrate metabolism	**0.4**	**0.4**	0.52	**0.5**	**0.4**	**0.5**
PP_5412	ATP synthase epsilon chain	Metabolism	Energy metabolism	**0.4**	**0.5**	**0.5**	0.6	0.54	0.6
PP_5414	ATP synthase subunit b	Metabolism	Energy metabolism	**0.4**	**0.5**	**0.5**	0.6	0.6	0.6

N.D. Protein not detected or protein ratio could not be determined.
[a,b] Functional annotation using KEGG orthology database with BRITE functional hierarchies.
Values indicating at least a twofold change (≥2 or ≤0.5) are highlighted in bold.
* Differentially regulated also at transcriptional level, as determined by previous transcriptome analyses (Shintani *et al*., 2010; Takahashi *et al*., 2015).

Table 2-9 KEGG pathway enrichment for acetylated proteins[a] in the logarithmic and stationary phases.

Term[b]	KEGG pathway	Count[c]	%[d]	*P*-value[e]	Fold enrichment[e]	Bonferroni[e]
		Log phase				
ppu03010	Ribosome	31	12.4	4.91E-08	2.26	3.63E-06
		Stationary phase				
ppu03010	Ribosome	31	10.8	8.89E-09	2.47	7.47E-07
ppu01120	Microbial metabolism in diverse environments	54	18.8	5.94E-05	1.53	0.005
ppu01200	Carbon metabolism	35	12.2	3.32E-04	1.67	0.028
ppu01130	Biosynthesis of antibiotics	56	19.4	6.44E-04	1.42	0.053
ppu00020	Citrate cycle (TCA cycle)	15	5.2	0.0011	2.24	0.091

[a] Proteins that contain reproducible acetylation sites (275 in the log phase and 311 in the stationary phase) were used for the analysis.
[b] Kyoto Encyclopedia of Genes and Genomes (KEGG) term.
[c] Number of genes matching a given KEGG term.
[d] Percentage of genes matching a given term divided by the total number of genes used for the analysis.
[e] Reproducibly detected proteins in the log (835 proteins) and stationary (1,259 proteins) phases, respectively, were used as background (*P*-value <0.01).

Table 2-10 KEGG pathway enrichment for succinylated proteins[a] in the logarithmic and stationary phases.

Term[b]	KEGG pathway	Count[c]	%[d]	*P*-value[e]	Fold enrichment[e]	Bonferroni[e]
		Log phase				
ppu03010	Ribosome	24	18.8	1.70E-07	2.77	9.86E-06
ppu00020	Citrate cycle (TCA cycle)	10	7.8	0.004	2.69	0.109
		Stationary phase				
ppu03010	Ribosome	12	16.9	1.61E-04	3.52	0.008

[a] Proteins that contain reproducible succinylation sites (138 in the log phase and 77 in the stationary phase) were used for the analysis.
[b] Kyoto Encyclopedia of Genes and Genomes (KEGG) term.
[c] Number of genes matching a given KEGG term.
[d] Percentage of genes matching a given term divided by the total number of genes used for the analysis.
[e] Reproducibly detected proteins in the log (835 proteins) and stationary (1,259 proteins) phases, respectively, were used as a background (*P*-value <0.01).

Table 2-11 Differentially regulated acetylation and succinylation sites by pCAR1 carriage[a].

Locus tag	Description	Position	R-value (pCAR1(+)/pCAR1(-))[b]	
			exp. 1	exp. 2
Acetylation sites upregulated in the pCAR1-harbouring strain in the log phase				
PP_0454	50S ribosomal protein L3	K123	KTPC[c]	KTPC
PP_0457	50S ribosomal protein L2	K37	KTPC	KTPC
PP_0480	50S ribosomal protein L17	K78	KTPC	KTPC
PP_0559	Acetyl-CoA carboxylase biotin carboxyl carrier protein subunit	K107	KTPC	KTPC
PP_1240	Phosphoribosylaminoimidazolesuccinocarboxamide synthase	K38	KTPC	KTPC
PP_1786	Glycosyl transferase family protein	K150	KTPC	KTPC
Acetylation sites upregulated in the pCAR1-harbouring strain in the stationary phase				
PP_0011	DNA polymerase III subunit beta	K236	2.03	2.62[d]
PP_0480	50S ribosomal protein L17	K78	KTPC	KTPC
PP_0559	Acetyl-CoA carboxylase biotin carboxyl carrier protein subunit	K107	KTPC	KTPC
PP_1776	Mannose-6-phosphate isomerase	K65	13.9	2.63
PP_1807	2-dehydro-3-deoxyphosphooctonate aldolase	K57	KTPC	KTPC
PP_5155	D-3-phosphoglycerate dehydrogenase	K75	2.13	KTPC
PP_5234	Nitrogen regulatory protein P-II	K58	KTPC	2.59
Acetylation sites upregulated in the pCAR1-free strain in the log phase				
PP_0440	Elongation factor Tu	K317	KT2440	KT2440
Acetylation sites upregulated in the pCAR1-free strain in the stationary phase				
PP_0440	Elongation factor Tu	K317	KT2440	KT2440
PP_1144	Diguanylate cyclase	K455	KT2440	KT2440
Succinylation site upregulated in the pCAR1-free strain in the log phase				
PP_0440	Elongation factor Tu	K317	KT2440	KT2440

[a]Acylation sites that were reproducibly differentially regulated in all three datasets obtained from each growth phase are shown.
[b]R-value (ratio of the pCAR1-harbouring to the pCAR1-free strain).
[c]The average value from the two replicates performed for ex2.
[d]KTPC, detected only in the pCAR1-harbouring strain; KT2440, detected only in the pCAR1-free strain.

Chapter 3

Investigation of the factors affecting the acylation status in pCAR1-free and -harbouring *Pseudomonas putida* KT2440

3.1 Introduction

The global proteome analyses of the pCAR1-free and -harbouring strains presented in Chapter 2 revealed that lysine acetylation and succinylation occur on hundreds of proteins with diverse functions. However, the mechanisms that regulate the acetylation levels in *P. putida* KT2440 are still unclear and functional KATs and KDACs have not been characterized. Therefore, in this chapter initial experiments have been performed in order to shed light on the factors that might affect the acetylation status in *P. putida* KT2440 and *P putida* KT2440(pCAR1). To this end, mutant strains that lack the three putative deacetylases (PP_4764, PP_5340 and PP_5402) were generated and phenotypic as well as anti-acetyllysine immunoblot analyses were conducted. Furthermore, to evaluate the extent to which acetyl-P levels in the cell might contribute to the global acetylation levels, a phosphotransacetyase (Pta), which catalyzes the reversible convesion of acetyl-CoA to acetyl-P was inactivated and anti-acetyllysine immunoblot analyses were performed in comparison to the control strains.

「本章の内容は，学術雑誌論文として出版する計画があるため，公表できない．1 年以内に出版予定．」

Chapter 4

Characterization of the N-terminal dimerization site of TurB- biochemical studies and crystallization

4.1 Preface

As described in the introduction, the crystal structure of TurB_nt$_{50}$-R8A and previous biochemical analyses identified a 'central dimerization site' and predicted a 'terminal dimerization site'. To confirm and study the properties of the 'terminal dimerization site' of MvaT homologues, protein variants truncated at the 'central dimerization site' were constructed. Those were subjected to chemical cross-linking analyses and crystallization screening.

「本章の内容は，学術雑誌論文として出版する計画があるため，公表できない．1 年以内に出版予定．」

References

AbouElfetouh, A., Kuhn, M.L., Hu L.I., Scholle, M.D., Sorensen, D.J., Sahu, A.K. *et al*. (2015) The *E. coli* sirtuin CobB shows no preference for enzymatic and nonenzymatic lysine acetylation substrate sites. *Microbiologyopen* **4**:66-83.

Allfrey V.G, Faulkner R., and Mirsky, A.E. (1964) Acetylation and methylation of histones and their possible role in the regulation of RNA synthesis. *Proc Natl Acad Sci U S A* **51**:786-94.

Ausubel, F.M., Brent, R., Kingston, R.E., Moore, D.D., Seidman, J.G., Smith, J.A., and Struhl K. (1990) *Current protocols in molecular biology*, New York, NY: John Wiley & Sons, Inc.

Bagdasarian, M., Lurz, R., Rückert, B., Franklin, F.C., Bagdasarian, M.M., Frey, J., and Timmis, K.N. (1981) Specific-purpose plasmid cloning vectors II. Broad host range, high copy number, RSF1010-derived vectors, and a host-vector system for gene cloning in *Pseudomonas*. *Gene* **16**:237-247.

Baltrus, D.A. (2013) Exploring the costs of horizontal gene transfer. *Trends Ecol Evol* **28**:489-495.

Barak, R., Welch, M., Yanovsky, A., Oosawa, K., and Eisenbach, M. (1992) Acetyladenylate or its derivative acetylates the chemotaxis protein CheY in vitro and increases its activity at the flagellar switch. *Biochemistry* **31**:10099-10107.

Bernal, P., Allsopp, L.P., Filloux, A., and Llamas, M.A. (2017) The *Pseudomonas putida* T6SS is a plant warden against phytopathogens. *ISME J* **11**:972-987.

Blander, G., and Guarente, L. (2004) The Sir2 family of protein deacetylases. *Annu Rev Biochem* **73**:417-435.

Bradford, M.M. (1976) A rapid and sensitive method for the quantitation of microgram quantities of protein utilizing the principle of protein-dye binding. *Anal Biochem* **72**:248-54.

Carabetta, V.J. and Cristea, I.M. (2017) Regulation, Function, and Detection of Protein Acetylation in Bacteria. *J Bacteriol* **199**:e00107-17

Carabetta, V.J., Greco, T.M., Tanner, A.W., Cristea, I.M., and Dubnau, D. (2016) Temporal Regulation of the of the *Bacillus subtilis* Acetylome and Evidence for a Role of MreB Acetylation in Cell Wall Growth. *mSystems* **1**:e00005-16.

Castaño-Cerezo, S., Bernal, V., Post, H., Fuhrer, T., Cappadona, S., Sánchez-Díaz, N.C., Sauer, U., Heck, A.J., Altelaar, A.F., and Cánovas, M. (2014) Protein acetylation affects acetate metabolism, motility and acid stress response in *Escherichia coli*. *Mol Syst Biol* **10**:762.

Choi, K.H., and Schweizer, H.P. (2005) An improved method for rapid generation of unmarked *Pseudomonas aeruginosa* deletion mutants. *BMC Microbiol* **5**:30.

Choudhary, C., Kumar, C., Gnad, F., Nielsen, M.L., Rehman, M., Walther, T.C., Olsen, J.V., and Mann, M. (2009) Lysine acetylation targets protein complexes and co-regulates major cellular functions. *Science* **325**:834-40.

Colak, G., Xie, Z., Zhu, A.Y., Dai, L., Lu, Z., Zhang, Y., *et al.* (2013) Identification of lysine succinylation substrates and the succinylation regulatory enzyme CobB in *Escherichia coli*. *Mol Cell Proteomics* **12**:3509-3520.

Dekel, E., and Alon, U. (2005) Optimality and evolutionary tuning of the expression level of a protein. *Nature* **436**:588-592.

Dorman, C.J. (2004) H-NS: a universal regulator for a dynamic genome. *Nat Rev Microbiol* **2**:391-400.

Doyle, M., Fookes, M., Ivens, A., Mangan, M.W., Wain, J. and Dorman, C.J. (2007) An H-NS-like stealth protein aids horizontal DNA transmission in bacteria. *Science* **315**:251-2.

de Lorenzo V., and Timmis, K.N. (1994) Analysis and construction of stable phenotypes in gram-negative bacteria with Tn5- and Tn10-derived mini-transposons. *Methods Enzymol* **235**:386-405.

Frost, L.S., Leplae, R., Summers, A.O., and Toussaint, A. (2005) Mobile genetic elements: the agents of open source evolution. *Nat Rev Microbiol* **3**:722-732.

Gardner, J.G., and Escalante-Semerena, J.C. (2008) Biochemical and mutational analyses of AcuA, the acetyltransferase enzyme that controls the activity of the acetyl coenzyme a synthetase (AcsA) in *Bacillus subtilis*. *J Bacteriol* **190**:5132-5136.

Gardner, J.G., Grundy, F.J., Henkin, T.M., and Escalante-Semerena, J.C. (2006) Control of acetyl-coenzyme A synthetase (AcsA) activity by acetylation/deacetylation without NAD(+) involvement in Bacillus subtilis. *J Bacteriol* 188:5460-5468.

Glozak, M.A., Sengupta, N., Zhang, X., and Seto, E. (2005) Acetylation and deacetylation of non-histone proteins. *Gene* 363:15-23.

Gu, W., and Roeder, R.G. (1997) Activation of p53 sequence-specific DNA binding by acetylation of the p53 C-terminal domain. *Cell* **90**:595-606.

Guan, K.L., and Xiong, Y. (2011) Regulation of intermediary metabolism by protein acetylation. *Trends Biochem Sci* **36**:108-116.

Guo, J., Wang, C., Han, Y., Liu, Z., Wu, T., Liu, Y., *et al.* (2016) Identification of Lysine Acetylation in *Mycobacterium abscessus* Using LC-MS/MS after Immunoprecipitation. *J Proteome Res* **15**:2567-78.

Haider, S., and Pal, R. (2013) Integrated analysis of transcriptomic and proteomic data. *Curr Genomics* **14**:91-110.

Hanahan, D. (1983) Studies on transformation of *Escherichia coli* with plasmids. *J Mol Biol* **166**:557-80.

Hentchel, K.L., and Escalante-Semerena, J.C. (2015) Acylation of Biomolecules in Prokaryotes: a Widespread Strategy for the Control of Biological Function and Metabolic Stress. *Microbiol Mol Biol Rev* **79**:321-346.

Hildmann, C., Riester, D., and Schwienhorst, A. (2007) Histone deacetylases-an important class of cellular regulators with a variety of functions. *Appl Microbiol Biotechnol* 75:487-497.

Hirschey, M.D., and Zhao, Y. (2015) Metabolic Regulation by Lysine Malonylation, Succinylation, and Glutarylation. *Mol Cell Proteomics* **14**:2308-2315.

Hishinuma, S., Yuki, M., Fujimura, M., and Fukumori, F. (2006) OxyR regulated the expression of two major catalases, KatA and KatB, along with peroxiredoxin, AhpC in *Pseudomonas putida*. *Environ Microbiol* **8**:2115-2124.

Hoang, T.T., Karkhoff-Schweizer, R.R., Kutchma, A.J., and Schweizer, H.P. (1998) A broad-host-range Flp-FRT recombination system for site-specific excision of chromosomally-located DNA sequences: application for isolation of unmarked *Pseudomonas aeruginosa* mutants. *Gene* **212**:77-86.

Hu, L.I., Chi, B.K., Kuhn, M.L., Fillipova, E.V., Walker-Peddakolta, A.J., Bäsell, K. *et al.* (2013) Acetylation of the response regulator RcsB controls transcription from a small RNA promoter. *J Bacteriol* **195**:4174-4186.

Hu, L.I., Lima, B.P., and Wolfe, A.J. (2010) Bacterial protein acetylation: the dawning of a new age. *Mol Microbiol* **77**:15-21.

Huang, D.W., Sherman, B.T., and Lempicki, R.A. (2009) Systematic and integrative analysis of large gene lists using DAVID bioinformatics resources. *Nature Protocols* **4**: 44-57.

Kim, S.C., Sprung, R., Chen, Y., Xu, Y., Ball, H., Pei, J., *et al.* (2006) Substrate and functional diversity of lysine acetylation revealed by a proteomics survey. *Mol Cell* **23**:607-18.

Kim, D., Yu, B.J., Kim, J. A., Lee, Y.J., Choi, S.G., Kang, S., and Pan, J.G. (2013) The acetylproteome of Gram-positive model bacterium *Bacillus subtilis*. *Proteomics* **13**:1726-36.

Kosono, S., Tamura, M., Suzuki, S., Kawamura, Y., Yoshida, A., Nishiyama, M. *et al.* (2015) Changes in the Acetylome and Succinylome of *Bacillus subtilis* in Response to Carbon Source. *PLoS One* **10**:e0131169.

Kuhn, M.L., Zemaitaitis, B., Hu, L.I., Sahu, A., Sorensen, D., Minasov, G., *et al.* (2014) Structural, kinetic and proteomic characterization of acetyl phosphate-dependent bacterial protein acetylation. *PLoS One* **9**:e94816.

Laemmli, U.K. (1970) Cleavage of structural proteins during the assembly of the head of bacteriophage T4. *Nature* **227**:680-685.

Lee, D.W., Kim, D., Lee, Y.J., Kim, J.A., Choi, J.Y., Kang, S., and Pan, J.G. (2013) Proteomic analysis of acetylation in thermophilic *Geobacillus kaustophilus*. *Proteomics* **13**:2278-2282.

Lee, S., Takahashi, Y., Oura, H., Suzuki-Minakuchi, C., Okada, K., Yamane, H., Nomura, N., and Nojiri, H. (2016) Effects of carbazole-degradative plasmid pCAR1 on biofilm morphology in *Pseudomonas putida* KT2440. *Environ Microbiol Rep* **8**:261-71.

Li, S., Zhao, H., Li, Y., Niu, S., and Cai, B. (2012) Complete genome sequence of the naphthalene-degrading *Pseudomonas putida* strain ND6. *J Bacteriol* **194**:5154-5155.

Li, T., Diner, B.A., Chen, J., and Cristea, I.M. (2012) Acetylation modulates cellular distribution and DNA sensing ability of interferon-inducible protein IFI16. *Proc Natl Acad Sci U S A* **109**:10558-10563.

Liao, G., Xie, L., Li, X., Cheng, Z., and Xie, J. (2014) Unexpected extensive lysine acetylation in the trump-card antibiotic producer *Streptomyces roseosporus* revealed by proteome-wide profiling. *J Proteomics* **106**:260-9.

Liu, J., Wang, Q., Jiang, X., Yang, H., Zhao, D., Han, J., Luo, Y., and Xiang, H. (2017) Systematic Analysis of Lysine Acetylation in the Halophilic Archaeon *Haloferax mediterranei*. *J Proteome Res* **16**:3229-3241.

Liu, L., Wang, G., Song, L., Lv, B., Liang, W. (2016) Acetylome analysis reveals the involvement of lysine acetylation in biosynthesis of antibiotics in *Bacillus amyloliquefaciens. Sci Rep* **6**:20108.

Liu, F., Yang, M., Wang, X., Yang, S., Gu, J., Zhou, J., Zhang, X.E., Deng, J., and Ge, F. (2014) Acetylome analysis reveals diverse functions of lysine acetylation in *Mycobacterium tuberculosis*. *Mol Cell Proteomics* **13**:3352-3366.

Lundby, A., Lage, K., Weinert, B.T., Bekker-Jensen, D.B., Secher, A., Skovgaard, T., *et al.* (2012) Proteomic analysis of lysine acetylation sites in rat tissues reveals organ specificity and subcellular patterns. *Cell Rep* **2**:419-431.

Macnab, R.M. (1996) Flagella and motility, p. 123–145. *In* F. C. Neidhardt, R. Curtiss III, J. L. Ingraham, E. C. C. Lin, K. B. Low, B. Magasanik, W. S. Reznikoff, M. Riley, M. Schaechter, and H. E. Umbarger (ed.), *Escherichia coli and Salmonella: Cellular and Molecular Biology*, 2nd ed. ASM Press, Washington, D.C.

Maeda, K., Nojiri, H., Shintani, M., Yoshida, T., Habe, H., and Omori, T. (2003) Complete nucleotide sequence of carbazole/dioxin-degrading plasmid pCAR1 in *Pseudomonas resinovorans* strain CA10 indicates its mosaicity and the presence of large catabolic transposon Tn4676. *J Mol Biol* **326**:21-33.

Marmorstein, R., and Roth, S.Y. (2001) Histone acetyltransferases: function, structure, and catalysis. *Curr Opin Genet Dev* **11**:155-61.

Miyakoshi, M., Nishida, H., Shintani, M., Yamane, H., and Nojiri, H. (2009) High-resolution mapping of plasmid transcriptomes in different host bacteria. *BMC Genomics* **10**:12.

Miyakoshi, M., Shintani, M., Terabayashi, T., Kai, S., Yamane, H., and Nojiri, H. (2007) Transcriptome analysis of *Pseudomonas putida* KT2440 harboring the completely sequenced IncP-7 plasmid pCAR1. *J Bacteriol* **189**:6849-6860.

Mizuno, Y., Nagano-Shoji, M., Kubo, S., Kawamura, Y., Yoshida, A., Kawasaki, H., *et al.* (2016) Altered acetylation and succinylation profiles in *Corynebacterium glutamicum* in response to conditions inducing glutamate overproduction. *Microbiologyopen* **5**:152-173.

Nelson, K.E., Weinel, C., Paulsen, I.T., Dodson, R.J., Hilbert, H., Martins dos Santos, V.A., *et al.* (2002) Complete genome sequence and comparative analysis of the metabolically versatile *Pseudomonas putida* KT2440. *Environ Microbiol* **4**:799-808.

Nikel, P.I., Martínez-García, E., and de Lorenzo, V. (2014) Biotechnological domestication of pseudomonads using synthetic biology. *Nat Rev Microbiol* **12**:368-379.

Nojiri, H., Habe, H., Omori, T. (2001) Bacterial degradation of aromatic compounds via angular dioxygenation. *J Gen Appl Microbiol* **47**:279-305.

Nojiri, H. (2012) Structural and molecular genetic analyses of the bacterial carbazole degradation system. *Biosci Biotechnol Biochem* **76**:1-18.

Nojiri, H. (2013) Impact of catabolic plasmids on host cell physiology. *Curr Opin Biotechnol* **24**:423-430.

Nojiri, H., Sekiguchi, H., Maeda, K., Urata, M., Nakai, S., Yoshida, T., *et al.* (2001) Genetic characterization and evolutionary implications of a *car* gene cluster in the carbazole degrader *Pseudomonas* sp. strain CA10. *J Bacteriol* **183**:3663-3679.

Nojiri, H., Shintani, M., and Omori, T. (2004) Divergence of mobile genetic elements involved in the distribution of xenobiotic-catabolic capacity. *Appl Microbiol Biotechnol* **64**:154-174.

Okanishi, H., Kim, K., Fukui, K., Yano, T., Kuramitsu, S., and Masui, R. (2017a) Proteome-wide identification of lysine succinylation in thermophilic and mesophilic bacteria. *Biochim Biophys Acta* **1865**:232-242.

Okanishi, H., Kim, K., Masui, R., and Kuramitsu, S. (2013) Acetylome with structural mapping reveals the significance of lysine acetylation in *Thermus thermophilus*. *J Proteome Res* **12**:3952-68.

Okanishi, H., Kim, K., Masui, R., and Kuramitsu, S. (2014) Lysine propionylation is a prevalent post-translational modification in *Thermus thermophilus*. *Mol Cell Proteomics* **13**:2382-2398.

Okanishi, H., Kim, K., Masui, R., and Kuramitsu, S. (2017b) Proteome-wide identification of lysine propionylation in thermophilic and mesophilic bacteria: *Geobacillus kaustophilus*, *Thermus thermophilus*, *Escherichia coli*, *Bacillus subtilis*, and *Rhodothermus marinus*. *Extremophiles* **21**:283-296.

Ong, S.E., Blagoev, B., Kratchmarova, I., Kristensen, D.B., Steen, H., Pandey, A. and Mann, M. (2002) Stable isotope labeling by amino acids in cell culture, SILAC, as a simple and accurate approach to expression proteomics. *Mol Cell Proteomics* **1**:376-86.

Ouchiyama, N., Zhang, Y., Omori, T. and Kodama, T. (1993). Biodegradation of Carbazole by *Pseudomonas* spp. CA06 and CA10. *Biosci Biotechnol Biochem* **57**:455-460.

Ouidir, T., Cosette, P., Jouenne, T., and Hardouin, J. (2015) Proteomic profiling of lysine acetylation in *Pseudomonas aeruginosa* reveals the diversity of acetylated proteins. *Proteomics* **15**:2152-2157.

Pan, J., Chen, R., Li, C., Li, W., and Ye, Z. (2015) Global Analysis of Protein Lysine Succinylation Profiles and Their Overlap with Lysine Acetylation in the Marine Bacterium *Vibrio parahemolyticus*. *J Proteome Res* **14**:4309-4318.

Pan, J., Ye, Z., Cheng, Z., Peng, X., Wen, L., and Zhao, F. (2014) Systematic analysis of the lysine acetylome in *Vibrio parahemolyticus*. *J Proteome Res* **13**:3294-3302.

Piperno, G., LeDizet, M., and Chang, X.J. (1987) Microtubules containing acetylated alpha-tubulin in mammalian cells in culture. *J Cell Biol* **104**:289-302.

Qian, L., Nie, L., Chen, M., Zhu, J., Zhai, L., Tao, S.C., *et al.* (2016) Global Profiling of Protein Lysine Malonylation in *Escherichia coli* Reveals Its Role in Energy Metabolism. *J Proteome Res* **15**:2060-2071.

Ramakrishnan, R., Schuster, M., and Bourret, R.B. (1998) Acetylation at Lys-92 enhances signaling by the chemotaxis response regulator protein CheY. *Proc Natl Acad Sci U S A* **95**:4918-4923.

Rimsky, S. (2004) Structure of the histone-like protein H-NS and its role in regulation and genome superstructure. *Curr Opin Microbiol* **7**:109-14.

Sambrook, J., and Russell, D.W. (2001) Molecular cloning: a laboratory manual, 3rd ed. Cold Spring Harbor, N.Y.: Cold Spring Harbor Laboratory Press.

Schäfer, A., Tauch, A., Jäger, W., Kalinowski, J., Thierbach, G., and Pühler, A. (1994) Small mobilizable multi-purpose cloning vectors derived from the *Escherichia coli* plasmids pK18 and pK19: selection of defined deletions in the chromosome of *Corynebacterium glutamicum*. *Gene* **145**:69-73.

Schilling, B., Christensen, D., Davis, R., Sahu, A.K., Hu, L.I., Walker-Peddakotla, A. *et al.* (2015) Protein acetylation dynamics in response to carbon overflow in *Escherichia coli*. *Mol Microbiol* **98**:847-863.

Schwartz, D., and Gygi, S.P. (2005) An iterative statistical approach to the identification of protein phosphorylation motifs from large-scale data sets. *Nat Biotechnol* **23**:1391-1398.

Shintani, M., Takahashi, Y., Tokumaru, H., Kadota, K., Hara, H., Miyakoshi, M., *et al.* (2010) Response of the *Pseudomonas* host chromosomal transcriptome to carriage of the IncP-7 plasmid pCAR1. *Environ Microbiol* **12**:1413-1426.

Shintani, M., Tokumaru, H., Takahashi, Y., Miyakoshi, M., Yamane, H., Nishida, H., and Nojiri, H. (2011) Alterations of RNA maps of IncP-7 plasmid pCAR1 in various *Pseudomonas* bacteria. *Plasmid* **66**:85-92.

Shintani, M., Yano, H., Habe, H., Omori, T., Yamane, H., Tsuda, M., and Nojiri, H. (2006) Characterization of the replication, maintenance, and transfer features of the IncP-7 plasmid pCAR1, which carries genes involved in carbazole and dioxin degradation. *Appl Environ Microbiol* **72**:3206-3216.

Shintani, M., Yoshida, T., Habe, H., Omori, T., and Nojiri, H. (2005) Large plasmid pCAR2 and class II transposon Tn4676 are functional mobile genetic elements to distribute the carbazole/dioxin-degradative *car* gene cluster in different bacteria. *Appl Microbiol Biotechnol* **67**:370-382.

Silva, J.C., Gorenstein, M.V., Li, G.Z., Vissers, J.P., and Geromanos, S.J. (2006) Absolute quantification of proteins by LCMSE: a virtue of parallel MS acquisition. *Mol Cell Proteomics* **5**:144-156.

Smets, B.F., and Barkay, T. (2005) Horizontal gene transfer: perspectives at a crossroads of scientific disciplines. *Nat Rev Microbiol* **3**:675-678.

Smith, K. T. and Workman, J. L. (2009) Introducing the acetylome. *Nat Biotechnol* **27:**917-919.

Starai, V.J., Celic, I., Cole, R.N., Boeke, J.D., and Escalante-Semerena, J.C. (2002) Sir2-dependent activation of acetyl-CoA synthetase by deacetylation of active lysine. *Science* **298**:2390-2392.

Starai, V.J., and Escalante-Semerena, J.C. (2004) Identification of the protein acetyltransferase (Pat) enzyme that acetylates acetyl-CoA synthetase in *Salmonella enterica*. *J Mol Biol* **340**:1005-1012.

Starai, V.J., Gardner, J.G., and Escalante-Semerena, J.C. (2005) Residue Leu-641 of Acetyl-CoA synthetase is critical for the acetylation of residue Lys-609 by the Protein acetyltransferase enzyme of *Salmonella enterica*. *J Biol Chem* **280**:26200-26205.

Sun, M., Xu, J., Wu, Z., Zhai, L., Liu, C., Cheng, Z., *et al.* (2016) Characterization of Protein Lysine Propionylation in *Escherichia coli*: Global Profiling, Dynamic Change, and Enzymatic Regulation. *J Proteome Res* **15**:4696-4708.

Sun, Z., Vasileva, D., Suzuki-Minakuchi, C., Okada, K., Feng, L., Igarashi, Y., and Nojiri, H. (2017) Growth phase-dependent expression profiles of three vital H-NS family proteins encoded on the chromosome of *Pseudomonas putida* KT2440 and on the pCAR1 plasmid. *BMC Microbiol* **17**:188.

Suzuki, C., Kawazuma, K., Horita, S., Terada, T., Tanokura, M., Okada, K., *et al.* (2014) Oligomerization mechanisms of an H-NS family protein, Pmr, encoded on the plasmid pCAR1 provide a molecular basis for functions of H-NS family members. *PLoS One* **9**:e105656.

Suzuki-Minakuchi, C., Hirotani, R., Shintani, M., Takeda, T., Takahashi, Y., Matsui, K., *et al.* (2015) Effects of three different nucleoid-associated proteins encoded on IncP-7 plasmid pCAR1 on host *Pseudomonas putida* KT2440. *Appl Environ Microbiol* **81**:2869-2880.

Suzuki-Minakuchi, C., Kawazuma, K., Matsuzawa, J., Vasileva, D., Fujimoto, Z., Terada, T., Okada, K., Nojiri, H. (2016) Structural similarities and differences in H-NS family proteins revealed by the N-terminal structure of TurB in *Pseudomonas putida* KT2440. *FEBS Lett* **590**:3583-3594.

Takahashi, Y., Shintani, M., Takase, N., Kazo, Y., Kawamura, F., Hara, H., *et al.* (2015) Modulation of primary cell function of host *Pseudomonas* bacteria by the conjugative plasmid pCAR1. *Environ Microbiol* **17**:134-155.

Takahashi, Y., Shintani, M., Li, L., Yamane, H., and Nojiri, H. (2009a) Carbazole-degradative IncP-7 plasmid pCAR1.2 is structurally unstable in *Pseudomonas fluorescens* Pf0-1, which accumulates catechol, the intermediate of the carbazole degradation pathway. *Appl Environ Microbiol* **75**:3920-9.

Takahashi, Y., Shintani, M., Yamane, H., and Nojiri, H. (2009b) The complete nucleotide sequence of pCAR2: pCAR2 and pCAR1 were structurally identical IncP-7 carbazole degradative plasmids. *Biosci Biotechnol Biochem* **73**:744-746.

Takeda, T., Yun, C.S., Shintani, M., Yamane, H., and Nojiri, H. (2011) Distribution of genes encoding nucleoid-associated protein homologs in plasmids. *Int J Evol Biol* **2011**:685015.

Tendeng, C., Soutourina, O.A., Danchin, A., and Bertin, P.N. (2003) MvaT proteins in *Pseudomonas* spp.: a novel class of H-NS-like proteins. *Microbiology* **149**:3047-3050.

Thao, S., Chen, C.S., Zhu, H., and Escalante-Semerena, J.C. (2010) Nε-lysine acetylation of a bacterial transcription factor inhibits Its DNA-binding activity. *PLoS One* **5**:e15123.

Thao, S., and Escalante-Semerena, J.C. (2011) Control of protein function by reversible Nε-lysine acetylation in bacteria. *Curr Opin Microbiol* **14**:200-204.

Tian, Z.X., Fargier, E., Mac Aogáin, M., Adams, C., Wang, Y.P., O'Gara, F. (2009) Transcriptome profiling defines a novel regulon modulated by the LysR-type transcriptional regulator MexT in

Pseudomonas aeruginosa. *Nucleic Acids Res* **37**:7546-7559.

Tu, S., Guo, S.J., Chen, C.S., Liu, C.X., Jiang, H.W. *et al.* (2015) YcgC represents a new protein deacetylase family in prokaryotes. *Elife* **4**.

Tucker, A.C., and Escalante-Semerena, J.C. (2013) Acetoacetyl-CoA synthetase activity is controlled by a protein acetyltransferase with unique domain organization in Streptomyces lividans. *Mol Microbiol* **87**:152-167.

Vasil, M.L. (2007) How we learnt about iron acquisition in *Pseudomonas aeruginosa*: a series of very fortunate events. *Biometals* **20**:587-601.

Vetting, M.W., S de Carvalho, L.P. Yu, M., Hegde, S.S., Magnet, S., Roderick, S.L. and Blanchard, J.S. (2005) Structure and functions of the GNAT superfamily of acetyltransferases. *Arch Biochem Biophys* **433**:212-226.

Vizcaíno, J.A., Csordas, A., del-Toro, N., Dianes, J.A., Griss, J., Lavidas, I., *et al.* (2016). 2016 update of the PRIDE database and related tools. *Nucleic Acids Res* **44**: D447-D456.

Wagner, G.R., and Payne, R.M. (2013) Widespread and enzyme-independent Nε-acetylation and Nε-succinylation of proteins in the chemical conditions of the mitochondrial matrix. *J Biol Chem* **288**:29036-29045.

Wang, Q., Zhang, Y., Yang, C., Xiong, H., Lin, Y., Yao, J., *et al.* (2010) Acetylation of metabolic enzymes coordinates carbon source utilization and metabolic flux. *Science* **327**:1004-1007.

Weinert, B.T., Iesmantavicius, V., Wagner, S.A., Schölz, C., Gummesson, B., Beli, P., *et al.* (2013a) Acetyl-phosphate is a critical determinant of lysine acetylation in *E. coli*. *Mol Cell* **51**:265-272.

Weinert, B.T., Schölz, C., Wagner, S.A., Iesmantavicius, V., Su, D., Daniel, J.A., and Choudhary, C. (2013b) Lysine succinylation is a frequently occurring modification in prokaryotes and eukaryotes and extensively overlaps with acetylation. *Cell Rep* **4**:842-851.

Weinert, B.T., Iesmantavicius, V., Moustafa, T., Schölz, C., Wagner, S.A., Magnes, C., Zechner, R., and Choudhary, C. (2014) Acetylation dynamics and stoichiometry in *Saccharomyces cerevisiae*. *Mol Syst Biol* **10**:716.

Wolfe, A.J. (2005) The acetate switch. *Microbiol Mol Biol Rev* **1**:12-50.

Xie, L., Wang, G., Yu, Z., Zhou, M., Li, Q., Huang, H., and Xie, J. (2016) Proteome-wide Lysine Glutarylation Profiling of the *Mycobacterium tuberculosis* H37Rv. *J Proteome Res* **15**:1379-1385.

Xie, L., Wang, X., Zeng, J., Zhou, M., Duan, X., Li, Q., *et al.* (2015) Proteome-wide lysine acetylation profiling of the human pathogen Mycobacterium tuberculosis. *Int J Biochem Cell Biol* **59**:193-202.

Yang, M., Wang, Y., Chen, Y., Cheng, Z., Gu, J., Deng, J., *et al.* (2015) Succinylome analysis reveals the involvement of lysine succinylation in metabolism in pathogenic *Mycobacterium tuberculosis*. *Mol Cell Proteomics* **14**:796-811.

Yang, X.J., and Seto, E. (2008) Lysine acetylation: codified crosstalk with other posttranslational modifications. *Mol Cell* **31**:449-461.

Yano, H., Garruto, C.E., Sota, M., Ohtsubo, Y., Nagata, Y., Zylstra, G.J., *et al.* (2007) Complete sequence determination combined with analysis of transposition/site-specific recombination events to explain genetic organization of IncP-7 TOL plasmid pWW53 and related mobile genetic elements. *J Mol Biol* **369**:11-26.

Yano, H., Miyakoshi, M., Ohshima, K., Tabata, M., Nagata, Y., Hattori, M., *et al.* (2010) Complete nucleotide sequence of TOL plasmid pDK1 provides evidence for evolutionary history of IncP-7 catabolic plasmids. *J Bacteriol* **192**:4337-4347.

Yu, B.J., Kim, J.A., Moon, J.H., Ryu, S.E., and Pan, J.G. (2008) The diversity of lysine-acetylated proteins in *Escherichia coli*. *J Microbiol Biotechnol* **18**:1529-1536

Yun, C.S., Suzuki, C., Naito, K., Takeda, T., Takahashi, Y., Sai, F., *et al.* (2010) Pmr, a histone-like protein H1 (H-NS) family protein encoded by the IncP-7 plasmid pCAR1, is a key global regulator that alters host function. *J Bacteriol* **192**:4720-4731.

Yun, C.S., Takahashi, Y., Shintani, M., Takeda, T., Suzuki-Minakuchi, C., Okada, K., *et al.* (2016) MvaT Family Proteins Encoded on IncP-7 Plasmid pCAR1 and the Host Chromosome Regulate the Host Transcriptome Cooperatively but Differently. *Appl Environ Microbiol* **82**:832-842.

Zhang, J., Sprung, R., Pei, J., Tan, X., Kim, S., Zhu, H., *et al.* (2009) Lysine acetylation is a highly abundant and evolutionarily conserved modification in *Escherichia coli*. *Mol Cell Proteomics* **8**:215-225.

Zhang, T., Wang, S., Lin, Y., Xu, W., Ye, D., Xiong, Y., *et al.* (2012) Acetylation negatively regulates glycogen phosphorylase by recruiting protein phosphatase 1. *Cell Metab* **15**:75-87.

Zhao, S., Xu, W., Jiang, W., Yu, W., Lin, Y., Zhang, T., *et al.* Regulation of cellular metabolism by protein lysine acetylation. *Science* **327**:1000-1004.

Acknowledgements

First and foremost I would like to express my gratitude to **Prof. Hideaki Nojiri** for giving me the opportunity to pursuit a doctoral degree in his laboratory and for his guidance and support. My grateful thanks are extended to **Associate Prof. Okada Kazunori** and **Assistant Prof. Chiho Suzuki-Minakuchi** for helpful discussions and support.

Furthermore, I would like to gratefully acknowledge **Associate Prof. Saori Kosono** for her support with preparation of the protein samples for MS, analysis of the data, useful discussions and critiques during the course of this study. I am also thankful to **Prof. Dr. Minoru Yoshida** from CSRS RIKEN for kindy providing the platform for performing the proteome and acylome studies. I thank **Kaori Ohtsuki**, **Masaya Usui**, and **Aya Abe** at the RRC centre of RIKEN-BSI for their technical assistance with the MS analysis. I would like also to thank **Dr. Zui Fujimoto** from NARO for providing the Hydra Plus-One robot and all chemicals for pre-crystallization screening of TurB N-terminal truncated variants.

This work was performed under the approval of the Photon Factory Program Advisory Committee (Proposal No. 2017G154). The synchrotron radiation experiments were performed at the BL26 of SPring-8 with the approval of the Japan Synchrotron Radiation Research Institute (JASRI) (Proposal No. 2017A2574 and 2017B2574).

I am thankful to all the present and former members of the **Laboratory for Environmental Biochemitsry at the University of Tokyo** who have immensely contributed to my personal and professional life in Japan.

I am especially grateful to my family for all their love, encouragement and infinite support in all my pursuits.